DISS. ETH NO. 22813

# SPATIALLY CONTROLLED IMMOBILIZATION OF ENZYMES ON SILICA SURFACES USING DENDRONIZED POLYMER-ENZYME CONJUGATES

A thesis submitted to attain the degree of

DOCTOR OF SCIENCES OF ETH ZURICH

(Dr. sc. ETH Zurich)

presented by

ANDREAS KÜCHLER

MSc ETH Interdisciplinary Sciences, ETH Zurich

born on January 9th, 1986

citizen of Horw (LU) and Sarnen (OW), Switzerland

accepted on the recommendation of

Prof. Dr. Peter Walde, examiner

Prof. Dr. A. Dieter Schlüter, co-examiner

Prof. Dr. Raffaele Mezzenga, co-examiner

Prof. Dr. André Studart, co-examiner

2015

## TABLE OF CONTENTS

## ABSTRACT

This work presents the synthesis, characterization and application of hybrid structures combining natural enzymes and synthetic dendronized polymers (denpols), bringing together the advantages and possibilities of the specific and efficient protein catalysts with the ability of the denpol to act as a macromolecular scaffold and mediator for stable surface adsorption. A linking chemistry based on the formation of a quantifiable bis-aryl hydrazone (BAH) bond was used for the formation of conjugates containing several copies of an enzyme along a single chain of a second generation denpol (*de*-PG2) dissolved in aqueous solution.

Such denpol-enzyme conjugates were prepared with three different enzymes, horseradish peroxidase (HRP), *Aspergillus* sp. glucose oxidase (GOD), and *Engyodontium album* proteinase K (proK). Additionally, a conjugate containing several copies of two different types of enzymes, GOD and HRP, on the same denpol chain was successfully synthesized. According to the composition determined by UV/vis spectrophotometric quantification of the amount of enzyme bound to the denpol during the conjugation reaction, an average 1400 repeating units long *de*-PG2 chain carried 108 HRP molecules (*de*-$PG2_{1400}$-BAH-$HRP_{108}$). Similarly, the composition of the other conjugates was determined to be *de*-$PG2_{1400}$-BAH-$GOD_{\approx 50}$, *de*-$PG2_{1400}$-BAH-($GOD_{\approx 25}$,$HRP_{\approx 78}$), and *de*-$PG2_{2000}$-BAH-$proK_{140}$. The attachment of the enzymes along the denpol chain was also confirmed by imaging of single conjugate chains adsorbed on mica with atomic force microscopy (AFM). Even though it was not possible to identify single enzyme molecules in the dry state, the thickness of the conjugates was significantly higher than the corresponding values for *de*-PG2, and was found to be in the range expected for a denpol chain with attached enzyme molecules.

Importantly, the enzymes remained active when attached to the denpols. The property of the denpol to adsorb very stably on unmodified glass surfaces was found to be a property of the denpol-enzyme conjugates as well. The absorption behavior was characterized *in situ* with the transmission interferometric adsorption sensor and the formed layers on glass surfaces were analyzed by AFM, indicating a layer thickness corresponding to a single layer of denpol-enzyme conjugate. The enzyme activity per surface area and the storage stability of the immobilized enzymes immersed in buffer solution were characterized using chromogenic enzyme substrates combined with UV/vis spectrophotometry.

The co-immobilization of GOD and HRP in a controlled ratio, which was possible with the denpol-enzyme conjugate containing both types of enzymes, allowed the observation of the catalysis of a two-step cascade reaction by the co-immobilized enzymes. Additional to the co-immobilization of GOD and HRP in a defined ratio using this two-enzyme conjugate, a system for the localized co-immobilization of GOD and HRP was developed by combination of enzyme immobilization within mesoporous silica nanoparticles (Hiroshima mesoporous materials, HMM) and the denpol mediated immobilization approach. This system resulted in a layered structure on unmodified glass surfaces, where a lower layer contained a first type of enzyme inside HMM particles and a covering layer contained the second type of enzyme in form of the denpol-enzyme conjugate. It was found that such a layered structure resulted in a good catalytic activity for the corresponding cascade reaction if GOD was adsorbed in the HMM particles and HRP added as a covering layer. The system with the HRP adsorbed in the HMM particles resulted in a low HRP activity and no product formation for the cascade reaction was observed. This behavior indicated the importance a proper choice of the enzyme immobilization protocol in such complex systems.

Complementing the results obtained for the activity and storage stability of the immobilized enzymes, a reactor for continuous flow operation was prepared for the characterization of the operational stability of the immobilized enzymes. Good stabilities were observed for reactors involving the two enzymes GOD and HRP in either a sequential setup with a first GOD reactor and a second, connected HRP reactor, or one single reactor containing the co-immobilized enzymes.

For proK, an excellent operational stability was observed in such a continuous flow setup using a tetrapeptide derivative as model-substrate. Additionally, the ability of the immobilized proK to digest a native protein in a microfluidic chip was demonstrated. This indicated the feasibility of the use of such a system for limited proteolysis in biotechnological applications. Additionally, the demonstrated possibility of the use of enzymes immobilized by this denpol-mediated approach together with macromolecular substrates offers also promising possibilities for the immobilization of enzymes used in synthetic applications involving macromolecules, such as for the preparation of modified proteins.

## ZUSAMMENFASSUNG

Diese Arbeit umfasst die Synthese, Charakterisierung und Anwendung von makromolekularen Hybriden, bestehend aus synthetischen dendronisierten polymeren Molekülen und natürlichen Enzymen. Diese hybriden Strukturen kombinieren die Vorzüge der Enzyme als effiziente Katalysatoren mit der Eigenschaft der dendronisierten Polymere, welche mit ihren langen, kettenförmigen und in jeder Wiederholungseinheit verzweigten Molekülen als Gerüst für die Verknüpfung mehrerer Enzymmoleküle dienen und gleichzeitig eine stabile Haftung auf Glasoberflächen vermitteln. Die Verknüpfung der Enzyme mit den Polymerketten wurde durch die Modifizierung beider Strukturen mit selektiv reaktiven Gruppen erreicht, welche miteinander unter Bildung einer bis-Arylhydrazon (BAH) Bindung reagieren. Durch dieses Vorgehen konnte eine Vielzahl von Enzymmolekülen entlang der einzelnen, in wässriger Lösung vorliegenden Polymerketten eines dendronisierten Polymers mit Dendronen der zweiten Generation (*de*-PG2) angebracht werden.

Drei verschiedene Enzyme, Meerrettichperoxidase (HRP), *Aspergillus* sp. Glucose-Oxidase (GOD) und *Engyodontium album* Proteinase K (proK), wurden zur Herstellung solcher Hybride verwendet. Zusätzlich wurde gezeigt, dass eine hybride Struktur, in welcher an den selben Polymerketten gleichzeitig mehrere Moleküle sowohl von der HRP als auch der GOD angeheftet sind, synthetisiert werden kann. Aufgrund der Absorption der während der Kupplung gebildeten BAH-Bindung im Bereich des ultravioletten und sichtbaren Lichtes konnte die Belegungsdichte der Polymerketten mit dem Enzym mittels *in situ* UV/vis-Spektralphotometrie bestimmt werden. Eine *de*-PG2 Kette mit einer durchschnittlichen Länge von 1400 Wiederholungseinheiten enthielt demnach 108 angehängte HRP Moleküle (abgekürzt als *de*-PG2$_{1400}$-BAH-HRP$_{108}$). Analog wurde die Zusammensetzung der weiteren Hybride bestimmt: *de*-PG2$_{1400}$-BAH-GOD$_{\approx 50}$, *de*-PG2$_{1400}$-BAH-(GOD$_{\approx 25}$,HRP$_{\approx 78}$) und *de*-PG2$_{2000}$-BAH-proK$_{140}$. Zusätzlich wurden einzelne Polymerketten der erhaltenen Hybride aus einer verdünnten Lösung auf Glimmer adsorbiert und im tockenen Zustand mittels Rasterkraftmikroskopie (AFM) untersucht. Obwohl eine Unterscheidung einzelner Enzymmoleküle im trockenen Zustand nicht möglich war, konnte aufgrund der gemessenen Höhen der Polymerketten der Hybride und dem Vergleich mit der Höhe von unmodifizierten Polymerketten eine Dichte Belegung entlang der Polymere gezeigt werden.

Die Hybride zeigten, ebenso wie *de*-PG2 selbst, eine sehr starke Neigung auf unbehandelten Glasoberflächen zu haften. Dieses Verhalten wurde ausgenützt um die ans Polymer gebundenen Enzyme mittels Adsorption an Glasoberflächen in einer katalytisch

aktiven Form zu immobilisieren. Der Adsorptionsvorgang wurde mittels TInAS (Transmission interferometric adsorption sensor) verfolgt und die adsorbierten Schichten auf der Oberfläche mittels AFM charakterisiert. Die gemessenen Schichtdicken der adsorbierten Hybride waren vergleichbar mit der Höhe einzelner Polymerketten welche auf Glimmer gemessen worden waren. Diese Tatsache bestätigte die Beobachtungen während der TInAS-Messungen, dass die Adsorption kontrolliert erfolgt und nach dem Erreichen einer bestimmten Menge stoppt. Die AFM Beobachtungen lassen den Schluss zu, dass die adsorbierten Schichten einer einzelnen Lage der adsorbierten Hybride entsprechen, und keine mehrlagigen Strukturen gebildet werden. Die Aktivität dieser immobilisierten Enzyme wurde mit Hilfe von chromogenen Enzymsubstraten mittels UV/vis Spektralphotometrie gemessen.

Aufgrund der Möglichkeit, die beiden Enzyme GOD und HRP an die selben Polymerketten anzuhängen, war es möglich durch Adsorption dieser Hybride die beiden Enzyme, welche zwei aufeinanderfolgende Schritte einer enzymatischen Kaskadenreaktion katalysieren, in klar definiertem Mengenverhältnis auf der Oberfläche zu immobilisieren. Zusätzlich zu diesem Ansatz der Co-Immobilisierung wurde ein System zur räumlich kontrollierten Co-Immobilisierung von Enzymen unter Einbezug eines Immobilisiersystems mittels mesoporösen Silikat-Nanopartikeln (Hiroshima Mesoporous Material, HMM) entwickelt. Dabei wurde durch schrittweise Adsorption eine mehrlagige Struktur auf einer unmodifizierten Glasoberfläche abgelagert, in welcher die untere Schicht aus HMM Partikeln aufgebaut war, welche in der porösen Struktur das eine Enzym enthielten, während das zweite Enzym in Form einer darüberliegenden adsorbierten *de*-PG2-Enzym Schicht präsent war. Dabei zeigte sich, dass die Lokalisierung der beiden Enzyme entscheidend für eine erfolgreiche Katalyse der enzymatischen Kaskadenreaktion ist. In einem System, in welchem GOD innerhalb der HMM Partikel immobilisiert wurde und HRP in der darüberliegenden Schicht als *de*-PG2-BAH-HRP Hybrid vorlag, wurde eine effiziente Katalyse der Kaskadenreaktion beobachtet. Im umgekehrten Fall wurde eine stark beeinträchtigte Aktivität der HRP nachgewiesen und die Kaskadenreaktion konnte nicht beobachtet werden. Diese Beobachtung wurde neben der sehr niedrigen HRP Aktivität der Tatsache zugeschrieben, dass das Zwischenprodukt in diesem Fall leichter in die freie Lösung diffundiert, während es im Falle der Produktion in der unteren Schicht durch die obere GOD Schicht diffundieren muss bevor es in die freie Lösung entweichen kann.

Des Weiteren wurden die Stabilitäten der immobilisierten Enzyme bei ständiger Aktivität bestimmt. Dazu wurden die Hybride innerhalb von Glasmikropipetten adsorbiert und so ein Durchflussreaktor hergestellt, durch welchen ein kontinuierlicher Substratfluss

aufrechterhalten wurde. Dabei zeigte sich eine gute Stabilität der Katalyse der Kaskadenreaktion durch HRP und GOD.

Die immobilisierte proK zeigte eine hervorragende Betriebsstabilität bei einem Test in einem solchen Durchflussreaktor mit einem Tetrapeptid-Derivat als Modelsubstrat. Zusätzlich wurde untersucht, ob die Protease nach der Immobilisierung auch die Verdauung von gefalteten Proteinen katalysieren kann. Dazu wurde die Proteinase im Kanal eines Mikrofluidik-Chips immobilisiert und ein fluoreszenzmarkiertes, gefaltetes Protein als Substrat zugegeben. Mittels Fluoreszenzmikroskopie wurde die erfolgreiche Hydrolyse des Substratproteins nachgewiesen. Die Möglichkeit, mit den durch die hier beschriebene Immobilisierungsmethode abgelagerten Enzymen auch Reaktionen makromolekularer Substrate zu katalysieren, ist von Bedeutung für mögliche Anwendungen in biotechnologischen und analytischen Systemen, sowie beispielsweise im Bereich der Synthese von modifizierten Proteinen.

# 1 AIM OF THE THESIS

The main aim of the thesis was the synthesis and characterization of hybrid structures of water soluble polycationic dendronized polymers (denpols) and enzymes and the investigation of a possible use of these hybrids for a simple enzyme immobilization on unmodified glass surfaces. The dendronized polymers should serve as a scaffold for the attachment of multiple copies of the enzymes horseradish peroxidase (HRP), glucose oxidase (GOD) or proteinase K (proK). A further aim was to investigate the possibility for the attachment of multiple copies of both, HRP and GOD, along the same denpol chain. These two enzymes serve as model enzymes and catalyze two consecutive steps in an enzymatic cascade reaction. Therefore, a co-immobilization of the two enzymes is of general interest.

After synthesis and characterization of these denpol-enzyme conjugates, the applicability of such conjugates for the immobilization of the enzymes on glass surfaces should be investigated, including a characterization of the adsorption procedure as well as the resulting enzymatic activity of the surface supported enzymes. For a potential further implementation of such an enzyme immobilization procedure, characterization of the performance under prolonged operating conditions should be addressed as well.

# 2 BACKGROUND

## 2.1 Concepts for enzyme immobilization on solid supports

The study of the properties of natural protein catalysts, *i.e.* enzymes, has been pursued since the discovery of diastase by Payen and Persoz in 1833 [1], preceding even the formulation of the general concept of catalysis by Berzelius [2, 3]. In their *Mémoire sur la diastase, les principaux produits de ses réactions et leurs applications aux arts industriels* the authors already point out the impact the preparation of an isolated enzyme product can have not only promoting the biochemical studies of the foundations of biocatalysis, but also enabling new processes of industrial use [1]. Isolation of enzymes in a pure form offers the great advantage of a fine control of the conditions used to study the enzymes function [4], as well as to tune reaction conditions in a way promoting the formation of a desired product in a synthetic or analytical application [5]. Apart from the possibility to produce pure enzyme preparations, another technological advance promoted the use of enzymes in various applications: The ability to immobilize enzyme molecules in a controlled way, *i.e.* to confine them on or in a support. Immobilized enzymes combine the advantages of a heterogeneous system in terms of product isolation and of enzymatic catalysts such as high reaction rates, and chemo-, regio-, and enantioselectivity, resulting in substrate specificity in some cases, and a broad acceptance of various substrates in other cases, both of which can be desirable depending on the application intended [6].

The field of enzyme immobilization was opened, among others, by the pioneering work of Katchalski-Katzir, pointing out the advantages of immobilized enzymes in terms of separation from reaction products [7, 8]. Additionally, the study of immobilized enzymes can also be used for further insights into mechanistic details of the catalytic activity [9]. At the same time, immobilized enzymes promised important advantages for industrial applications, as the isolation of the reaction product can be simplified significantly, and regeneration of the active enzyme catalyst is generally possible, while in a homogeneous system enzyme recovery is not normally feasible [10-12]. In addition to the advantages in terms of separation and catalyst recycling, the possibility to immobilize enzymes on solid supports opened a new field of activity by enabling the construction of bioelectrodes with a specific electrochemical activity determined by the immobilized enzyme [13].

A wide range of enzyme immobilization approaches have been described, varying in the concept of immobilization as well as in the type of enzyme suitable for a specific approach [14-16]. Conceptually different methods for enzyme immobilization are described here in more details. However, it has to be taken into account that the intrinsic differences of different types of enzymes as well as the varying prerequisites of the

applications resulted in a plethora of approaches, which often combine aspects of conceptually different methods in one practical example.

The most simple and straightforward enzyme immobilization technique is a direct adsorption of the enzyme on the surface of the solid support (**Figure 2.1.1a**) [17, 18]. As the interactions mediating such physisorption are normally of a weak nature, desorption of the enzyme is often observed in these systems. The desorption of enzyme can be a anticipated feature of immobilized enzymes used [19], but often a stable adsorption without loss of enzyme to the solution is needed. This limitation can be overcome by activating the surface in a way to allow a covalent binding of the enzymes coming in contact with the surface (**Figure 2.1.1b**). Various chemical linkers have been used for a direct linking of enzymes to solid supports, often exploiting surface exposed lysine residues presenting amino groups as reactive nucleophiles for the immobilization reaction [20]. Often, a surface modification of the support is carried out to obtain an aldehyde presenting surface, which can react with enzymes by Schiff base formation with available amino groups [21]. Due to the dynamic nature of the imine bond, such approaches normally rely on multiple interactions of the solid support with each enzyme molecule to prevent leaching of the immobilized enzyme [22]. A variation of this approach which is often employed is the preparation of an amine decorated surface, which then can be modified with glutaraldehyde in order to bind the enzyme. This leads to a combination of ionic interactions of the ammonium groups with the enzyme in a first step of the

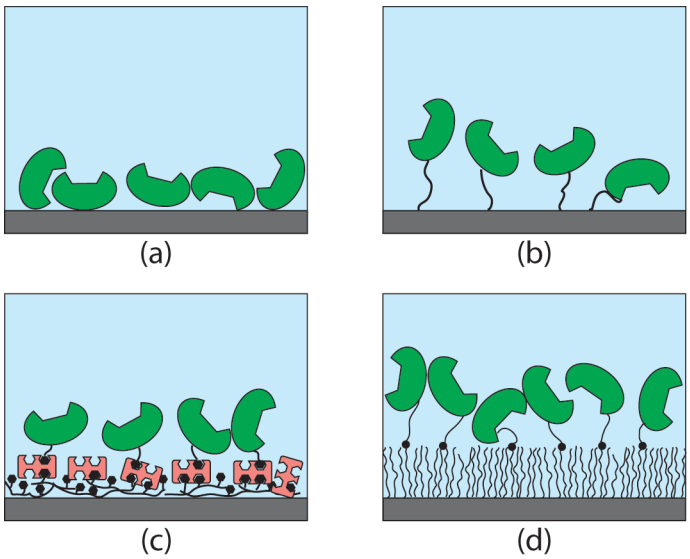


**Figure 2.1.1** Schematic representation of a selection of the different enzyme immobilization methodologies on a solid support (gray). **a)** Immobilization of enzymes (green) by adsorption on the solid support offers the simplest approach. **b)** Covalent attachment of the enzyme can be used to inhibit desorption of enzymes from the support, yielding better stabilities. c) Binding of avidin (red) on a surface presenting biotin moieties forms an intermediate organic layer. Biotinylated enzymes are stably bound by avidin. **d)** Grafting of polymer brushes from the surface and subsequent post-polymerization functionalization with enzymes allows the formation of an intermediate organic layer between support and enzymes.

immobilization, and subsequent covalent binding of the adsorbed enzyme via an aldehyde moiety of glutaraldehyde [23]. Other direct covalent enzyme attachment approaches base on the presence of thiols in cysteine containing proteins, which can be exploited for selective reactions such as the formation of disulfide bonds and the thiol-ene click reaction [24, 25].

As an alternative to the direct covalent linking of the enzyme of interest to a support, the high affinity of the natural protein avidin (or its bacterial homolog streptavidin) towards the vitamin biotin, with a dissociation constant of about $10^{-15}$ M one of the strongest non-covalent bonds known [26], has been exploited for enzyme immobilizations in numerous examples (**Figure 2.1.1c**) [27]. A modification of the support surface with biotin moieties can be achieved in different ways, such as deposition of a supported lipid bilayer including biotin modified lipids, to which then a layer of avidin binds, presenting biotin binding sites towards the solution. On such substrates, biotinylated enzymes can be readily immobilized [28]. Other possibilities to prepare biotin presenting supports for enzyme immobilization include the deposition of biotinylated synthetic polymers on the surface of the support. Using glass surfaces with a negative surface charge when present in neutral aqueous solutions, polycationic polymers can be used for this purpose. Different types of such polymers, as for example biotinylated poly(L-lysine)-*graft*-poly(ethylene glycol) (PLL-*g*-PEG) or a polycationic dendronized polymer (denpol) have been successfully used for this approach [29, 30]. Using such a biotin-avidin mediated approach is accompanied by the feature that the enzyme is not in direct contact with the surface of the solid support, as in the case of a direct adsorption or using a direct covalent linker. The avidin binding to the surface exposed biotin forms an intermediate organic layer between the solid support and the enzyme of interest.

A different approach which also features an intermediate organic layer between the immobilized enzymes and the support is a surface modification presenting polymer brushes (**Figure 2.1.1d**) [31]. A dense polymer layer grafted from the support can be obtained by surface initiated polymerization of a suitable monomer, which allows the attachment of the enzymes *via* post polymerization modifications [32]. Depending on the synthetic procedure and the length of the polymer brushes, the thickness of the protein containing layer on the surface of the support, and therefore the amount of enzyme per surface area, can be tuned, arriving at amounts exceeding monolayer coverage of the surface [33].

Aiming as well for high enzyme coverage per surface area exceeding monolayer thickness, the use of layered deposition similar to the biotin-avidin based procedure

described above has been described for the preparation of more complex structures. In a layer-by-layer adsorption procedure, several enzyme containing layers can be built up on the surface of a solid support. In the traditional layer-by-layer technique, polyelectrolyte multilayers are formed by stepwise adsorption of oppositely charged polyelectrolytes [34, 35]. To exploit such a behavior for enzyme immobilization, an enzyme can be deposited as one of the polyelectrolyte layers if the pH is chosen such that the protein structure exhibits a pronounced excess surface charge [36]. Apart from the formation of conventional polyelectrolyte based layer-by-layer structures, other types of interactions have been exploited for similar enzyme immobilization protocols. These include the formation of pure protein layers by the use of multiply biotinylated enzymes and avidin, which allows repetitive deposition of avidin and the multiply biotinylated protein, which then presents again free biotin moieties capable of binding a next layer of avidin [37]. In a similar way, the interaction of the protein concanavalin A (Con A) and sugars was exploited. Using glycosylated enzymes for the layer-by-layer assembly, the interaction between Con A and the sugars present on the surface of the glycosylated enzymes allows the formation of stable layered structures on solid supports [38]. As the interaction of the individual layers does not normally depend on the further underlying layers, a thickness of these structures can be achieved by repetitive deposition of the alternating layers. As a drawback, it has been shown that an increase in enzymatic activity may be only seen for a small number of layers, as mass transport of enzymatic substrates inside the layer-by-layer structure may become limiting and therefore subjacent enzyme layers cannot contribute to the overall reaction [39].

Additionally to the variation of the attachment strategies for enzymes onto supporting surfaces, the solid support itself offers a different level of variation for the development of immobilized enzyme materials. As already seen in the case of layer-by-layer assembled structures on the surface, the amount of immobilized enzyme can be increased significantly when departing from mere surface covering. The most extreme examples in this direction are virtually support free structures such as cross linked enzyme crystals (CLEC, [40, 41]) and cross linked enzyme aggregates (CLEA, [11, 42, 43]). In these materials, the enzymes are not only involved as catalytically active species, but at the same time constitute the major amount of the supporting structure, complemented only by small molecular linkers. After crystallization or aggregation of the enzyme molecules, these structures are stabilized by multiple crosslinking, often performed with glutaraldehyde [40, 43]. In contrast to the surface confined systems consisting of a thin layer of catalyst on the solid support, such approaches offer a considerably higher mass

fraction of catalyst. Possible disadvantages may arise if macromolecular substrates are considered, where the accessibility of the active site can become a limiting factor.

Another method for the preparation of immobilized enzymes which allow subsequent dispersion of the catalytically active material is based on the use of mesoporous silicate materials. Various mesoporous materials, with ordered or non-ordered pore structures have been used for the preparation of immobilized enzyme materials [44-48]. The use of such porous silicate supports allowed the combination of high surface areas, which are essential for high catalyst loading, with favorable mechanical properties of the silicate materials in terms of further handling of the immobilized enzymes. As in the case of non-porous surfaces, a variety of immobilization chemistries can be applied. In contrast to the flat surfaces, mesoporous structures can offer additional interactions due to the curvature of the pores, which is in the same order of magnitude as the size of the enzymes, and therefore allows a multipoint interaction between enzymes and support [49].

Apart from the direct properties of the mesoporous silica materials as a support for the immobilization of enzymes, the confined environment inside the mesoporous structure can have a direct influence on the enzymatic activity. Local pH changes induced by the silanol groups of the silica support have been characterized [50], but also local concentration effects as well as stabilization or destabilization of the enzyme structure due to interactions with the support are pronounced in the mesopores and can induce both, increase or decrease of enzymatic activity [48, 51].

Such findings indicate the importance of the availability of various different protocols for enzyme immobilization. Specific advantages and disadvantages of individual approaches, depending on enzyme, application and immobilization method used, indicate the necessity of the development of further alternatives in the field of enzyme immobilization. Even though this short list of different enzyme immobilization concepts is not encyclopedic and numerous variations and combinations of the described methods exist, there is a need for further enzyme immobilization techniques in order to explore the potential and the understanding of such surface confined biocatalysts. A special focus in this area was recently also set on the methods allowing a simple and reliable immobilization procedure feasible in micro- and nanostructured devices [52-54].

## 2.2 The dendronized polymer *de*-PG2

A possibility for a straightforward enzyme immobilization on non-modified silicate glass surfaces, excluding surface chemical approaches involving chemical functionalization and activation of the glass surface, was investigated in the present work. An approach including the conjugation of the enzymes of interest to a synthetic polymer, which serves as a macromolecular scaffold for enzyme attachment and at the same time mediates the immobilization of the enzymes on the glass surface, was chosen. Aiming for the synthesis of water soluble polymer-enzyme conjugates to be used for enzyme immobilization on glass surfaces, there is a set of prerequisites for the selection of a suitable polymer. Using unmodified glass as a solid support for the immobilization, the polymer has to mediate a strong and stable adsorption on this surface without significant desorption, while still exhibiting a good water solubility to enable synthesis of the polymer-enzyme conjugate in aqueous solution, which is required for most enzymes to prevent deactivation of the enzyme during the conjugate synthesis. Furthermore, the polymer itself must not impact the activity of the enzyme of interest and needs to have functional groups which allow the attachment of linkers in order to form the polymer-enzyme conjugate.

A class of polymers which can fulfill all the requirements listed above are polymeric structures which carry free primary amines in the side chains. Of these, a special interest was recently directed towards dendronized polymers (denpols) [55, 56]. This term describes polymers which carry on every repeating unit of the polymer chain a dendron, *i.e.* a regularly branched side chain [57, 58]. These denpols present a well-defined structure, formed by the polymer backbone in the core, surrounded by the dendron

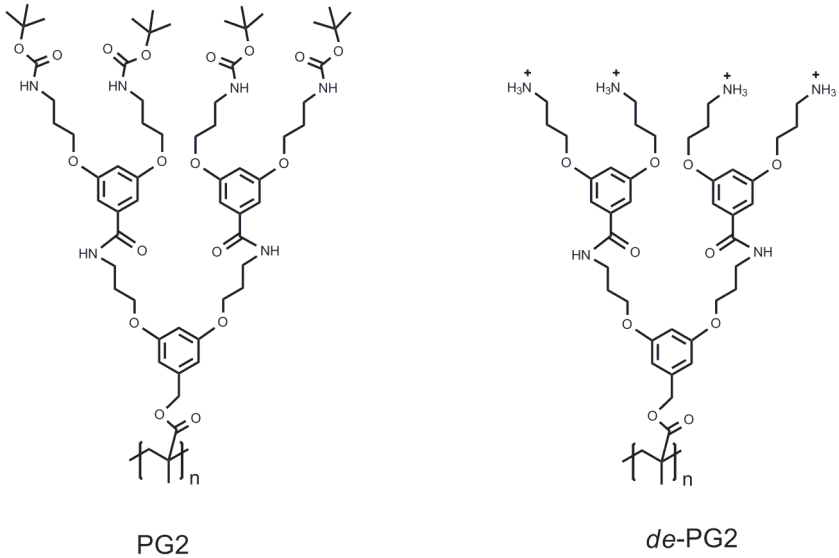


**Figure 2.2.1** The poly methacrylate based second generation dendronized polymer PG2 and the deprotected polycationic, water soluble *de*-PG2 (the fully protonated form is shown, counter-ions are omitted).

structure presenting the dendron's peripheral functional groups on the surface of a cylindrical object-like macromolecule [59, 60].

A specific type of denpols, based on a polymethacrylate backbone and dendrons built from 3,5-bis(aminopropyloxy)-benzamide branching units (**Figure 2.2.1**), has been extensively investigated in terms of synthetic accessibility of high dendron generation [61] as well as in terms of high molecular weight of the polymer backbone [62]. By increasing the dendron generation of such high molecular weight denpols by iterative grafting of an additional branching unit of the dendron to the existing denpol, it is possible to obtain extraordinary high molecular weight structures. Additionally to the synthetic accessibility of high generation denpols with excellent structural perfection in terms of dendron coverage, the grafting from approach also opens the path towards the synthesis of homologous series of denpols consisting of the same polymer backbone in terms of length and polydispersity, and only differing in the generation of the attached dendrons [55]. Such a series of homologous denpols gives access to studies of the influence of the dendron generation on the properties of the polymer chain such as an increasing rigidity and the emergence of an intrinsically cylindrical shape [60, 63].

While during synthesis, characterization and application of the denpol in organic solvents a *tert*-butyloxycarbonyl (Boc) protecting group is used to mask the peripheral amines of the dendrons, deprotection of the denpol results in a polycationic species presenting a surface covered with ammonium groups (**Figure 2.2.1**). The charges localized on the ammonium groups render these denpols water soluble at pH values below about 8, where a major part of the amines are protonated, offering then a polymer which fulfills the above mentioned criteria needed to present a promising platform for enzyme attachment to the denpol [56, 64, 65] and further use of the conjugates for enzyme immobilization on non-modified silica surfaces.

A generic nomenclature implemented for denpols to distinguish the different generations available can be used assigning **PG1** to a **p**olymer of **g**eneration **1** and **PGX** to a **p**olymer of **g**eneration **X**, respectively. Here this nomenclature is used for the above discussed case of the polymethacrylate based denpol carrying 3,5-bis(aminopropyloxy)-benzamide dendrons (**Figure 2.2.1**). In contrast to the PGX including the peripheral Boc protecting groups, the corresponding **de**protected, water soluble, polycationic **p**olymer of **g**eneration **X** is abbreviated as ***de*-PGX**. Additionally, an indication of the average number of repeating units per polymer chain can be used to differentiate denpols of different lengths. Using such a nomenclature, *de*-$PG2_{1400}$ describes a deprotected second generation

denpol with a number-average degree of polymerization of 1400, as it was used for major parts of the work described here.

## 2.3 Enzyme immobilization on $SiO_2$ surfaces with *de*-PG2 and the biotin-avidin system

Recently, the use of such denpols for enzyme immobilization has been demonstrated [30, 66, 67]. In a stepwise approach, and exploiting the biotin-avidin linker system, the feasibility of using *de*-$PG2_{1000}$ for an efficient adsorption on silica surfaces has been proven. The affinity of the protein avidin (and it's homolog streptavidin) to bind selectively to the small molecule biotin, with a dissociation constant in the femtomolar range [26], has been exploited in numerous applications including labelling protocols [68-70], protein purification [71] as well as various enzyme immobilization procedures [29].

A partial modification of the peripheral amino groups of *de*-$PG2_{1000}$ with biotin by reaction with an activated ester (in this case a sulfo-*N*-hydroxysuccinimidyl ester of a biotin derivative) allowed installing biotin moieties on the denpol. As a result of the high abundance of amino groups on the denpol, more than 100 biotin moieties per *de*-$PG2_{1000}$ could be installed without changing the adsorption properties of the denpol on $SiO_2$ surfaces, as this corresponded to a modification of less than 3 % of the amino groups which mediate the polymer adsorption. After adsorption of the biotinylated denpol on a $SiO_2$ surface, avidin was able to bind the biotin groups presented from the polymer layer. As the avidin tetramer presents four biotin binding sites, it was possible to adsorb on this avidin layer *via* remaining free biotin binding sites a further layer of biotinylated protein [30]. As the subjacent denpol and avidin layers were independent of the protein layer on top, the same immobilization procedure could be used for various different types of biotinylated enzymes [67]. Preparation of the necessary biotinylated enzymes was performed by reaction of surface exposed amino groups as present in lysine side chains, which can be modified using activated ester reagents, similar to the modification of the denpol amino groups.

Using this stepwise approach for *de*-PG2 mediated enzyme immobilization, horseradish peroxidase (HRP), *Aspergillus* sp. glucose oxidase (GOD), and *Escherichia coli* β-galactosidase(β-Gal) were separately immobilized on non-modified glass surfaces of microscopy slides and inside glass micropipettes and in the channels of a microfluidic chip [66, 67]. This allowed the preparation of an enzymatic reactor catalyzing a 3-step cascade reaction. In a first step, lactose was hydrolyzed by β-Gal yielding D-galactose and D-glucose. The glucose was then oxidized by the GOD and dissolved dioxygen, which in turn produced glucono-δ-lactone and hydrogen peroxide. In a third step, the oxidation of the chromogenic substrate *o*-phenylenediamine, yielding the chromophore 2,3-diaminophenazine, was catalyzed by HRP.

## 2.4 Formation of denpol-enzyme conjugates in aqueous solution

While the use of the biotin-avidin system allowed a stable denpol mediated immobilization of enzymes on $SiO_2$ surfaces when applied in a stepwise adsorption procedure, the synthesis of denpol-enzyme conjugates in solution poses different problems when approached with this linking system. The homotetrameric structure of native avidin features four biotin binding sites with comparable binding constants [26]. Given the desired design of a denpol-enzyme conjugate which carries several copies of an enzyme on a single polymer chain, each polymer chain carries several reactive units during the conjugation reaction. Addition of a tetravalent reaction partner to the modified polymer would in such a case induce network formation, leading to an insoluble and ill-defined product.

Aiming for water soluble, well-defined denpol-enzyme conjugates without crosslinking of the individual polymer chains, it has been shown that a bio-orthogonal linker chemistry based on the formation of a bis-aryl hydrazone (BAH) can be applied [56, 64]. Among various other bio-orthogonal protein modification chemistries, the BAH linker introduced in the 2000s offers the advantage of the possibility for a direct quantification of the conjugation reaction by quantitative UV/vis spectrophotometry due to a characteristic absorption band of the bis-aryl hydrazone moiety formed during the conjugation reaction [72-74]. Such a linking chemistry requires installation of a benzaldehyde and a 2-hydrazinopyridine moiety on the enzyme and the denpol, respectively, which then condense upon combining the two macromolecules, yielding a stable bis-aryl hydrazone (**Figure 2.4.1**). Both of the required linker moieties can be introduced using amino reactive *N*-hydroxysuccinimidyl esters, using on the side of the denpol the peripheral amino groups for the attachment of the linker, and on the side of the enzyme the amines presented by the side chains of surface localized lysines. The modification of the enzymes

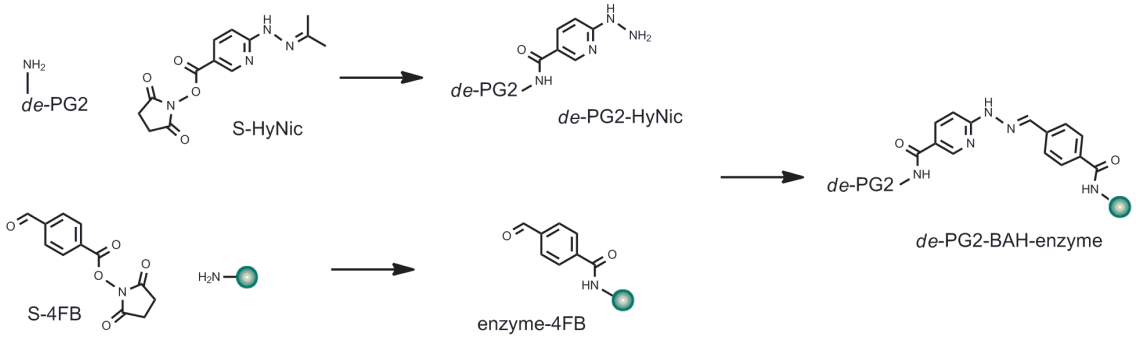


**Figure 2.4.1** The conjugation system used in this work is based on the modification of the protein of interest and the synthetic polymer with bio-orthogonal moieties, a 4-formylbenzamide (4FB) and a 6-hydrazinonicotinamide (HyNic), respectively. Selective reaction of the HyNic and the 4FB moieties yields a stable bis-aryl hydrazone, with a characteristic UV/vis absorption band at about 350 nm.

was adjusted in a way that the a minimal fraction of enzyme molecules carried more than one linker moiety, as this would result in crosslinking of the denpol chains as discussed above. With such precautions, it was possible to synthesize denpol-enzyme conjugates involving the enzymes HRP and bovine erythrocyte superoxide dismutase (SOD) [56].

Exploiting the UV/vis signature of the BAH conjugation reaction, it has been possible to not only monitor the course of the conjugation, but also to quantitatively evaluate the extent of enzyme binding to the denpol. The synthesis of a conjugate of *de*-PG1$_{2000}$ carrying HRP and SOD in a defined ratio along the denpol chain was described. The conjugate also included a fluorescein tag which was attached to the polymer using the same linker moieties. Such a conjugate was described as *de*-PG1-BAH-(FL$_{20}$,HRP$_{120}$,SOD$_{60}$), indicating the presence of 120 HRP molecules, 60 SOD molecules, and 20 fluorescein tags on a single polymer chain of the length of 2000 r.u. which were all linked to the polymer *via* bis-aryl hydrazone linkers [56].

Similar conjugates were also synthesized and characterized with a second generation denpol *de*-PG2$_{2000}$, and it was shown that a *de*-PG2$_{2000}$-BAH-(FL$_{100}$,HRP$_{100}$) conjugate could be entrapped in 1-palmitoyl-2-oleoyl-*sn*-glycero-3-phosphocholine (POPC) giant vesicles formed by the water droplet transfer method [64].

Apart of the potential application of such conjugates for enzyme entrapment yielding high enzyme concentrations inside vesicles, the synthesis of denpol-BAH-enzyme conjugates offers the possibility to control the abundance of different types of enzymes within a single macromolecular structure, which in turn allows controlling the ratio of the different types of enzymes in further applications using these conjugates. This is of special interest in regard to enzyme co-immobilization, where a certain ratio of two different types of enzymes is aimed for to achieve specific performance characteristics.

## 2.5 Enzymes used in this work

### 2.5.1 Horseradish peroxidase

Peroxidase (HRP, EC 1.11.1.7: donor:hydrogen-peroxide oxidoreductase) from horseradish (*Armoracia rusticana*) is a monomeric protein, represented by several acidic, neutral and basic isoenzymes [75, 76]. Due to its high abundancy, the basic isoenzyme C (isoelectric point pI ≈ 9, [76]) was used for most of the work involving HRP [77] and represents the prototypic class III plant peroxidase *per se* [78]. It consists of a 308 amino acid polypeptide with 8 heterogeneously modified glycosylation sites [79-81]. This results in an average molar mass of 44 kDa with a carbohydrate content of about 20 mass%. HRP additionally contains two bound calcium ions and the active site includes a prosthetic heme group [82]. The UV/vis absorbance of the heme group has been used for quantification of the enzyme ($\varepsilon_{403nm}$ = 102000 $M^{-1}cm^{-1}$, [76]) as well as for the characterization of enzyme purity by correlation to the protein absorption at 280 nm (Reinheitszahl: R.Z. = $A_{403nm}/A_{280nm}$, [83]). In the resting state, the heme group is present in a reduced form. Oxidation by hydrogen peroxide yields the reactive compound I, which then is reduced to the resting state by two one-electron transfer reactions oxidizing two reducing substrate molecules per catalytic cycle (**Figure 2.5.1**).

An interesting property of HRP is the acceptance of a variety of reducing substrates. Several of these can be used as chromogenic substrates with direct quantification of the

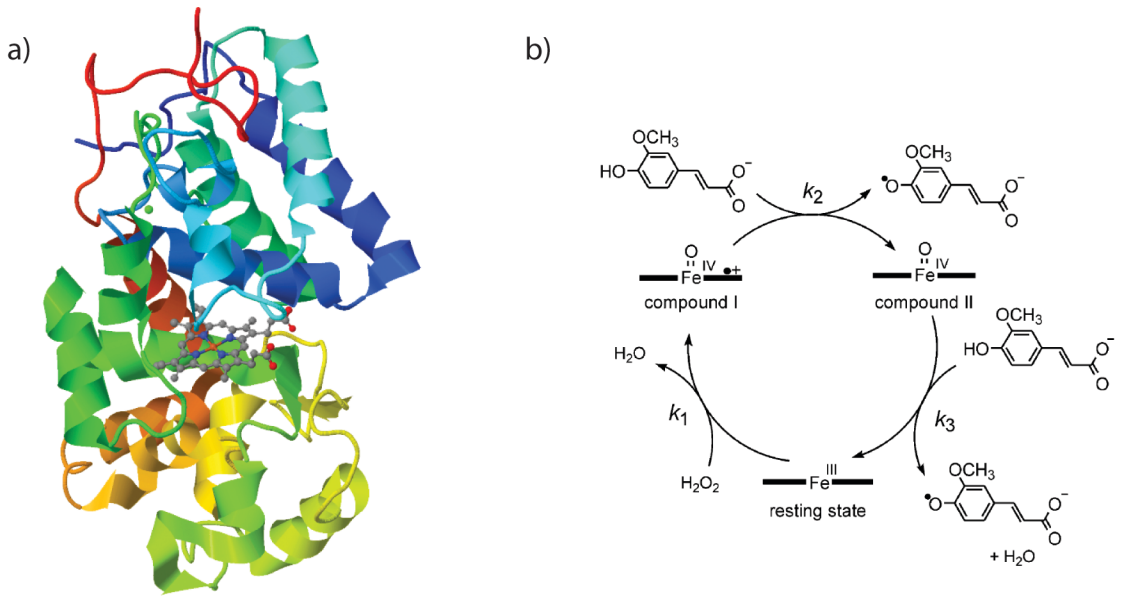


**Figure 2.5.1 a)** Cartoon representation of the structure of HRP as determined by X-ray crystallography of a recombinant, non-glycosylated enzyme (PDB entry: 1H5A). **b)** Catalytic cycle of HRP with ferulate as reducing substrate. Oxidation of the resting state yields the reactive compound I, which is reduced *via* two one-electron transfers (Figure from Veitch [77]).

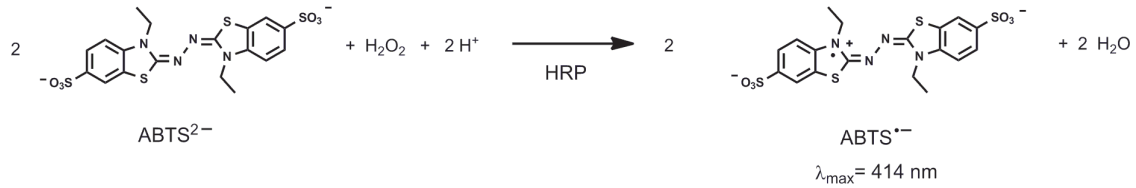


**Figure 2.5.2** HRP catalyzed oxidation of $ABTS^{2-}$ with $H_2O_2$ yielding the blue-green colored, stable radical $ABTS^{\bullet-}$.

product by UV/vis spectrophotometry or as fluorogenic substrates for fluorescence analysis of the product formation [82]. Due to this characteristics, HRP was used as a reporter enzyme already in one of the first examples of the enzyme linked immunosorbent assay (ELISA) [84].

Among the different chromogenic substrates of HRP, two are discussed here in more detail. 2,2′-Azino-bis(3-ethylbenzothiazoline-6-sulfonate) ($ABTS^{2-}$), normally used in the form of the well soluble diammonium salt, is readily oxidized by HRP in a one-electron oxidation yielding the green to blue $ABTS^{\bullet-}$ radical (**Figure 2.5.2**). This radical is stable enough to allow reaction times of several minutes without interfering decay of the product concentration and has a high absorption coefficient ($\varepsilon_{414nm}$ = 36000 $M^{-1}cm^{-1}$), resulting in easy detection of the product formed [85]. An additional broad absorption band between about 550 and 850 nm with three maxima would allow detection as well in a higher wavelength area if needed due to interfering absorptions at 414 nm.

A second, widely used reducing substrate for HRP is 1,2-diaminobenzene (*o*-phenylene diamine, OPD). In contrast to the case of $ABTS^{2-}$ oxidation, where the direct product of the enzymatic reaction can be observed, the OPD reaction is more complex. Upon enzymatic oxidation of OPD, a dimerization and a subsequent non-enzymatic oxidation step is observed, yielding 2,3-diaminophenazine as product (**Figure 2.5.3**) [86, 87]. Due to the complex nature of the assay reaction, side product formation can become significant if the reaction conditions are not controlled rigorously [87]. Additionally, assay solutions are light sensitive and therefore require special precautions, such as storage and incubation in a dark environment and limited exposure to light during UV/vis spectrophotometric quantification of the product formation. Despite these limitations, the stable product formed allows for elongated incubation times, and therefore very low detection limits routinely down to picomolar concentrations of HRP [87]. Additionally, the

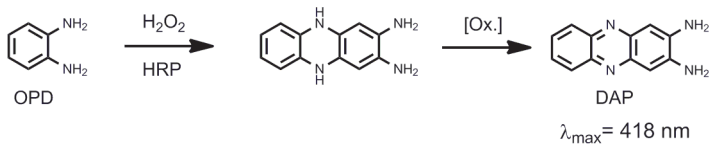


**Figure 2.5.3** Reaction scheme of the enzymatic oxidation of OPD by HRP. After subsequent dimerization and non-enzymatic oxidation, the yellow product DAP is obtained.

fluorescence observed for the reaction product DAP allows fluorimetric detection if needed [88].

### 2.5.2 Glucose oxidase

Glucose oxidase (GOD, EC 1.1.3.4: β-D-glucose:oxygen 1-oxidoreductase) from *Aspergillus* sp. is a glycosylated, homodimeric protein with a pI of 4.2 [89]. Each monomer is formed from a 583 amino acid long polypeptide chain and includes a tightly but non covalently bound flavin adenine dinucleotide (FAD) as a prosthetic group located at the active site and involved in the catalytic cycle [90]. The two subunits are connected via covalent disulfide bonds. The molar mass of the glycosylated enzyme has been reported to be about 150 kDa and the FAD cofactor was shown to be released only under denaturing conditions [89]. The presence of the FAD group results in a characteristic UV/vis spectrum with absorption maxima at 278 nm, 383 nm and 452 nm. The extinction coefficients at 450 nm and 280 nm have been determined and allow UV/vis spectrophotometric quantification of the enzyme ($\varepsilon_{450nm}$ = 28200 $M^{-1}cm^{-1}$, [91]; $\varepsilon_{280nm}$ = 270000 $M^{-1}cm^{-1}$, [92]).

In the resting state of GOD, the FAD cofactor is present in the oxidized form. Upon oxidation of D-glucose, yielding glucono-δ-lactone, the dinucleotide is reduced. Re-oxidation of the cofactor occurs *via* reduction of dissolved dioxygen, yielding hydrogen peroxide as byproduct (**Figure 2.5.4**) [93, 94].

Various applications of GOD in fields ranging from food processing, use as

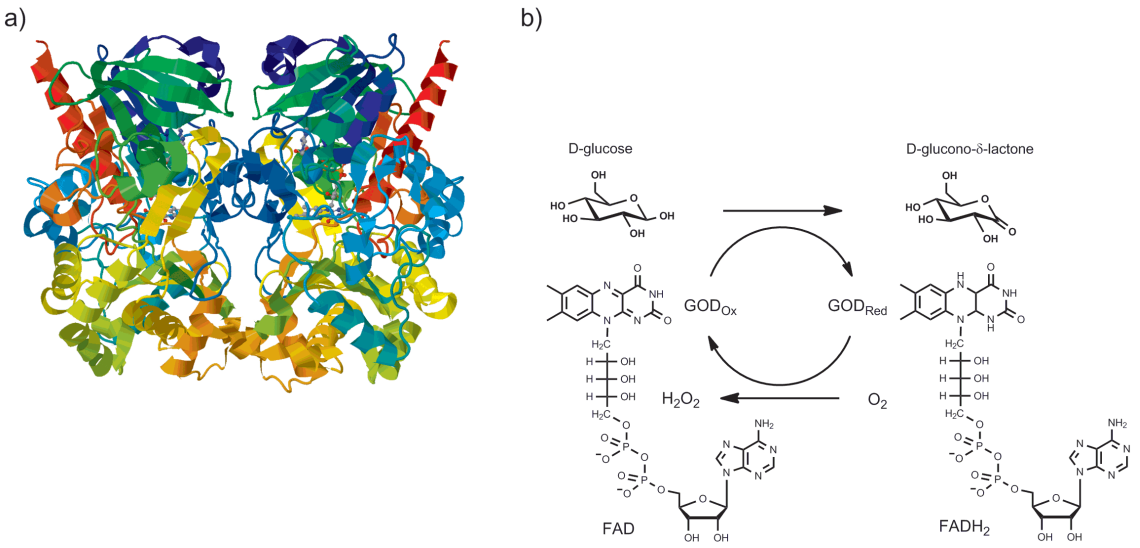


**Figure 2.5.4 a)** Cartoon representation of the crystal structure of a deglycosylated GOD dimer (PDB-entry: 3QVP). **b)** Catalytic cycle of GOD: The oxidized enzyme ($GOD_{Ox}$: falvin adenine dinucleotide cofactor in oxidized form FAD) converts glucose to glucono-δ-lactone. In a second reaction, the reduced enzyme ($GOD_{Red}$: flavin adenine cofactor in reduced form $FADH_2$) is re-oxidized by dissolved dioxygen, producing $H_2O_2$ as byproduct.

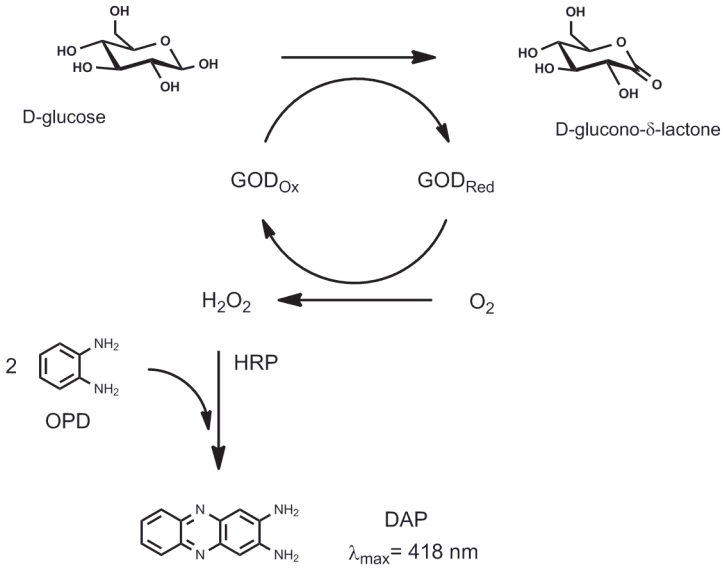


**Figure 2.5.5** Coupled assay for UV/vis spectrophotometric quantification of active GOD. The hydrogen peroxide formed by GOD serves as oxidizing substrate for a subsequent HRP catalyzed transformation of the chromogenic substrate OPD to the chromophore DAP.

antioxidant and food preservative, and synthesis of gluconic acid have been reviewd by Wong *et al.* [95]. A special focus for the application of GOD as immobilized enzyme is in the field of bioelectrode fabrication [95, 96]. In the area of biofuel cells, glucose oxidation is often used as model system, but with the drawback of a low energy content of the substrate compared to other systems [96]. A prominent area with numerous well-estabished applications of GOD bioelectrodes is the fabrication of biosensors, with a focus on devices for glucose quantification especially in medical diagnostics [95].

In contrast to HRP, there is no direct chromogenic assay available for the quantification of the activity of GOD. The formation of hydrogen peroxide as one of the products has been used for the development of coupled assays. Addition of HRP and a suitable reducing substrate allow quantification of the $H_2O_2$ formed during the enzymatic oxidation of D-glucose by the subsequent HRP catalyzed oxidation of the chromogenic substrate (**Figure 2.5.5**). Using an excess of HRP, transformation of the intermediate $H_2O_2$ proceeds quantitatively and the product formation can be directly correlated to the GOD activity. Different chromogenic substrates for HRP have shown compatibility in such assays, among others *o*-dianisidine and OPD [97, 98].

### 2.5.3 Proteinase K

The serine protease proteinase K (proK, EC 3.4.21.64: peptidase K) from *Engyodontium album* (formerly *Tritirachium album*) is a subtilisin homolog (peptidase family S8) capable of hydrolyzing native keratin, and exhibits a preferred cleavage after

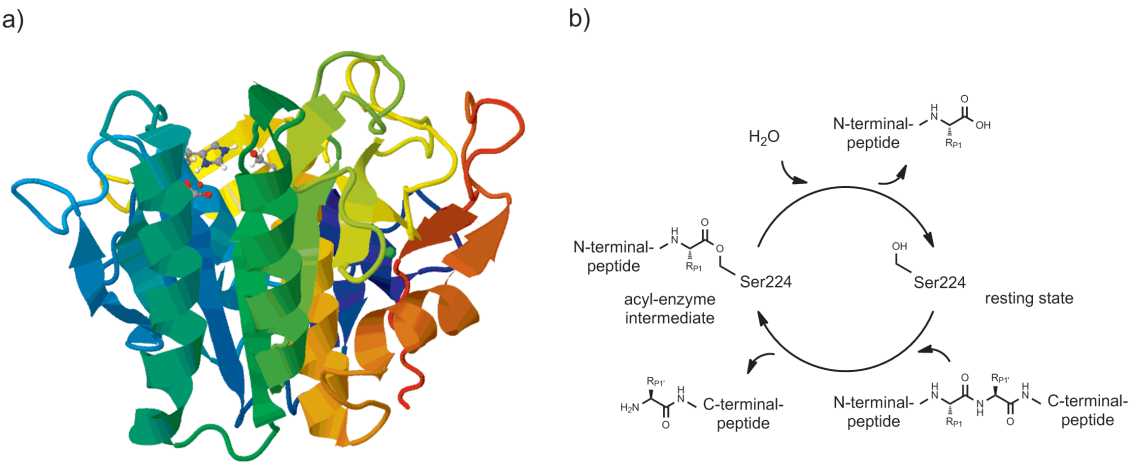


**Figure 2.5.6 a)** Cartoon representation of the crystal structure of proK (PDB-entry: 1IC6). The active site residues Ser224, His69 and Asp39 are depicted in the ball-stick-model. **b)** The catalytic cycle of proK follows the classical reaction scheme of serine proteases. The peptidic substrate is attacked by the nucleophilic active site serine, resulting in an acyl-enzyme intermediate and release of the C-terminal peptide. In a second step, the acyl-enzyme adduct is hydrolyzed, releasing the N-terminal peptide and reconstituting the free enzyme.

hydrophobic aromatic or aliphatic amino acids. The basic enzyme with a pI of 8.9 has a primary sequence of 278 amino acids and contains two calcium ions in the tertiary structure, with a molar mass of 28930 Da as determined from the amino acid sequence [99, 100]. The active site is formed by the classical catalytic triad of serine proteases, formed by Ser224, His69 and Asp39 [101]. Apart from the natural activity catalyzing the hydrolysis of amide bonds in peptides (**Figure 2.5.6**), a hydrolytic activity for ester and thioester substrates is known for proK [102, 103]. Further on, the catalysis of transesterifications in room temperature ionic liquids has been reported as well as the proK catalyzed synthesis of peptides in organic solvents with low water concentrations [104].

A major application of proK has been established in the area of molecular biology. The ability of proK to inactivate nucleases was detected already in the 1970's [105-107], and resulted in the use of proK in many standard DNA and RNA extraction protocols. Addition of proK to crude lysates results in an efficient digestion of RNases and DNases and therefore allows isolation of non-digested DNA or RNA in good yields.

Another application of proK is in the area of prion protein detection. Missfolding and aggregation of prion proteins are involved in the development and transmission of transmissible spongiform encephalopathies, including bovine spongiform encephalopathy (mad cow disease) and the Creutzfeldt-Jakob disease in human. The detection of the abnormal form of prion protein involved in these processes is based on its resistance against proK digestion, while the normally produced native protein is degraded during incubation with proK [108, 109]. This possibility of degrading the native protein is of

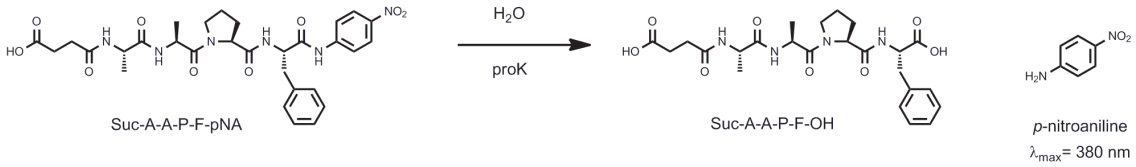


**Figure 2.5.7** Enzymatic hydrolysis of the chromogenic proK substrate Suc-AAPF-pNA yields the chromophore *p*-nitroaniline by selective hydrolysis of the activated amide bond of the *p*-nitroanilide. The peptide sequence is chosen according to the specificity of proK. The N-terminal succinyl protecting group increases the water solubility of the peptide.

special importance as the two forms contain the same primary structure and therefore cannot be distinguished with methods requiring denaturing of the analyte protein.

Studies of the specificity for a preferred cleavage sequence of proK for peptide hydrolysis have been carried out with synthetic peptide substrates. Common chromogenic substrates for such studies of proK are peptidyl *para*-nitroanilides [110]. The activated amide present in the *p*-nitroanilide allows specific hydrolysis of this peptide bond under release of the chromophore *p*-nitroaniline, which can be quantified by UV/vis spectrophotometry (**Figure 2.5.7**). Using such substrates with varying peptide sequences N-terminal of the *p*-nitroanilide cleavage site, the sequence specificity and dependence of the catalytic efficiency from the substrate peptide length have been investigated [111, 112]. These reports indicate excellet hydrolytic activity of proK for the tetrapeptide succinyl-L-alanyl-L-alanyl-L-prolyl-L-phenylalanyl-*p*-nitroanilide (Suc-AAPF-pNA, **Figure 2.5.7**), commercially available also as α-chymotrypsin substrate, enabling characterization of proK even at low concentrations.

# 3 RESULTS AND DISCUSSION

## 3.1 Immobilization of HRP and GOD with *de*-PG2-BAH-GOD, *de*-PG2-BAH-HRP, and *de*-PG2-BAH-(GOD,HRP) on $SiO_2$ surfaces

### 3.1.1 Introduction

The synthesis of the denpol-enzyme conjugates was performed in a procedure described by Grotzky *et al*. for the preparation of fluorescently labelled denpol-enzyme conjugates [56, 64]. The bis-aryl hydrazone (BAH) linking chemistry allowed the *in situ* monitoring of the conjugation reaction due to its characteristic UV/vis absorption band at 354 nm [72, 113]. In order to be able to exploit the use of this linking chemistry, both the polymer and the enzymes needed to be modified with a suitable linker moiety, *i.e*. a 2-hydrazinopyridine and a benzaldehyde. While the 2-hydrazinopyridine linker moiety does not interfere with the functional groups present in proteins nor in the denpol, the benzaldehyde moiety can react with the primary amino groups of the denpol and of lysine side chains present on the protein surface, forming a Schiff base. However, the reversibility of this interfering reaction still allowed the use of the BAH linker chemistry, but had to be considered for the choice of which linker was to be used on the denpol and the enzyme, respectively. As the conjugates were designed to carry multiple copies of the enzyme on each denpol chain, the polymer had to be modified with a high number of linker moieties per chain. This excluded the benzaldehyde linker moiety to be used on the denpol, as its reactivity towards the peripheral amino groups, even though reversible, might lead to a crosslinking of the polymer chains, resulting in the formation of network structures. On the side of the enzyme it had to be assured that each enzyme molecule carried not more than one linker, as each enzyme with two or more linkers would act as a crosslinking species during the conjugation reaction.

### 3.1.2 Preparation of *de*-PG2-BAH-HRP

For the synthesis of the *de*-PG2-BAH-HRP conjugate, a *de*-$PG2_{1400}$, *i.e.* a deprotected second generation denpol with a number average of 1400 repeating units per chain, was used. The general procedure for the synthesis of *de*-PG2-BAH-HRP was carried out as described by Grotzky *et al.* [56, 64].To install the HyNic linker moieties on the denpol, some of the peripheral amino groups were reacted with S-HyNic (**Figure 3.1.1**). As the reaction was carried out in aqueous solution and the positively charged ammonium groups are essential for the water solubility of the denpol, the reaction was carried out at pH 7.6; well below the p$K_a$ of a regular primary ammonium group, but in a range where a polyamine species contains a considerable amount of non-protonated amino groups [114].

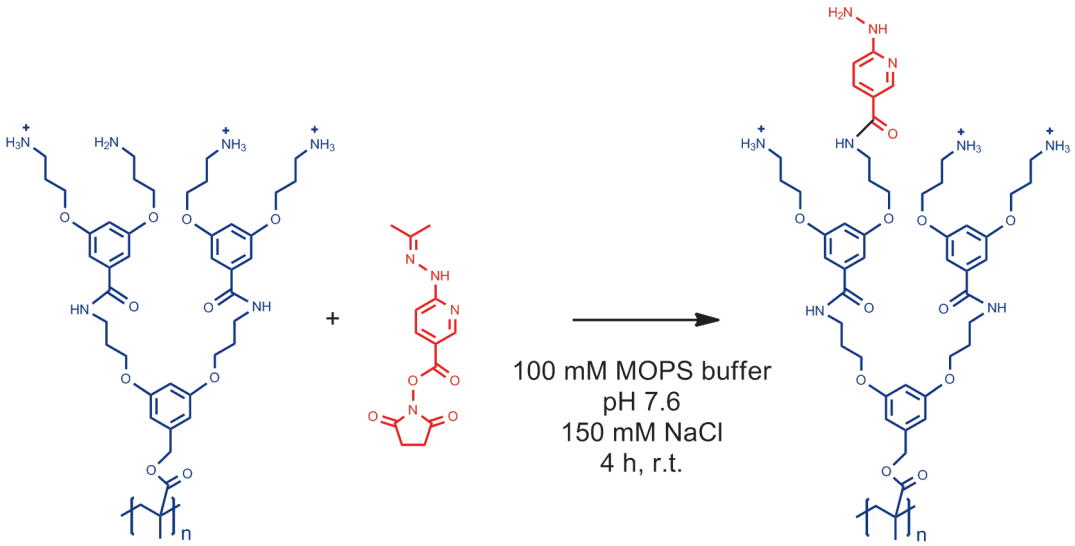


**Figure 3.1.1** Modification of *de*-PG2 (blue) with the HyNic linker moiety (red). Upon reaction of partially deprotonated *de*-PG2 (1 eq. r.u.) with 0.4 eq. S-HyNic, the linkers were statistically distributed on the polymer with an average of 1 linker every 6 r.u. The acetone protecting group of the hydrazinopyridine was removed during the workup at pH 4.7.

These non-protonated amines readily reacted with the *N*-hydroxysuccinimide ester yielding the modified denpol *de*-PG2-HyNic.

Purification of the modified *de*-PG2-HyNic from hydrolyzed HyNic and the reaction byproduct *N*-hydroxysuccinimide was crucial to avoid cross reaction of free HyNic with the 4FB modified enzymes during the conjugation reaction. Removal of the low molar mass linker molecules was obtained by repetitive ultrafiltration at a nominal molecular weight cutoff of 100 kDa, allowing simultaneous buffer exchange to obtain a *de*-PG2-HyNic solution in the conjugation buffer at pH 4.7. This buffer exchange leads as well to a hydrolysis of the acetone protecting group present on the HyNic linker, leaving the free HyNic on the denpol (see **Figure 3.1.1**). To determine the extent of modification of the denpol, the repeating unit concentration of the denpol as well as the concentration of the HyNic moiety in the *de*-PG2-HyNic solution were determined independently.

Even though the polymer has a quantifiable UV/vis absorption band at 285 nm, the

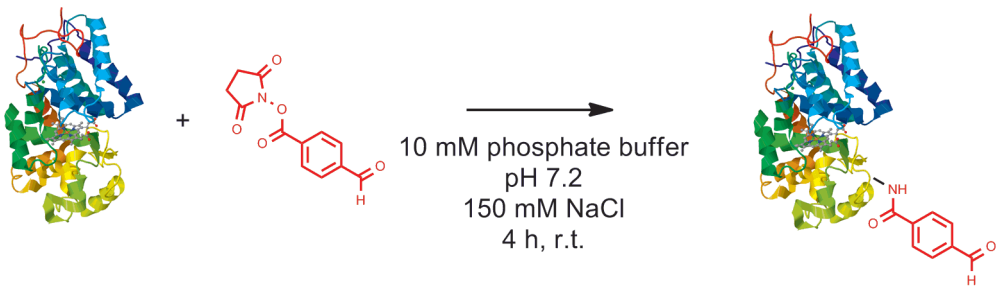


**Figure 3.1.2** Modification of HRP with the 4 FB linker moiety. Reaction of 1 eq. HRP with 6 eq. of S-4FB resulted in an average of 0.85 linkers/HRP. This ensured a minimal presence of HRP molecules modified with more than one linker moiety per enzyme molecule in the sample.

interference with the HyNic absorption at this wavelength hindered direct quantification of the polymer concentration by UV/vis spectrophotometry. Therefore, an indirect quantification method was applied, exploiting the complexation of the anionic dye trypan blue by polycations and subsequent quantitative precipitation [115]. Using a calibration curve recorded with known concentrations of *de*-PG2 (see **Experimental Part: Figure 5.3.1**), the repeating unit concentration in a sample of *de*-PG2-HyNic was determined under the assumption that a modification of a low percentage of the amino groups with the HyNic moiety does not influence the complexation and precipitation behavior during the trypan blue assay. The quantification of the HyNic concentration in the *de*-PG2-HyNic solution was performed by derivatization of the HyNic moiety with 4-nitrobenzaldhyde, yielding a BAH with a characteristic UV/vis signature at 390 nm ($\varepsilon_{390nm}$ = 24000 $M^{-1}$ $cm^{-1}$) [113].

Performing the *de*-PG2 modification with 0.1 equivalents of S-HyNic per amino group, a modification of about 4 % of the amines of the denpol was obtained. The *de*-PG2-HyNic polymer consequently contains 16 HyNic linkers per 100 r.u., *i.e.* about 1 HyNic every 6 r.u. This ensures the capability of a high enzyme coverage on the denpol, but at the same time maintaining the water solubility and adsorption properties mediated by the denpol's amino groups.

The preparation of the 4FB modified HRP was carried out as described by Grotzky *et al.* [56, 64]. O'Brien *et al.* have shown that the modification of HRP with *N*-succinimidyl esters occurs preferentially at the lysine residue at position 232, distant from the active site [78]. Performing the modification of HRP at pH 7.2 with 6 equivalents of S-4FB for 4 hours resulted in a modification ratio of about 0.85 linker/HRP (**Figure 3.1.2**). As mentioned above, a linker/HRP ratio of less than 1 is an important requirement to prevent polymer crosslinking during the subsequent conjugation reaction. The excess of hydrolyzed 4FB linker was removed by repetitive ultrafiltration to avoid quenching of the HyNic groups on the denpol by free 4FB linker molecules. At the same time, the ultrafiltration step was used for a buffer exchange to the conjugation buffer at pH 4.7. The modification ratio was determined exploiting the UV/vis absorption of the heme group of HRP at 403 nm ($\varepsilon_{403nm}$ = 102000 $M^{-1}$ $cm^{-1}$ [76]) for the determination of the HRP concentration, and by derivatization of the 4FB linker moiety with 2-hydrazinopyridine, yielding a BAH moiety quantifiable by UV/vis spectrophotometry ($\varepsilon_{350nm}$ = 24500 $M^{-1}$ $cm^{-1}$) [113]. Separation of modified HRP-4FB from non-modified HRP was not attempted and might be hardly feasible, due to the minimal differences between these two species. As there was no non-specific interaction of HRP with *de*-PG2-HyNic observed, native HRP

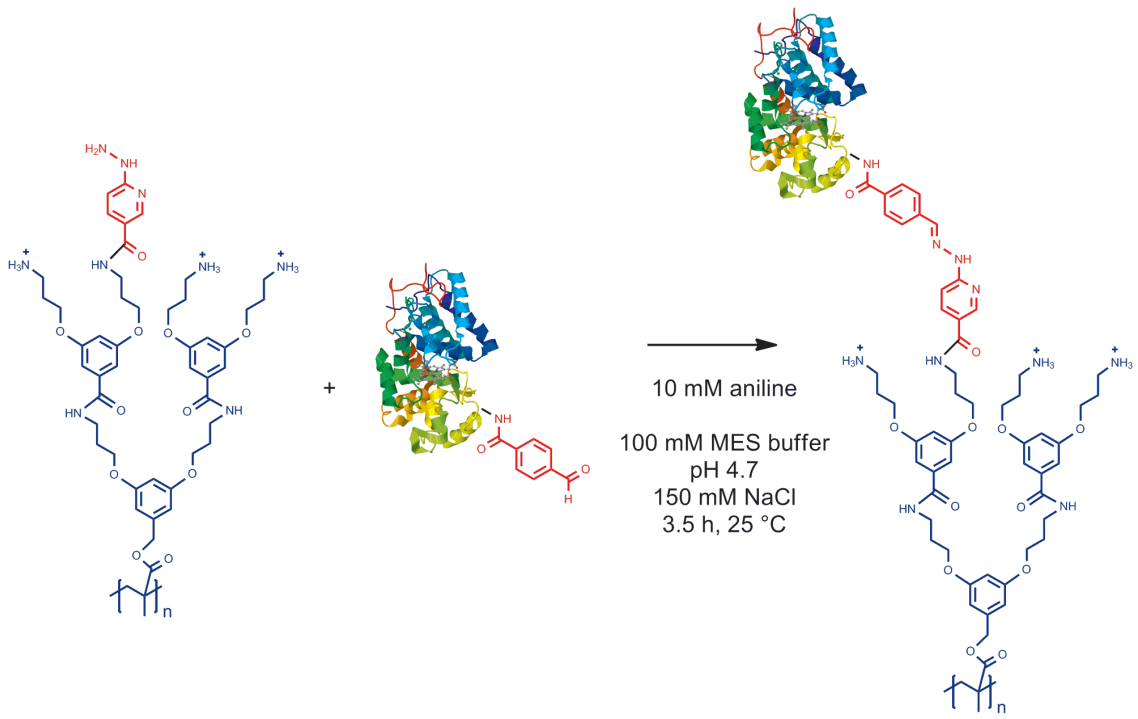


**Figure 3.1.3** Conjugation of *de*-PG2-HyNic with HRP-4FB yielding *de*-PG2-BAH-HRP. The formation of the BAH bond (red) by reaction of the HyNic moiety on the *de*-PG2 and the 4FB moiety on the HRP could be monitored due to the characteristic UV/vis signal at 354 nm. Aniline was added as nucleophilic catalyst for the BAH formation [73].

could be removed during workup of the conjugation reaction, removing native HRP and remaining free HRP-4FB in a single step, as demonstrated earlier [65].

For the conjugation of HRP-4FB to *de*-PG2-HyNic, yielding *de*-PG2-BAH-HRP (see **Figure 3.1.3**), a ratio of 1.5 equivalents HyNic / 1 equivalent 4FB was chosen. Using *de*-PG2-HyNic in a slight excess improves the conversion of HRP-4FB, thus maximizing the yield of the conjugation reaction, while the high modification ratio of 16 HyNic linkers per 100 r.u. still allowed good enzyme coverage on the denpol. The conjugation reaction was carried out at pH 4.7 and with 10 mM aniline as a nucleophilic catalyst for the hydrazone formation, as described by Dirksen *et al.* [73]. Due to the characteristic UV/vis absorption of the BAH moiety, the conjugation reaction could be monitored *in situ* by UV/vis spectrophotometry. The reaction was carried out directly in 1 mm quartz cuvettes and spectra recorded every 5 minutes (**Figure 3.1.4a**). Even though the Soret band of HRP at 403 nm interferes with the BAH absorption band at 354 nm, the evolution of a shoulder in the spectrum of the conjugation reaction mixture can be observed, and evaluating the data as difference spectra using the initial spectrum as reference, the appearance of the BAH absorption band can be extracted and the corresponding reaction progress analyzed and quantified (**Figure 3.1.4b**).

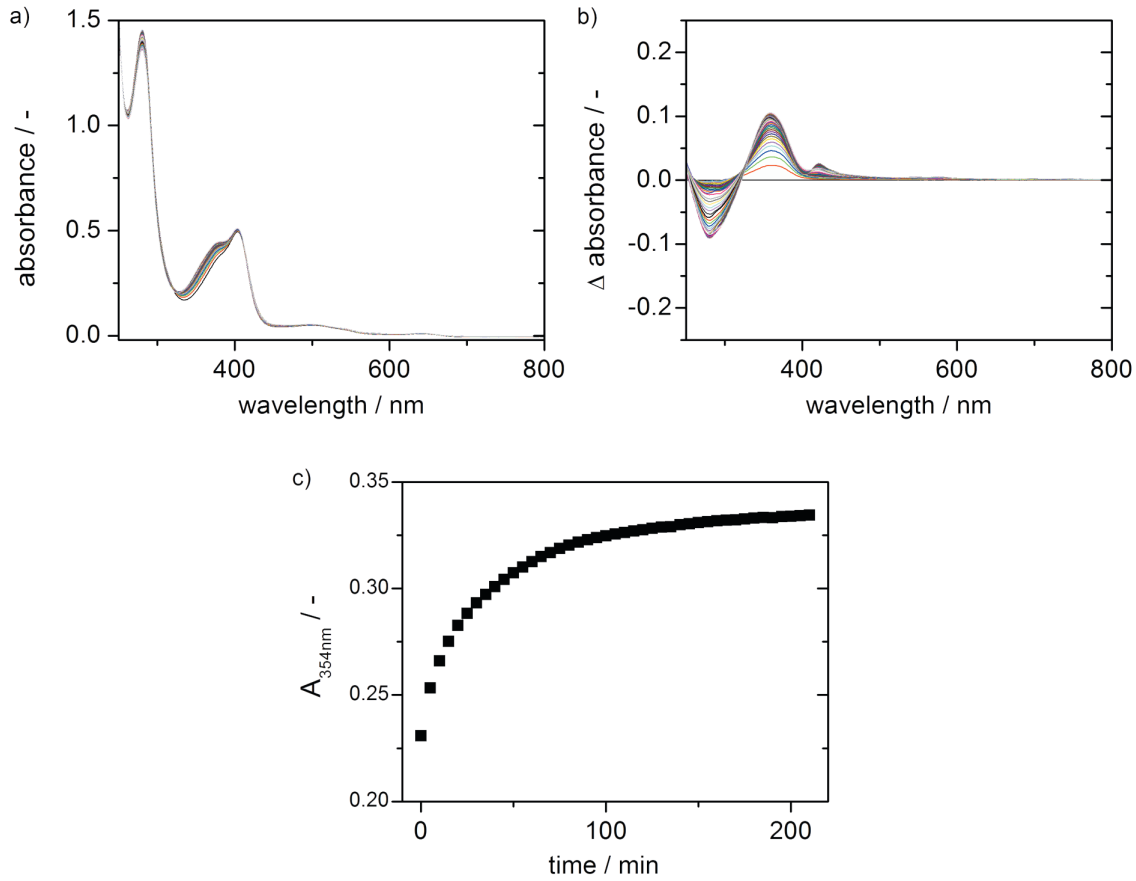


**Figure 3.1.4** *In situ* UV/vis spectrophotometric analysis of the conjugation of *de*-PG2-HyNic with HRP-4FB at pH 4.7. **a)** Spectra of the conjugation reaction solution recorded at intervals of 5 min. The increasing absorbance at 354 nm due to the formation of the BAH bond is visible as an emerging shoulder from the absorption of the Soret band of HRP at 403 nm. **b)** Difference spectra obtained by subtraction of the initial spectrum (t = 0 min) indicate the increasing peak of the BAH bond at 354 nm and the reduced absorption at about 280 nm due to consumption of the free linker moieties. **c)** Evaluation of the evolution of the absorbance at 354 nm allowed to determine the conversion of the conjugation reaction. No further significant changes were observed after about 3.5 h of reaction.

The conjugation reaction was run for about 3.5 hours, after which time no further increase of absorbance at λ =354 nm was observed (**Figure 3.1.4c**). The increase in absorption at 354 nm of 0.104 absorption units corresponded to a BAH concentration of 36 µM in the reaction mixture. The 75 µM HyNic present in the reaction mixture corresponded to a r.u. concentration of 470 µM with the given linker/r.u. ratio of 0.16. The formation of 36 µM BAH bonds, and therefore the attachment of the same amount of HRP to the denpol chains, resulted in an average attachment of 108 HRP molecules to a denpol chain of a length of 1400 r.u. The obtained denpol-enzyme conjugate can therefore be abbreviated as *de*-PG2$_{1400}$-BAH-HRP$_{108}$. Removal of the remaining free HRP and non-conjugated HRP-4FB as well as the aniline present in the reaction mixture was obtained by repetitive ultrafiltration, yielding the purified *de*-PG2-BAH-HRP ( = *de*-PG2$_{1400}$-BAH-HRP$_{108}$) in aqueous solution.

Knowledge of the molecular weight of the non-modified denpol and the composition of the conjugate allowed an estimation of the molecular weight of the *de*-$PG2_{1400}$-$BAH\text{-}HRP_{108}$ conjugate. With a molecular weight of 1.2 MDa for a *de*-$PG2_{1400}$ chain, and the additional 108 times the 44 kDa for each HRP molecule attached to the denpol chain, an overall molecular weight of about 5.9 MDa could be calculated for this conjugate. These numbers indicate that in terms of molecular weight only a minor part of the conjugate was contributed by the denpol, while most of it was constituted by the HRP enzymes.

### 3.1.3 Preparation of *de*-PG2-BAH-GOD

In order to obtain a denpol-enzyme conjugate of the enzyme GOD, a modification of GOD to obtain GOD-4FB (**Figure 3.1.5**) was performed similar to the modification of HRP described above. As GOD reacted much more efficiently with S-4FB, 1.2 equivalents of this linker reagent per 1 equivalent of GOD homodimer were sufficient for a modification ratio of about 0.65 linkers per GOD. After removal of hydrolyzed 4FB, the linker/GOD ratio was determined by independent quantification of the GOD and 4FB concentration in the GOD-4FB solution. The GOD concentration could be determined directly via the characteristic UV/vis absorption band of the flavin adenine dinucleotide (FAD) at 450 nm ($\varepsilon_{450nm}$ = 28200 $M^{-1}$ $cm^{-1}$ for a GOD homodimer [91]). The 4FB concentration was determined by derivatization of the 4FB group with 2-hydrazinopyridine, yielding a BAH moiety with a characteristic UV/vis absorption at 350 nm ($\varepsilon_{350nm}$ = 24500 $M^{-1}$ $cm^{-1}$) [113].

For the preparation of *de*-PG2-BAH-GOD, the same *de*-PG2-HyNic as for the preparation of *de*-PG2-BAH-HRP was used (**Figure 3.1.6**). The reaction conditions elaborated for the synthesis of the *de*-PG2-BAH-HRP conjugate had to be modified in order to be applicable for the conjugation of GOD to the denpol. Mixing of a *de*-PG2-HyNic solution and a GOD-4FB solution in the standard conjugation buffer (100 mM MES, 150 mM NaCl, pH 4.7) resulted in the immediate formation of insoluble aggregates. This

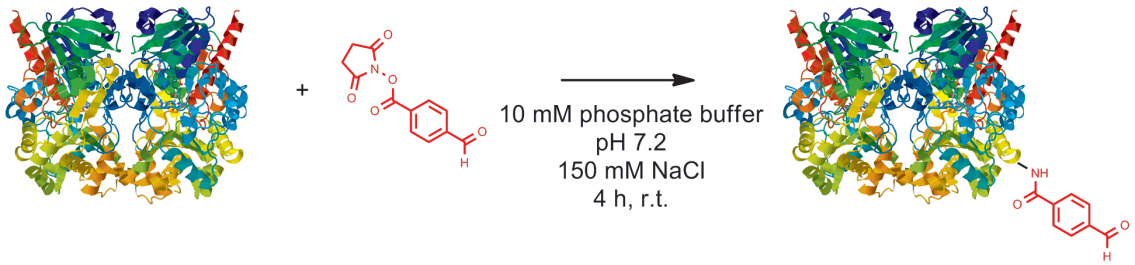


**Figure 3.1.5** Modification of GOD with the 4FB linker moiety. Reaction of 1 eq. GOD with 1.2 eq. S-4FB resulted in an average of 0.65 linker moieties per GOD homodimer. A linker/GOD ratio <1 reduced the presence of GOD dimers containing more than one linker moiety, preventing crosslinking during the subsequent conjugation reaction.

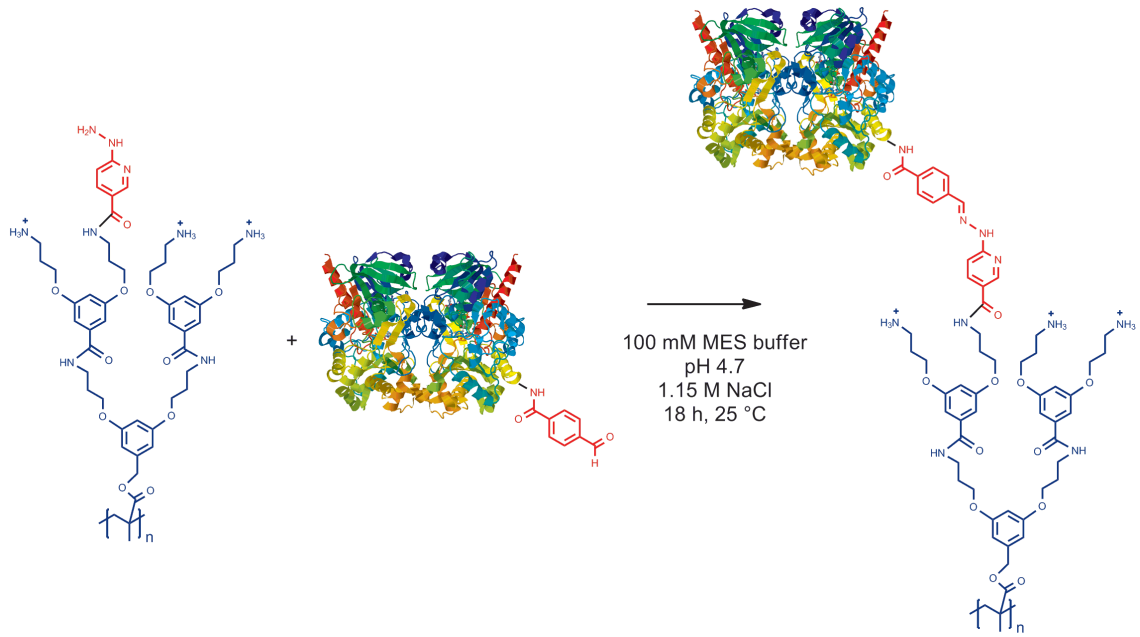


**Figure 3.1.6** Conjugation of *de*-PG2-HyNic and GOD-4FB yielding *de*-PG2-BAH-GOD. The formation of the BAH bond (red) upon reaction of the HyNic and the 4FB moieties could be monitored by UV/vis spectrophotometry due to its characteristic absorption band at 354 nm.

observation was attributed to the fact that GOD at pH 4.7 has a negative overall charge, as the isoelectric point of GOD is at 4.2 [89]. To overcome aggregation of the negatively charged GOD and the positively charged denpol, a modified conjugation buffer with high ionic strength was used (100 mM MES, 1.15 M NaCl, pH 4.7), which allowed mixing of all components in a homogeneous solution. As in the case of the conjugation of HRP-4FB to *de*-PG2-HyNic, the conjugation reaction was monitored *in situ* by UV/vis spectrophotometry (**Figure 3.1.7a**). The evolution of the BAH absorption band at 354 nm was observed after correction for the interfering absorption band of the prosthetic FAD group present in GOD by subtraction of the initial spectrum of the reaction mixture (**Figure 3.1.7b**). The UV/vis spectra recorded during the conjugation reaction also indicated an additional contribution from scattered light during progress of the reaction. This was clearly seen by the increasing absorbance at wavelengths above about 550 nm, where no absorption peaks are present (**Figure 3.1.7a&b**). The contribution of the scattered light in the range of the BAH band can only be roughly estimated and therefore a degree of uncertainty in the determination of the amount of bound GOD on the denpol arises. Even though the attenuance at 354 nm can be used to calculate an apparent BAH concentration in the reaction mixture, it has to be taken into account that this value can only serve as an upper limit of the actual conjugation efficiency.

Despite the limits mentioned above, the UV/vis signature of the BAH bond allows to monitor the progress of the conjugation reaction during the synthesis of *de*-PG2-BAH-GOD, indicating no further changes after 18 hours (**Figure 3.1.7c**). Calculating an apparent BAH

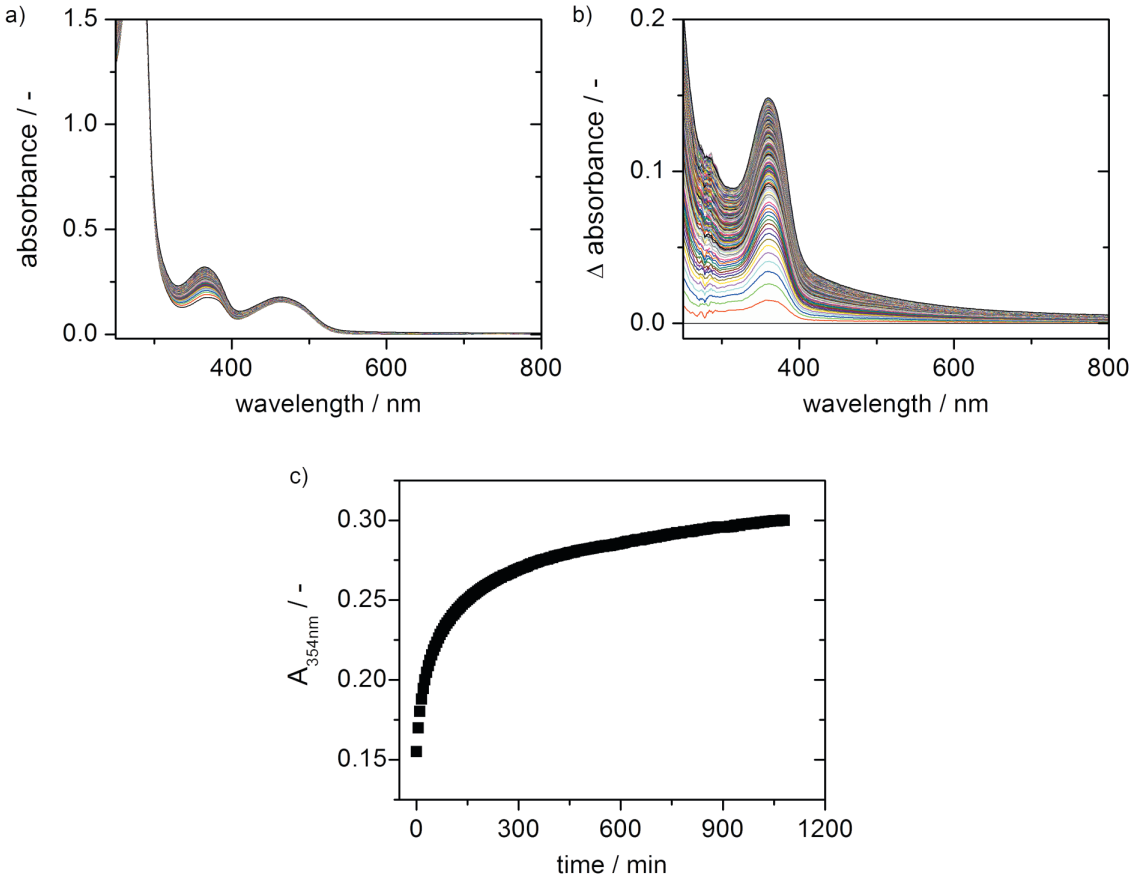


**Figure 3.1.7** *In situ* UV/vis spectrophotometric analysis of the conjugation of *de*-PG2-HyNic and GOD-4FB at pH 4.7. **a)** Spectra of the conjugation reaction solution were measured in intervals of 5 min. The emerging absorption band of the BAH bond at 354 nm is overlapping with the absorption of the prosthetic FAD group present in the GOD molecule. **b)** Difference spectra obtained by subtraction of the initial spectrum (t = 0 min) identified the increasing absorption peak at 354 nm. Increasing scattering of light, probably due to the size of the conjugates formed, resulted in an increasing turbidity of the sample as seen by the increase in absorption at wavelengths above about 400 nm in the difference spectra. This phenomenon hindered as well the observation of the reduction in absorbance at around 280 nm due to the consumption of the free linker moieties as it was possible in the case of the formation of the *de*-PG2-BAH-HRP conjugate. **c)** Evaluation of the absorbance reading at 354 nm allowed monitoring the reaction progress. The contribution of scattered light to the absorbance reading, resulting in a value for attenuation instead of absorption, limited the quantitative evaluation of the conjugation reaction to an estimation of an upper limit of conjugated GOD instead of a precise quantification as in the case of HRP.

concentration from the increase in attenuance at 354 nm of 0.145, the reaction mixture contained 50 µM bound GOD. With a *de*-PG2-HyNic concentration of 470 µM r.u. in the reaction mixture, this resulted in a value of about 150 GOD on a 1400 r.u. denpol chain. As mentioned above, this value represents an upper limit of GOD coverage on the denpol.

Removal of remaining free GOD-4FB and GOD from the *de*-PG2-BAH-GOD conjugate showed to be not possible with ultrafiltration or aqueous size exclusion chromatography. Permeation of GOD through ultrafiltration membranes with a nominal cutoff of 300 kDa from a solution containing *de*-PG2-BAH-GOD was inefficient, and aqueous gel permeation chromatography resulted in loss of the conjugate on the column. Therefore, purification of

the conjugate was achieved by precipitation with ammonium sulfate, exploiting the fact that the conjugate precipitated at lower salt concentrations than the free GOD. After four times precipitation of *de*-PG2-BAH-GOD from a 60 % saturated ammonium sulfate solution, the supernatant did not contain any residual GOD as determined by UV/vis spectrophotometric analysis. Quantification of the total content of GOD in the collected supernatants indicated as well that the amount of GOD bound to the denpol was considerably lower than the upper limit determined by UV/vis spectrophotometry during the conjugation reaction. While the increase in attenuance at 354 nm during the conjugation reaction corresponded to the binding of 150 GOD molecules on a 1400 r.u. chain, the recovery of non-bound GOD (free GOD-4FB and non-modified GOD) in the supernatant during precipitation of the *de*-PG2-BAH-GOD conjugate indicated the binding of about 50 molecules GOD per 1400 r.u. denpol chain. Therefore, the obtained conjugate was designated as *de*-$PG2_{1400}$-BAH-$GOD_{\approx 50}$. Calculating the molecular weight of such a conjugate according to this ratio of GOD per r.u., a *de*-$PG2_{1400}$ denpol chain of 1.2 MDa would have attached 50 times 153 kDa, resulting in an average molecular weight of 8.8 MDa. As in the case of *de*-PG2-BAH-HRP, the enzyme has a major contribution to the overall molecular mass of the *de*-PG2-BAH-GOD conjugate.

### 3.1.4 Preparation of *de*-PG2-BAH-(GOD,HRP)

Apart from the two conjugates *de*-PG2-BAH-HRP and *de*-PG2-BAH-GOD, a third denpol-enzyme conjugate containing both types of enzymes on the same polymer molecule was synthesized. In contrast to a simple mixture of the individual HRP and GOD conjugates described above, such a conjugate allows the co-immobilization of two different types of enzymes in a defined ratio, without a bias of the enzyme ratio due to different adsorption behaviors of the two conjugates. Considering the size of the two enzymes, the larger, dimeric GOD was chosen to be attached to the denpol in a first step, leaving gaps in between the individual enzymes large enough for a smaller enzyme to still reach the polymer backbone. After this first conjugation step, resulting in a *de*-PG2-BAH-GOD conjugate with remaining free HyNic linker moieties present on the polymer backbone, the second, smaller enzyme, *i.e.* HRP, was attached using the same linker chemistry (**Figure 3.1.8**).

The denpol and the enzymes modified with the corresponding linker moieties, *i.e.* *de*-PG2-HyNic, GOD-4FB and HRP-4FB, used for the synthesis of the *de*-PG2-BAH-(GOD,HRP) conjugate were as prepared for the synthesis of the conjugates containing only one type of enzyme. The conjugation conditions were modified in a way to ensure the

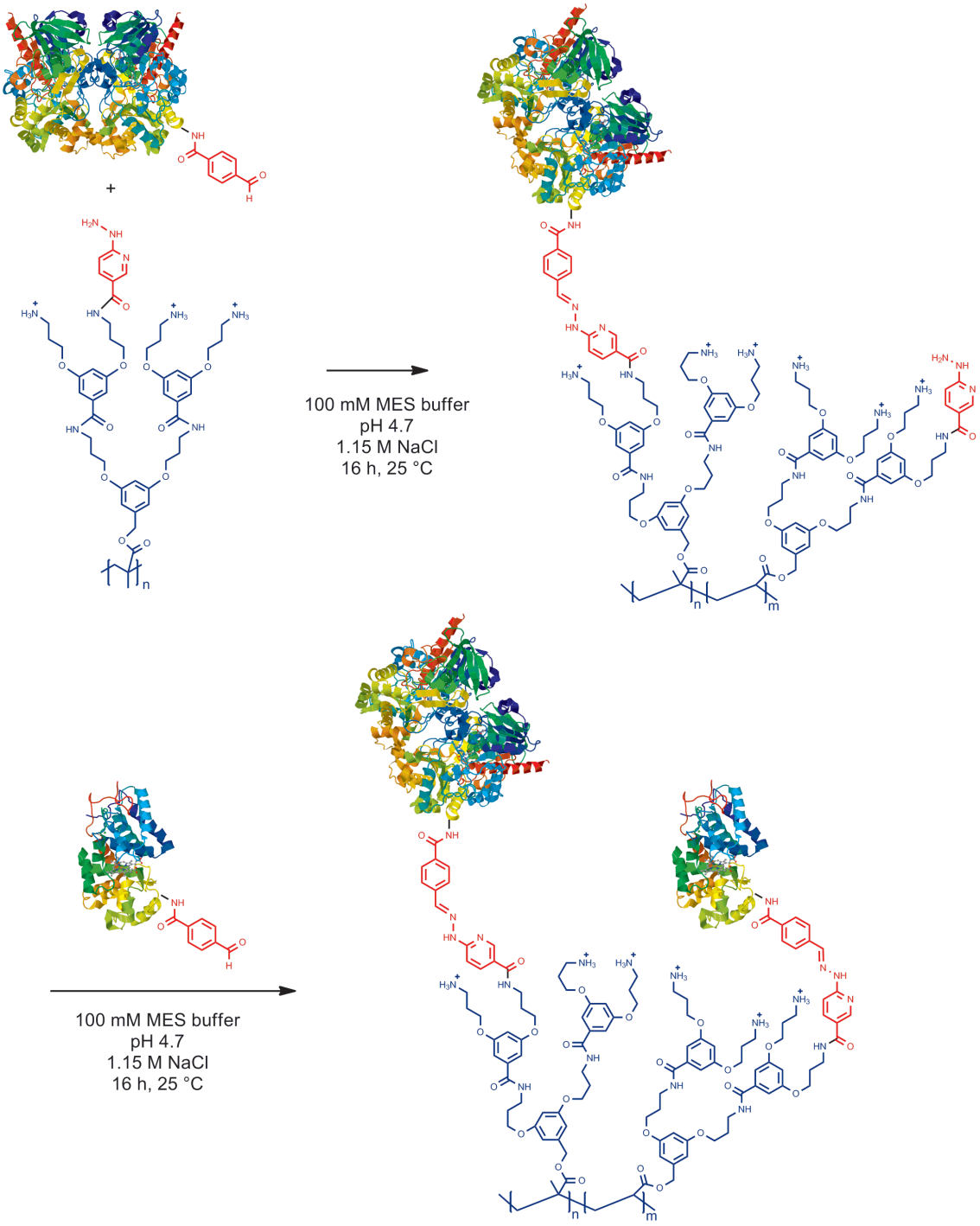


**Figure 3.1.8** Stepwise conjugation of *de*-PG2-HyNic with GOD-4FB and HRP-4FB in a stepwise reaction. After the reaction of *de*-PG2-HyNic with GOD-4FB remaining free linkers are still available for further conjugation of HRP after addition of HRP-4FB to the reaction mixture. The reaction progress of the BAH bond formation could be followed by monitoring the characteristic UV/vis absorption at 354 nm.

availability of free HyNic linkers for the second conjugation step. Therefore, a HyNic/4FB ratio of 2/1 was chosen for the first conjugation step. After mixing of *de*-PG2-HyNic and GOD-4FB, the reaction progress was observed by UV/vis spectrophotometry until no further change in absorbance was detected (**Figure 3.1.9a**). As before, the UV/vis data was evaluated by subtraction of the initial spectrum to monitor the evolution of the

absorption band of the BAH bond at 354 nm (**Figure 3.1.9b**). After about 16 h, the increase in attenuance at 354 nm was negligible, indicating no further reaction between *de*-PG2-HyNic and GOD-4FB (**Figure 3.1.9e**). At this point, the second enzyme, *i.e*. HRP-4FB, was added to the reaction mixture. After mixing of the reaction solution, the conjugation reaction was followed again by *in situ* UV/vis spectrophotometry (**Figure 3.1.9c**), and an increase of attenuance at 354nm was observed (**Figure 3.1.9d&e**), indicating reaction of the remaining HyNic moieties present on the intermediate *de*-PG2-BAH-GOD with HRP-4FB, yielding the two enzyme conjugate *de*-PG2-BAH-(GOD,HRP).

During the conjugation of GOD-4FB to *de*-PG2-HyNic, a similar interference of scattered light was observed as during the preparation of *de*-PG2-BAH-GOD described above. The resulting attenuance measured by UV/vis spectrophotometry accordingly overestimates the concentration of BAH bonds formed, if directly evaluated as an absorbance value. Therefore, the obtained value for GOD-4FB attached to *de*-PG2-HyNic was only considered as an upper limit of the real amount of enzymes linked to the denpol. Considering the increase in attenuance of 0.095 at 354 nm (see **Figure 3.1.9e**), the upper limit of GOD conjugated to the denpol was 33 µM in a reaction mixture containing 625 µM *de*-PG2 r.u., corresponding to about 75 GOD molecules bound to an average denpol of 1400 r.u. During the second conjugation step, attaching HRP-4FB to the *de*-PG2-BAH-GOD intermediate, the increase in attenuance at 354 nm was measured as 0.075 absorbance units (see **Figure 3.1.9e**), corresponding to a BAH concentration of 26 µM. As the reaction of GOD-4FB was allowed to proceed until no further enzyme was attached to the denpol, the subsequent formation of BAH bonds after addition of the smaller enzyme HRP was designated as the conjugation of HRP-4FB to the denpol chain at positions which were not accessible for the larger GOD, but still allowed the smaller HRP-4FB to react with remaining free HyNic linkers. Therefore, the concentration of 26 µM BAH formed during the second conjugation step were assigned to the same amount of HRP bound to the denpol. With the denpol concentration of 469 µM r.u. during the second conjugation step, this results in an amount of 78 molecules of HRP per average 1400 r.u. *de*-PG2 chain.

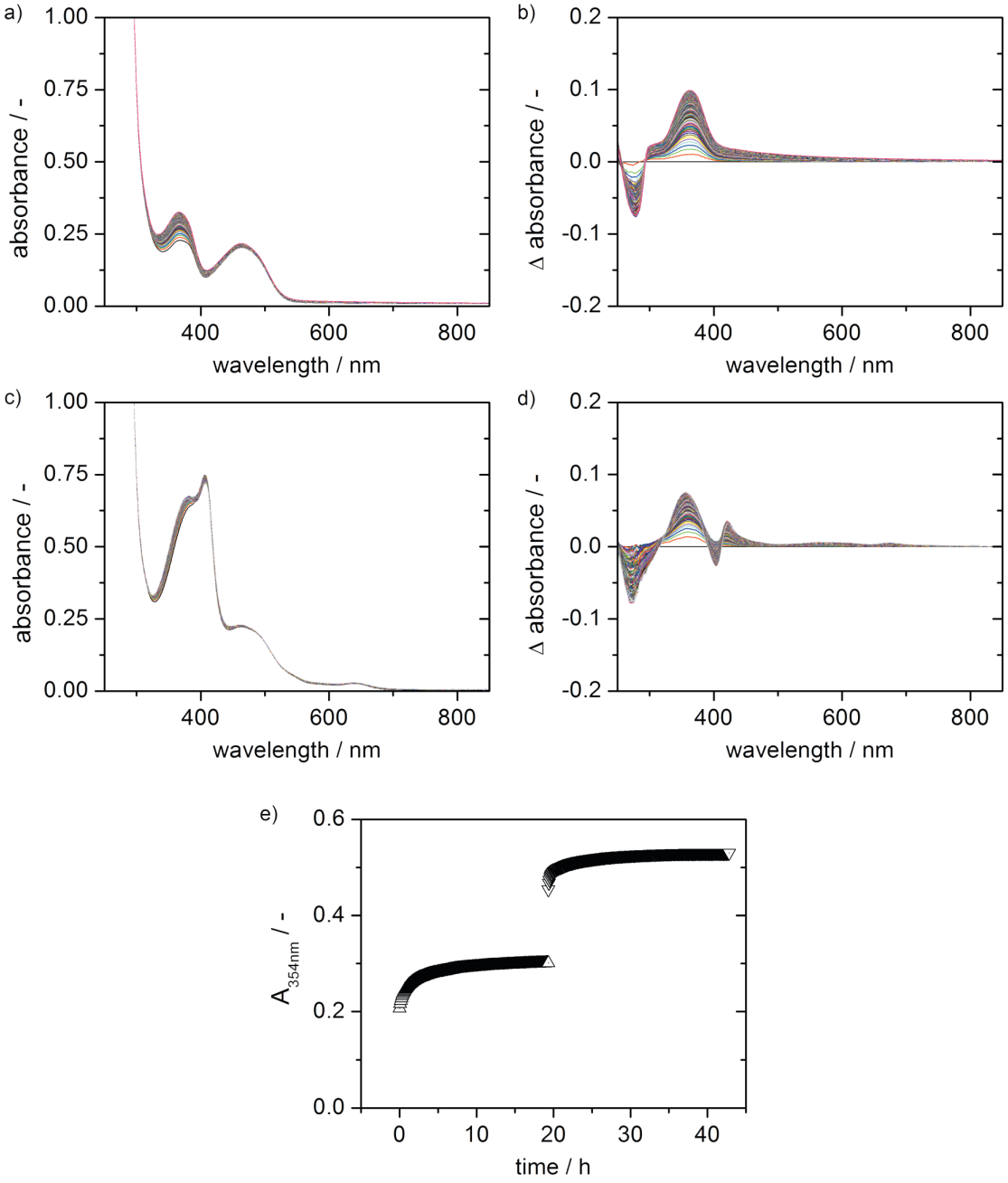


**Figure 3.1.9** *In situ* UV/vis spectrophotometric analysis of the consecutive conjugation reaction of *de*-PG2-HyNic with GOD-4FB and HRP-4FB at pH 4.7. **a)** Spectra of the conjugation of *de*-PG-HyNic with GOD-4FB recorded in intervals of 5 min and **b)** difference spectra obtained by subtraction of the first spectrum (t = 0 min), indicating the increasing absorbance of the BAH moiety at 354 nm. **c)** Spectra recorded in 5 min intervals upon addition of HRP-4FB to the intermediate *de*-PG2-BAH-GOD and **d)** difference spectra obtained by subtraction of the first spectrum measured after the addition of HRP-4FB. **e)** The increasing absorbance at λ = 354 nm upon addition of GOD-4FB (Δ) and HRP-4FB (∇) was correlated to the BAH bond formed and therefore to the amount of enzyme bound.

The purification of *de*-PG2-BAH-(GOD,HRP) was performed by precipitation with ammonium sulfate, as for the conjugate containing only GOD. In contrast to the case of *de*-PG2-BAH-GOD, where the upper limit of GOD attachment to the denpol, as estimated from

the UV/vis spectrophotometric monitoring of the conjugation reaction, was complemented by an estimation of the bound GOD by a UV/vis spectrophotometric determination of free GOD in the supernatant of the precipitation, such an indirect estimation of bound GOD was not possible for *de*-PG2-BAH-(GOD,HRP) due to the interference of the absorption spectra of GOD and HRP, which were both present in the supernatant. Considering the 3 fold overestimation of bound GOD observed during the synthesis of *de*-PG2-BAH-GOD, the real amount of GOD attached to the two enzyme conjugate *de*-PG2-BAH-(GOD,HRP) was estimated to be not as high as the upper limit of 75 molecules of GOD per 1400 r.u. chain, but rather at a value of about 25 GOD molecules per *de*-$PG2_{1400}$. The obtained conjugate was therefore described as *de*-$PG2_{1400}$-BAH-($GOD_{\approx 25}$,$HRP_{\approx 78}$), indicating the average composition of a conjugate of 1400 r.u. *de*-PG2 carrying about 25 GOD and 78 HRP molecules covalently bound to the denpol chain. In terms of molecular weight, this results in a *de*-$PG2_{1400}$ chain of 1.2 MDa with 25 times 153 kDa attached by the linked GOD molecules and 78 times 44 kDa attached through the HRP included in the conjugate, resulting in an overall molecular weight of the conjugate of 8.4 MDa.

### 3.1.5 Characterization of the denpol-enzyme conjugates of GOD and HRP by AFM

In order to characterize the conjugates *de*-PG2-BAH-HRP, *de*-PG2-BAH-GOD and *de*-PG2-BAH-(GOD,HRP), single denpol chains of these conjugates were analyzed by atomic force microscopy (AFM). The denpol-enzyme conjugates were adsorbed from dilute aqueous solution onto freshly cleaved mica, washed with Milli-Q water and dried by air. This allowed analysis of single chains of the conjugates, including a determination of their height along the denpol chain in a dry state. Such longitudinal height profiles can provide information about the coverage of the denpol chain with enzyme, as the thickness of a non-modified denpol chain for *de*-PG2 is significantly smaller than the diameter of either HRP or GOD.

The height of *de*-$PG2_{1400}$ was measured as about 1-1.5 nm (**Figure 3.1.10a**), in good agreement with earlier determinations of the height of this denpol in a dry state on mica [64]. In contrast to this, the longitudinal height profile of *de*-$PG2_{1400}$-BAH-$HRP_{108}$ indicated a height between 2 nm and 4 nm (**Figure 3.1.10b**), without significant parts of the denpol chain with a height of less than 2 nm. The relatively uniform height profile indicates a good coverage of the denpol backbone with enzymes, as larger free segments of the denpol would result in a longitudinal height profile with pronounced areas of a height of around 1.5 nm. Even more pronounced was the increased denpol chain thickness in the case of *de*-

$PG2_{1400}$-BAH-$GOD_{50}$ (**Figure 3.1.10c**). A longitudinal height profile of this conjugate indicated a height between about 6 nm and 15 nm. No significant part of denpol chains without attached enzymes were detected. The increased thickness of *de*-PG2-BAH-GOD compared to *de*-PG2-BAH-HRP is consistent with the bigger size of GOD (6.0 x 5.2 x 7.7 $nm^3$ for the GOD dimer [90])compared to HRP (about 6.5 x 4.9 x 4.2 $nm^3$ as determined from the crystal structure [116]).

Considering the number of enzyme molecules bound to an average denpol chain of 1400 r.u. as determined from the UV/vis spectrophotometric measurements of the conjugation reactions for *de*-PG2-BAH-HRP and *de*-PG2-BAH-GOD, an estimation of the length of a virtual line formed by lining up these molecules could be calculated. Comparison of the length of this line with the length of a *de*-$PG2_{1400}$ chain gave a measure for the density of the enzyme attached along the denpol chain. The spacing of the denpol is defined by the two carbon atoms per repeating unit of the poly methacrylate backbone, resulting in a length of about 0.25 nm/r.u. In the case of *de*-$PG2_{1400}$-BAH-$HRP_{108}$, the 108 HRP molecules line up to a length of 454 nm (108 x 4.2 nm, considering the smallest dimension of HRP), compared with a denpol length of 350 nm. For *de*-$PG2_{1400}$-BAH-$GOD_{50}$, the GOD dimers line up to a length of 260 nm (50 x 5.2 nm, considering the smallest dimension of the dimer). Considering that the crystal structures were obtained from a non-glycosylated recombinant protein in the case of HRP [116] and from a partially deglycosylated form of GOD [90], and the fact that in a denpol-enzyme conjugate not all enzymes were attached with their smallest dimension along the denpol chain, these values corroborated the observation that the denpol chain was covered densely with enzymes. The fact that the length of 108 lined up HRP molecules exceeded the length of the *de*-$PG2_{1400}$ chain indicated that the HRP molecules were attached such that parts of the enzymes were overlapping along the denpol chain. In the case of GOD, such geometric considerations indicated that the coverage of the denpol chain was less dense, which might be a result of a reduced accessibility of the denpol chain close to the considerably larger GOD. Additionally, it has to be considered that the determination of the amount GOD on the *de*-PG2-BAH-GOD conjugate was less precise than for HRP on the *de*-PG2-BAH-HRP conjugate due to the interference during the conjugation reaction as described above. Despite this uncertainty of the exact composition of the *de*-PG2-BAH-GOD conjugate, the AFM images clearly indicated a good coverage of the denpol chain with enzyme in this conjugate.

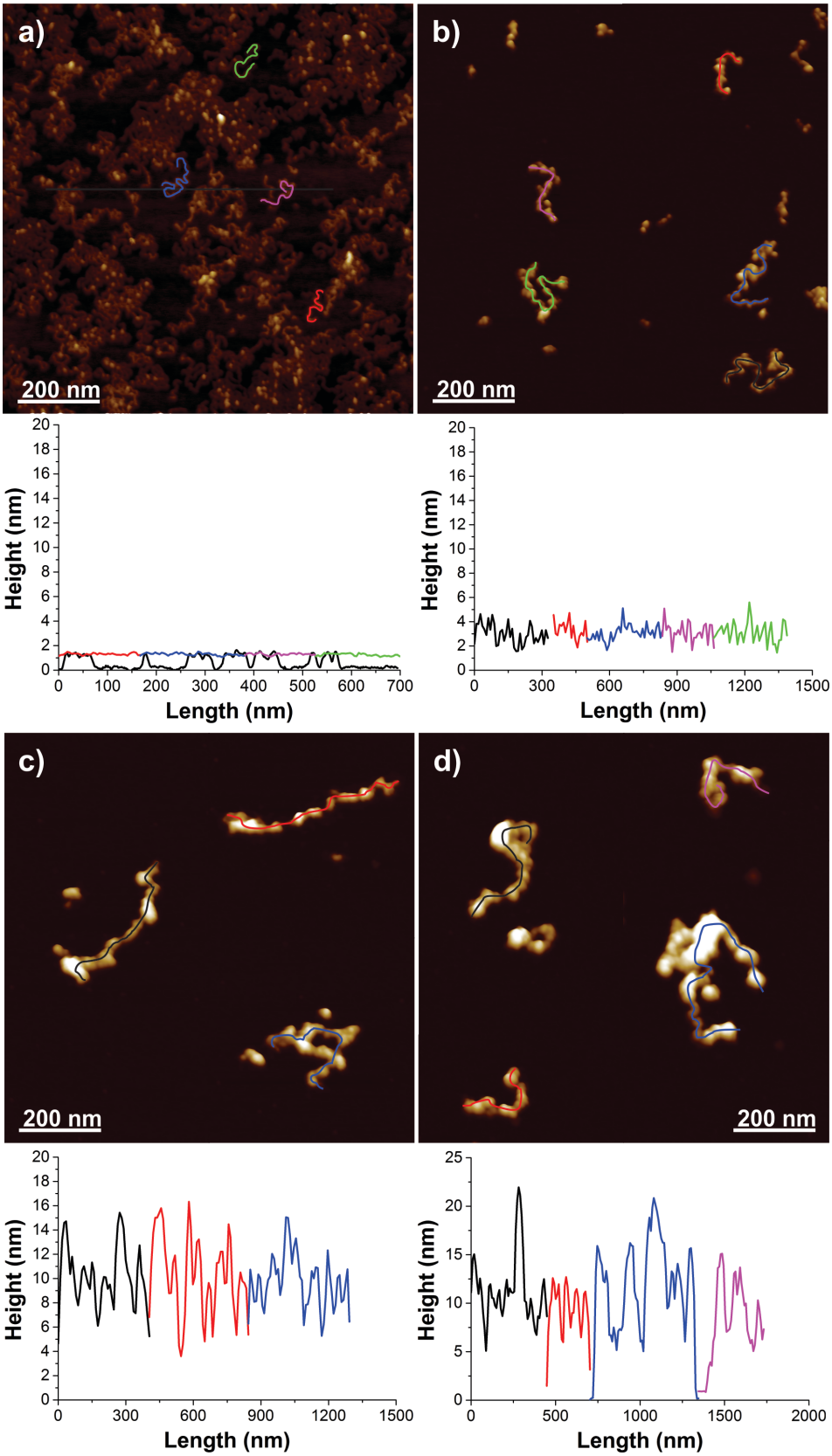


**Figure 3.1.10** Tapping mode 3D AFM images of **a)** the adsorbed denpol *de*-PG2 and the denpol-enzyme conjugates **b)** *de*-PG2-BAH-HRP, **c)** *de*-PG2-BAH-GOD, and **d)** *de*-PG2-BAH-(GOD,HRP) on freshly cleaved mica, deposited from a pH 5.0 solution. Longitudinal height profiles of the individual chains are given in different colors as indicated by the colored lines in the images. The black height profile in **a)** corresponds to the transversal height profile indicated by the straight black line in the image.

The AFM images of the *de*-$PG2_{1400}$-BAH-($GOD_{25}$,$HRP_{78}$) conjugate (**Figure 3.1.10d**) indicated larger variations in the longitudinal height profile of the conjugate, but a similar average height as in the case of *de*-PG2-BAH-GOD. Even though a less homogeneous height might be expected for this conjugate due to the presence of two types of enzymes of different sizes, the large variations in the height profiles were partially also due to more clustered areas along the denpol chain. A less elongated denpol chain on the mica substrate might be promoted in this conjugate due to the additional interactions between GOD and HRP. Even though the surface of the two enzymes is shielded by the glycosylation present on both types of enzymes, the large difference in the isoelectric points of GOD and HRP, 4.2 [89] and about 9 [76], respectively, might result in a propensity to form clustered areas with increased direct interactions of GOD and HRP as compared to an elongated conformation of the denpol.

In the AFM images of all three types of denpol-enzyme conjugates, *de*-PG2-BAH-HRP, *de*-PG2-BAH-GOD and *de*-PG2-BAH-(GOD,HRP), there was no free enzyme visible on the mica surface. This indicates the feasibility of the approach to immobilize enzymes in a controlled way by synthesizing such denpol-enzyme conjugates in solution, followed by adsorption of the full conjugates from the solution resulting in a defined layer of adsorbed conjugates without any free denpol or free enzyme present.

### 3.1.6 Immobilization of the denpol-enzyme conjugates of GOD and HRP on $SiO_2$ surfaces

After completion of the synthesis of the denpol-enzyme conjugates containing HRP and GOD as described above, the adsorption of these conjugates on $SiO_2$ surfaces was studied. The transmission interferometric adsorption sensor (TInAS, see [117, 118]) was used as the method of choice to monitor the adsorption of the denpol-enzyme conjugates on a sputtered $SiO_2$ surface from an aqueous solution. The TInAS setup allowed *in situ* monitoring of the adsorption process using a flow cell and a feed of dilute denpol-enzyme conjugate solutions. To calculate the adsorbed dry mass from the optical mass measured with the TInAS, the refractive index increments of the denpol-enzyme conjugates needed to be estimated, as a precise determination was not possible due to the fact that the concentration of the denpol-enzyme conjugates could be only roughly estimated by UV/vis spectrophotometry due to overlapping absorption bands of the enzymes, the BAH moiety and the denpol.

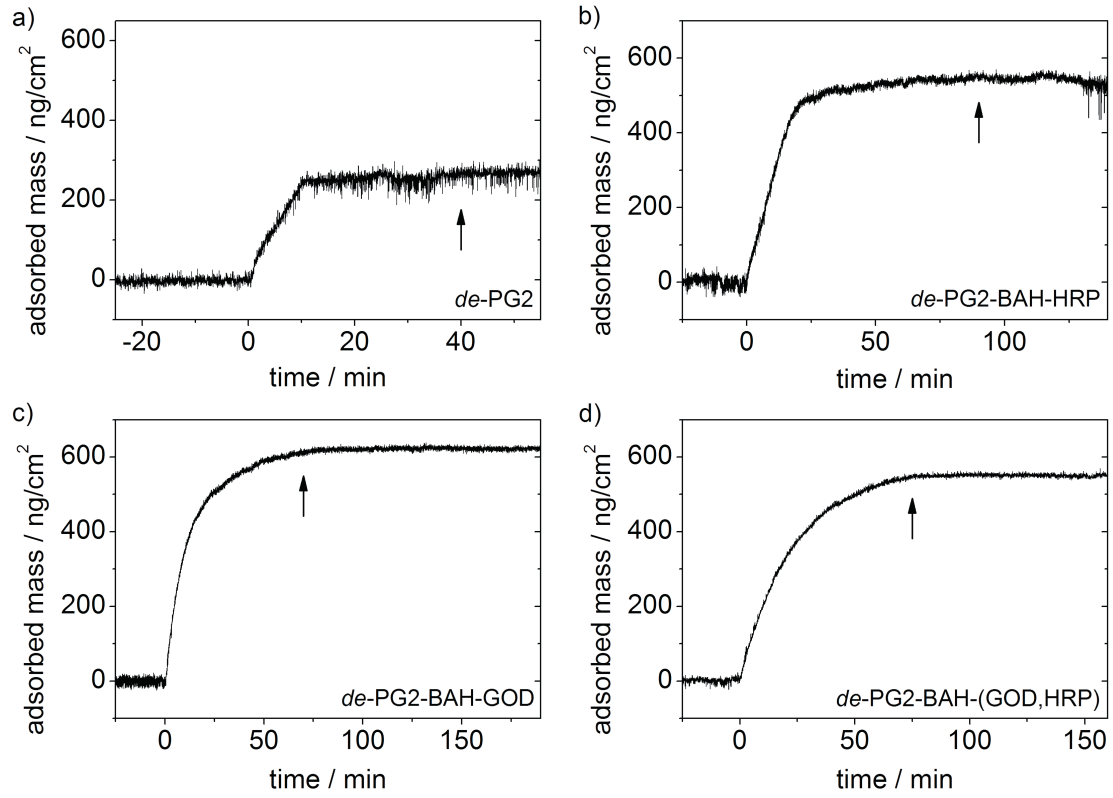


**Figure 3.1.11** TInAS analysis of the adsorption of **a)** *de*-PG2, **b)** *de*-PG2-BAH-HRP, **c)** *de*-PG2-BAH-GOD, and **d)** *de*-PG2-BAH-(GOD,HRP) on a $SiO_2$ sputtered surface at pH 5.0. After recording a baseline at a continuous flow of buffer, the denpol or denpol-enzyme conjugate was introduced at t = 0 min into the flow cell using continuous flow conditions. After adsorption on the surface, the denpol or denpol-enzyme conjugates were removed from the flow cell by purging with buffer (⇑) and subsequent continuous flow of buffer indicated a good stability of the adsorbed layer without any detectable desorption of denpol or denpol-enzyme conjugate, respectively.

The refractive index increment of *de*-PG2 had been determined previously to be dn/dc = 0.140 $cm^3/g$ [30]. To obtain a value for the denpol-enzyme conjugates, a linear combination of the refractive index increments of the denpol, the polypeptide content of the enzyme and the carbohydrate content of the enzyme attached was calculated, according to their contribution to the total mass of the conjugate [119]. The refractive index increments for the polypeptide content of proteins has previously been reported to be dn/dc = 0.186 $cm^3/g$ and the corresponding value for the carbohydrate content as dn/dc = 0.136 $cm^3/g$ [120]. With a molecular weight of 44 kDa for HRP and an average glycosylation content of 20 mass% [82], the calculated refractive index increment for a *de*-$PG2_{1400}$-BAH-$HRP_{108}$ conjugate was dn/dc = 0.170 $cm^3/g$. In the case of GOD, the molecular weight specified by the supplier was 153 kDa [121], with an average glycosylation of 16.2 mass% [122]. For a *de*-$PG2_{1400}$-BAH-$GOD_{50}$ conjugate the calculated refractive index increment was therefore dn/dc = 0.174 $cm^3/g$, and for the conjugate containing both types of enzymes, *de*-$PG2_{1400}$-BAH-($GOD_{25}$,$HRP_{78}$), a value of dn/dc = 0.173 $cm^3/g$ was calculated.

The amount of adsorbed denpol-enzyme conjugate as measured with the TInAS was comparable for the three conjugates *de*-PG2-BAH-HRP (**Figure 3.1.11b**), *de*-PG2-BAH-GOD (**Figure 3.1.11c**) and *de*-PG2-BAH-(GOD,HRP) (**Figure 3.1.11d**), all resulting in the range of 550-650 ng/cm$^2$. The different size of the enzymes present in the conjugates was not reflected in the amount of adsorbed mass. As the TInAS measurements result in an average surface concentration, this might indicate that the thicker *de*-PG2-BAH-GOD and *de*-PG2-BAH-(GOD,HRP) conjugate adsorbed in a less dense layer on the $SiO_2$ surface than the *de*-PG2-BAH-HRP conjugate. After adsorption of each conjugate, the flow cell was purged with buffer and the adsorbed mass monitored during at least 1 hour under continuous flow of buffer in order to test the stability of the adsorbed layer on the $SiO_2$ surface. In all cases, there was no desorption of conjugate detected, indicating the formation of a stable layer of denpol-enzyme conjugate on the surface.

As a reference value for the adsorption measurements of the denpol-enzyme conjugates, the adsorption of the non-modified denpol *de*-$PG2_{1400}$ was monitored with the TInAS as well (**Figure 3.1.11a**). The adsorbed mass of *de*-PG2 was about 250 ng/cm$^2$, and therefore considerably lower than in the case of the denpol-enzyme conjugates. Comparable to the results obtained with the denpol-enzyme conjugates, there was no detectable desorption of *de*-PG2 during a rinsing of the TInAS flow cell with buffer. This confirmed previously published results indicating a very stable adsorption of denpols of the type of *de*-PG2, outperforming comparable polymers decorated with primary amino groups such as poly-D-lysine [30].

From the results of the TInAS measurements, the obtained dry mass of adsorbed denpol-enzyme conjugates was used to calculate the amount of enzymes present on the $SiO_2$ surface. In the case of *de*-$PG2_{1400}$-BAH-$HRP_{108}$ and considering an average adsorbed dry mass of 600 ng/cm$^2$, this results in 11 pmol/cm$^2$, and for *de*-$PG2_{1400}$-BAH-$GOD_{50}$, the amount of GOD on the $SiO_2$ surface was correspondingly determined to be 3.4 pmol/cm$^2$. In the case of *de*-$PG2_{1400}$-BAH-($GOD_{25}$,$HRP_{78}$) the calculated amount of immobilized HRP was 5.6 pmol/cm$^2$, while the amount of immobilized GOD with the same conjugate was 1.8 pmol/cm$^2$. These values confirmed a good efficiency of this denpol mediated enzyme immobilization with a surface concentration of the enzyme comparable to the results reported using alternative enzyme immobilization approaches [30, 67, 123-125].

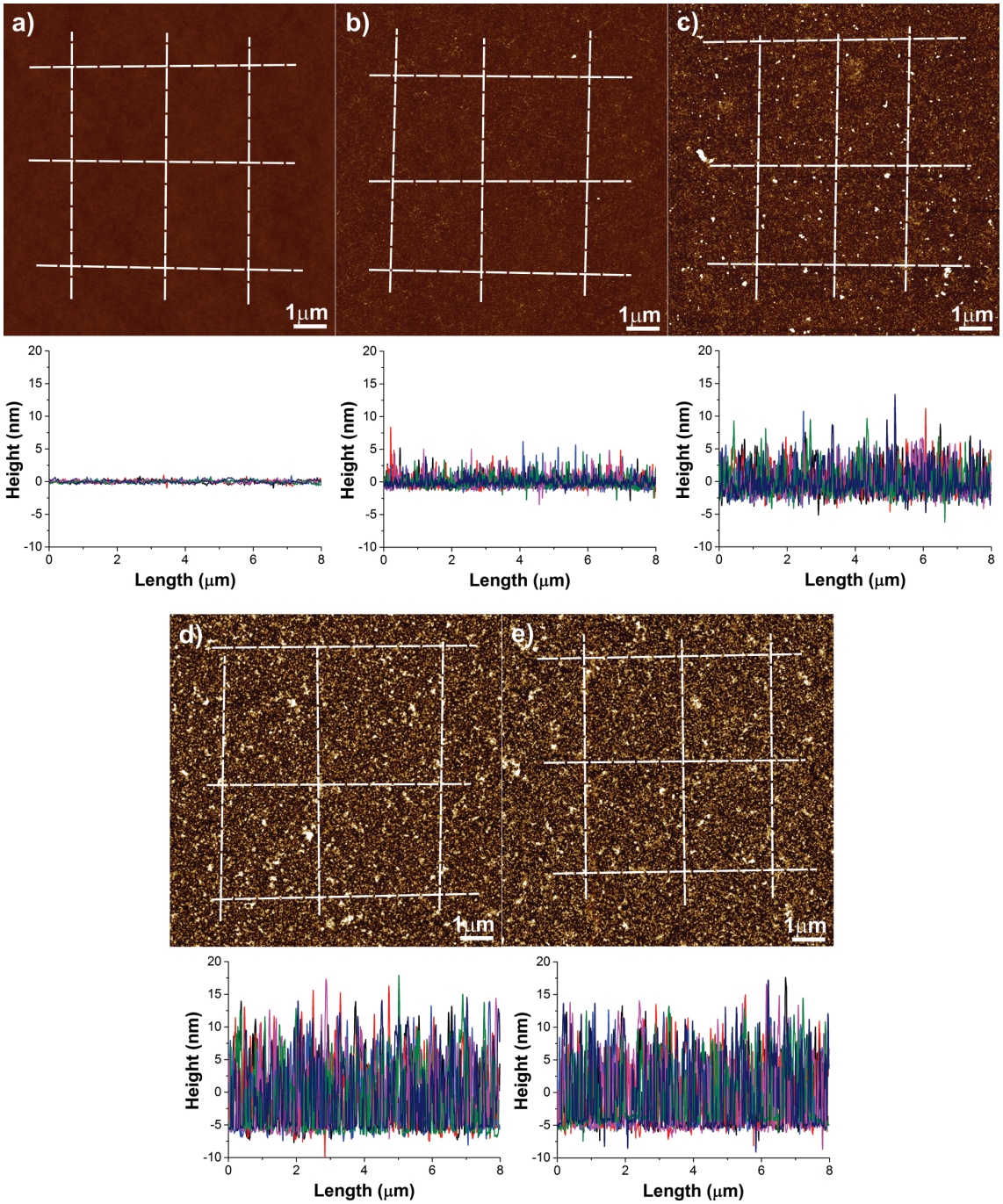


**Figure 3.1.12** Tapping mode 3D AFM images of microscopy glass coverslips with corresponding height profiles. **a)** The clean glass surface of the coverslips had a roughness below 1 nm. **b)** Adsorbed *de*-PG2 formed a homogeneous layer with a surface roughness of 1-2 nm with a few peaks up to about 5 nm. Adsorption of the denpol-enzyme conjugates **c)** *de*-PG2-BAH-HRP, **d)** *de*-PG2-BAH-GOD, and **e)** *de*-PG2-BAH-(GOD,HRP) resulted in the formation of homogeneous layers of a thickness of about 7 nm in the case of *de*-PG2-BAH-HRP and about 15 nm in the case of *de*-PG2-BAH-GOD and *de*-PG2-BAH-(GOD,HRP). The adsorption was done at pH 5.0.

After confirmation of the adsorption of the denpol-enzyme conjugates on $SiO_2$ surfaces with the TInAS measurements, the formed layers on silicate glass were analyzed by AFM. For this purpose, cleaned microscopy glass coverslips were coated with the denpol-enzyme conjugates by immersion of the coverslips into dilute solutions of the

conjugates for 1 hour and subsequent washing of the coverslips with buffer to remove excess denpol-enzyme conjugates. After rinsing of the coverslips with Milli-Q water and drying with air, the adsorbed layer of denpol-enzyme conjugates on the coverslips was analyzed by AFM. As a reference, a glass coverslip was coated with the unmodified *de*-PG2 using the same protocol.

A characterization of a clean glass coverslip without any adsorbed layer confirmed a flat surface of the glass with a roughness clearly below 1 nm on an area of several micrometers per edge (**Figure 3.1.12a**). The glass coverslip coated with *de*-PG2 indicated a dense layer of denpol resulting in an increased surface roughness of 1-2 nm, with a few peaks up to more than 5 nm (**Figure 3.1.12b**). The homogeneity of the adsorbed layer and the thickness corresponding roughly to the thickness of a single *de*-PG2 chain indicated a controlled deposition of a single layer of the polycationic denpol on the negatively charged $SiO_2$ surface. Considering a non-ordered deposition of the denpol chains on the surface, the height of two chains crossing each other would be expected to be in the range of 2-3 nm if compared to the thickness of 1-1.5 nm measured for a single denpol chain (see **Figure 3.1.10a**). Except for a few peaks, this value was not exceeded in an analyzed area of several micrometers per edge.

For a glass coverslip coated with *de*-PG2-BAH-HRP, the surface roughness was considerably increased to about 7 nm (**Figure 3.1.12c**). As in the case of the non-modified denpol, this value corresponded well to the thickness expected from two *de*-PG2-BAH-HRP chains crossing each other on the surface. Even though a few larger aggregates were observed on an analyzed area of several micrometers per edge, the homogeneity of the layer indicated a well-defined adsorption of the denpol-enzyme conjugate, resulting in a mainly monolayer covered surface.

For the glass coverslips with adsorbed *de*-PG2-BAH-GOD (**Figure 3.1.12d**) and *de*-PG2-BAH-(GOD,HRP) (**Figure 3.1.12e**), the increase in surface roughness was even more pronounced than in the case of *de*-PG2-BAH-HRP, corresponding to the observed higher heights seen in the longitudinal profiles of single denpol-enzyme conjugates on mica (see **Figures 3.1.10c&d**). In both cases, a surface roughness of about 15 nm was observed, indicating a monolayer coverage of the glass surface as seen for *de*-PG2 and *de*-PG2-BAH-HRP. Despite the higher roughness, the surface coverage was again homogeneous over an area of several micrometers per edge.

The observation of monolayer surface coverage for all different denpol-enzyme conjugates indicated a good control of the immobilization process. The homogeneity of the

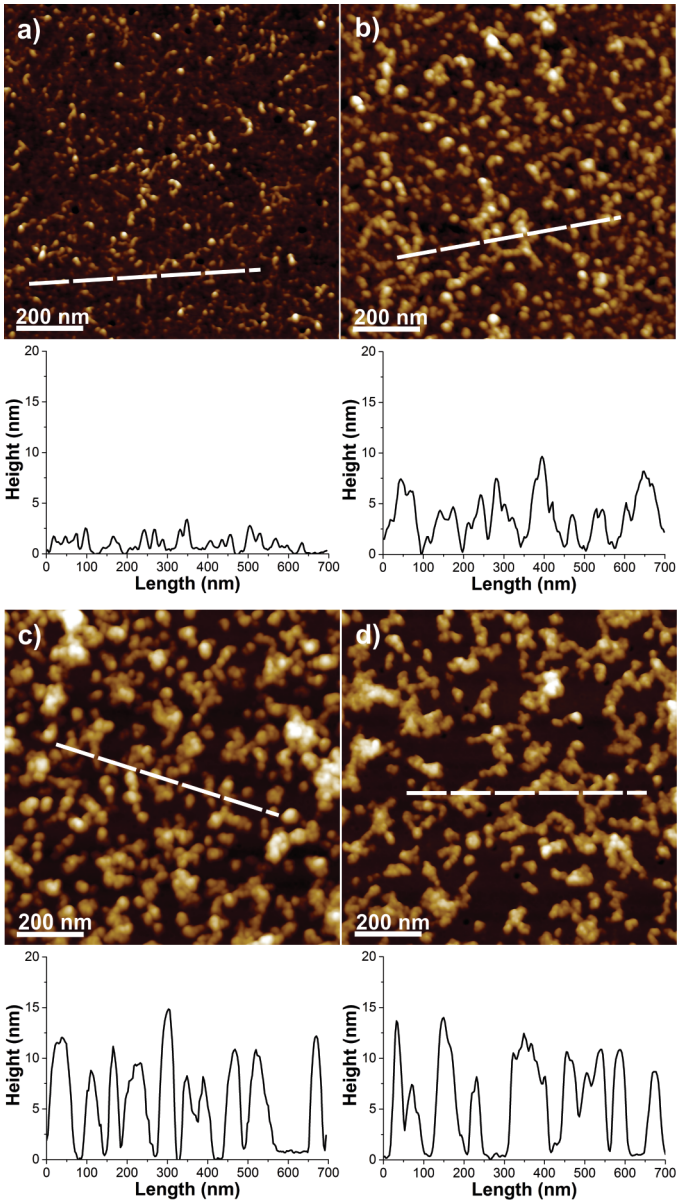


**Figure 3.1.13** Tapping mode 3D AFM images of **a)** *de*-PG2 and the denpol-enzyme conjugates **b)** *de*-PG2-BAH-HRP, **c)** *de*-PG2-BAH-GOD, and **d)** *de*-PG2-BAH-(GOD,HRP) on microscopy glass coverslips with corresponding height profiles. The homogeneous layer on the surface indicates a controlled adsorption of the denpol and the denpol-enzyme conjugates from a pH 5.0 solution, without formation of large clusters or multilayered structures.

surface confirmed the presence of well-defined adsorbed layers. To further analyze the adsorbed denpol-enzyme conjugates, AFM images of the denpol-enzyme conjugates on the glass coverslips were evaluated at higher resolution.

The high resolution AFM images of *de*-PG2 (**Figure 3.1.13a**), *de*-PG2-BAH-HRP (**Figure 3.1.13b**), *de*-PG2-BAH-GOD (**Figure 3.1.13c**), and *de*-PG2-BAH-(GOD,HRP) (**Figure 3.1.13d**) adsorbed on the glass coverslips confirmed the presence of a single layer of denpol or denpol-enzyme conjugate, respectively. The denpol chains were adsorbed in a non-ordered way, resulting in overlapping chains. The height of the individual chains forming the adsorbed layer was comparable to the values determined for single chains

adsorbed on mica (see **Figures 3.1.10a-d**). The presence of overlapping chains resulted in higher areas, consistent with the results obtained from the visualization of larger areas of the glass coverslips (see **Figures 3.1.12b-d**). A height profile across the *de*-PG2 chains showed heights of 1-3 nm (**Figure 3.1.13a**), whereas the profile across the adsorbed *de*-PG2-BAH-HRP layer showed values of around 4-6 nm (**Figure 3.1.13b**), but including features of up to 10 nm in height. For the *de*-PG2-BAH-GOD layer, the height profile indicated a thickness of the chains between about 8-12 nm with some even larger features (**Figure 3.1.13c**). The *de*-PG2-BAH-(GOD,HRP) layer resulted in a slightly higher variation in the height profile than observed for the adsorbed *de*-PG2-BAH-GOD, with values of about 7-13 nm (**Figure 3.1.13d**).

As in the case of the imaging of single denpol-enzyme conjugates on mica (**Figures 3.1.10b-d**), the height profiles measured across the adsorbed layers resulted in all cases in heights comparable to the expected thickness of conjugates according to the enzyme present in the conjugate. Considering the homogeneous coverage of the surface observed in the AFM images analyzing areas of several micrometers per edge, it has to be noted that the high resolution imaging clearly indicated a surface coverage with non-dense packing. This seemed to be pronounced in the case of *de*-PG2-BAH-GOD and *de*-PG2-BAH-(GOD,HRP), while the adsorbed *de*-PG2-BAH-HRP forms a denser layer. The observation of a thicker but less dense layer in the case of *de*-PG2-BAH-GOD and *de*-PG2-BAH-(GOD,HRP) compared to *de*-PG2-BAH-HRP was consistent with the results obtained from the TInAS measurements for the quantification of an average adsorbed dry mass of the conjugates. The thickness and the density of the adsorbed layers of denpol-enzyme conjugates affected the average surface concentration in opposite directions, resulting in comparable TInAS readings for all three denpol-enzyme conjugates.

### 3.1.7 Catalytic activity and stability of denpol-enzyme conjugates of GOD and HRP on $SiO_2$ surfaces

After successful deposition of the three denpol-enzyme conjugates *de*-PG2-BAH-HRP, *de*-PG2-BAH-GOD and *de*-PG2-BAH-(GOD,HRP) on microscopy glass coverslips, the catalytic activity of the coated surfaces was investigated. This was performed by immersion of the coated coverslips in a defined volume of substrate solution for the corresponding enzymes for a defined period of time and subsequent analysis of the product concentration in the solution. For a quantitative evaluation of the enzymatic activity, the obtained rates of product formation were compared to the rates observed for

known concentrations of native enzyme in solution. The direct correlation of the enzymatic activity measured on a defined surface area with a certain concentration of native enzyme in solution includes the assumption of similar kinetic constants in both cases. This might not be true in most cases, as the interaction of the enzymes with the surface and the denpol induced changes in the enzyme's environment and conformation, leading to altered enzyme kinetics. Nevertheless, the values obtained from such a comparison were used to calculate an apparent enzyme concentration on the surface, which was expressed as picomol enzyme per square centimeter surface area. Comparison of the values obtained in this way with the values obtained from the TInAS measurements of the adsorption process allowed an estimation of the catalytic efficiency of the immobilized enzymes.

*Catalytic activity of immobilized HRP*. The catalytic activity of immobilized HRP was measured by immersion of a microscopy glass coverslip with adsorbed *de*-PG2-BAH-HRP into a solution containing the chromogenic HRP substrate $ABTS^{2-}$ and subsequent UV/vis spectrophotometric quantification of the product formed (see **Background: Figure 2.5.2**). For a correlation of the measured activity to an apparent surface concentration of HRP as described above, a calibration curve was measured with known amounts of native HRP in solution and with 1 mM $ABTS^{2-}$ and 0.2 mM $H_2O_2$ as substrates. The initial reaction rate of these measurements were recorded by UV/vis spectrophotometry, calculating the rate of product formation with the known absorption coefficient of $ABTS^{\bullet-}$ at 414 nm ($\varepsilon_{414nm}$ = 36000 $M^{-1}\,cm^{-1}$ [85]). The calibration curve obtained indicated a linear correlation of the product formation rate and the HRP concentration for enzyme concentrations of 0.25-8 nM HRP under the conditions used (see **Experimental Part: Figure 5.9.1**). This allowed a direct correlation of the apparent amount of immobilized enzyme within the range of this calibration.

In the case of immobilized HRP, the reaction could not be followed *in situ* by UV/vis spectrophotometry due to the heterogeneous nature of the system. Instead, the glass coverslips were immersed into a defined volume of the same substrate solution as used for the calibration, and after a defined incubation time, typically 1 minute, the formation of the chromophore $ABTS^{\bullet-}$ was measured by UV/vis spectrophotometry. The assay conditions for the immobilized HRP were chosen such that the amount of product formation corresponded to a HRP concentration within the range of the calibration curve. The amount of product formation measured for the immobilized HRP could in this way be directly correlated to the apparent amount of HRP present in the reaction mixture and therefore assigned to the defined surface of the microscopy coverslip supporting the immobilized enzyme. Using the denpol-enzyme conjugate *de*-PG2-BAH-HRP, the

determination of the HRP activity per surface area indicated an apparent HRP surface concentration of 1.4 pmol/cm² (**Figure 3.1.14**). This value was considerably lower than the value calculated from the TInAS adsorption measurements of *de*-PG2-BAH-HRP, which indicated an HRP surface concentration of 11 pmol/cm² (see above). The difference between the surface concentration determined *via* the adsorption measurement and the apparent surface concentration estimated from the catalytic activity could originate from different phenomena, as discussed below.

In addition to the quantification of the catalytic activity of the immobilized HRP, the stability of the enzyme during storage was monitored (**Figure 3.1.14**). For storage, the coated glass coverslips were kept in a polypropylene tube filled with phosphate buffer (pH = 7) at 4 °C. After defined times, the activity of the immobilized HRP was re-measured using the same procedure as for the initial quantification of the apparent surface concentration of the enzyme. In an initial phase, a decrease of activity to a level corresponding to an apparent surface concentration of about 0.7 pmol/cm² was observed within 7 days. At this value, corresponding to about 50 % of the initial activity, the HRP activity stabilized for a storage time as long as 10 weeks. Even though the decrease during the first phase was considerable, the remaining activity after a storage time as long as 10 weeks indicated a good storage stability of the immobilized HRP when kept in a wet state at 4 °C.

*Catalytic activity of immobilized GOD*. For the determination of the GOD activity of glass coverslips coated with *de*-PG2-BAH-GOD, a similar approach was followed as in the

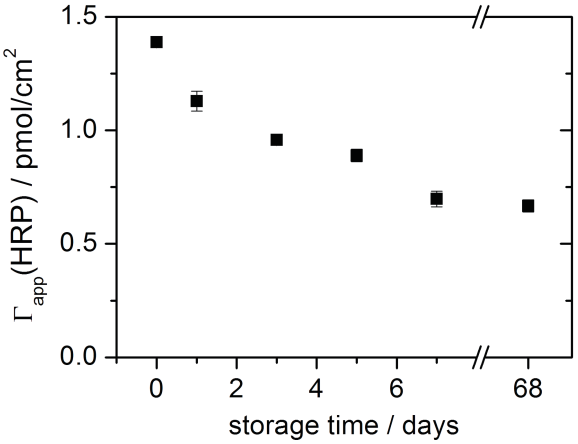


**Figure 3.1.14** Catalytic activity and stability of HRP immobilized by adsorption of *de*-PG2-BAH-HRP on a glass coverslip. For activity measurements, a substrate solution containing 1 mM $ABTS^{2-}$ and 0.2 mM $H_2O_2$ (pH 7.0) was added to the reaction tube containing the glass coverslip for 1 min at room temperature. After removal of the substrate solution, the concentration of $ABTS^{\bullet-}$ formed was quantified spectrophotometrically and the apparent surface concentration of HRP $\Gamma_{app}$(HRP) calculated by correlation of the measured activity to the activity of native HRP in solution. Between measurements, the coverslips were stored at pH 7.0 at 4 °C.

case of immobilized HRP. As there was no chromogenic substrate available for GOD, an indirect assay was used for the quantification of the activity of immobilized GOD. In a coupled assay exploiting an enzymatic cascade reaction involving GOD and HRP, the $H_2O_2$, produced upon oxidation of D-glucose with $O_2$ catalyzed by GOD, was quantified by further conversion with HRP leading to the oxidation of a chromogenic HRP substrate. In contrast to the quantification of HRP as described above, the chromogenic HRP substrate OPD was used instead of $ABTS^{2-}$ (see **Background: Figure 2.5.5**). As OPD forms a dimer upon oxidation, instead of a radical chromophore species as in the case of $ABTS^{\bullet-}$, longer incubation times are experimentally accessible without further reaction of the chromophore species interfering with the determination of the product concentration.

As in the case of the quantification of the activity of immobilized HRP, a calibration curve correlating the rate of product formation to the concentration of native GOD in solution was measured. Using a substrate mix containing 3.45 mM D-glucose, dissolved oxygen (approximately 0.25 mM [126]), 3.14 mM OPD and 2 nM HRP, a linear relationship between the rate of product formation and the GOD concentration was observed in the range of 0.3-2.4 nM GOD (see **Experimental Part: Figure 5.9.2**). For the determination of the apparent surface concentration of immobilized GOD, a coverslip coated with *de*-PG2-BAH-GOD was immersed into an assay solution as used for the calibration curve, and the product formation was quantified after a defined time, typically 20 minutes, by UV/vis spectrophotometry. Comparison with the calibration curve indicated an apparent GOD surface concentration of 1.3 pmol/cm² (**Figure 3.1.15**). As in the case of HRP, the stability of immobilized GOD during storage in phosphate buffer (pH = 7) at 4 °C was monitored by

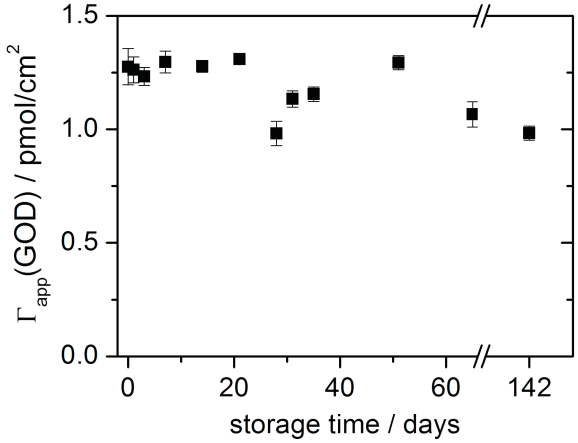


**Figure 3.1.15** Catalytic activity and stability of GOD immobilized by adsorption of *de*-PG2-BAH-GOD on a microscopy glass coverslip. For the activity measurements, an assay solution containing 3.45 mM D-glucose, dissolved $O_2$, 3.14 mM OPD, and 2 nM HRP (pH 7.0) was added to the reaction tube containing the glass coverslip for 20 min at room temperature. After removal of the assay solution, the concentration of the DAP formed was quantified spectrophotometrically and the apparent surface concentration of GOD $\Gamma_{app}$(GOD) calculated by correlation of the measured activity to the activity of native GOD in solution. Between measurements, the coverslips were stored at pH 7.0 at 4 °C.

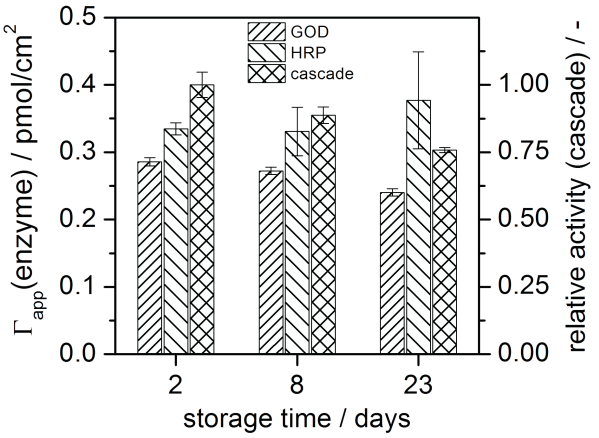


**Figure 3.1.16** Catalytic properties of co-immobilized GOD and HRP upon adsorption of *de*-PG2-BAH-(GOD,HRP) on microscopy glass coverslips from a pH 5.0 solution. The apparent surface concentration of GOD and HRP were determined by correlation of the individual activity of the enzymes with a corresponding calibration of native enzymes in solution. The relative performance of the enzymatic cascade reaction involving both immobilized enzymes was determined at room temperature using an assay solution containing 3.45 mM D-glucose, dissolved $O_2$ and 3.14 mM OPD as substrates (pH 7.0). Between measurements, the coverslips were stored at pH 7.0 at 4 °C.

repeated measurements of the remaining activity. The storage stability of GOD was very high during the first few weeks, and no initial decrease of activity as in the case of HRP was observed. Even after 20 weeks a remaining activity corresponding to an apparent surface concentration of 1 pmol/cm$^2$ was detected, corresponding to about 75 % of the initial activity (**Figure 3.1.15**).

*Catalytic activity of immobilized GOD and HRP*. Similar to the measurement of the enzymatic activity of the adsorbed denpol-enzyme conjugates *de*-PG2-BAH-HRP and *de*-PG2-BAH-GOD, the catalytic activity of the adsorbed conjugate carrying both enzymes on the same denpol chain, *i.e. de*-PG2-BAH-(GOD,HRP), was determined. For the characterization of the catalytic properties of this conjugate adsorbed on glass coverslips, the determination of the catalytic activity of HRP and GOD was performed as for the conjugates including only one type of these enzymes. Additionally, the cascade reaction involving both enzymes adsorbed on the $SiO_2$ surface was characterized using D-glucose and OPD as substrates, as for the determination of the apparent surface concentration, but without any additional HRP in solution. Therefore, the second step of the enzymatic cascade reaction was catalyzed exclusively by the immobilized HRP present in the adsorbed *de*-PG2-BAH-(GOD,HRP) conjugate.

The quantification of the HRP activity of adsorbed *de*-PG2-BAH-(GOD,HRP) on an $SiO_2$ surface indicated an apparent surface concentration of 0.33 pmol/cm$^2$, while the GOD activity of the same surface corresponded to an apparent surface concentration of 0.28 pmol/cm$^2$ (**Figure 3.1.16**). Remarkably, and in contrast to the results obtained for the HRP stability of adsorbed *de*-PG2-BAH-HRP, the HRP activity was not reduced during

storage. After 3 weeks of storage of the *de*-PG2-BAH-(GOD,HRP) coated glass coverslip in phosphate buffer (pH = 7) at 4 °C, no significant reduction in HRP activity was detected. During the same time, the GOD activity was reduced to 0.24 pmol/cm$^2$, corresponding to a decrease of about 15 %. For the cascade reaction observed in this system, rate of product formation was not directly correlated to the concentration of one of the enzymes, but rather observed as a relative measure for the overall efficiency of the enzymatic cascade reaction. Within 3 weeks of storage, the relative efficiency of the cascade reaction dropped to about 75 % of the initial value (**Figure 3.1.16**).

In a comparison of the values obtained as apparent surface concentrations of the enzymes measured through determination of the catalytic activity and as the surface concentrations calculated from the adsorbed mass as determined with the TInAS, the activity based determination resulted in all cases in a lower apparent surface concentration than the adsorbed mass suggested. In the case of adsorbed *de*-PG2-BAH-HRP, the immobilized HRP was quantified as 1.4 pmol/cm$^2$ (activity) *vs.* 11 pmol/cm$^2$ (TInAS) and in the case of adsorbed *de*-PG2-BAH-GOD, the immobilized GOD was quantified as 1.3 pmol/cm$^2$ (activity) *vs.* 3.4 pmol/cm$^2$ (TInAS). A similar trend was observed in the case of the co-immobilization of GOD and HRP with *de*-PG2-BAH-(GOD,HRP), where the amount of immobilized HRP was determined as 0.33 pmol/cm$^2$ (activity) *vs.* 5.6 pmol/cm$^2$ (TInAS) and the amount of immobilized GOD as 0.28 pmol/cm$^2$ (activity) *vs.* 1.8 pmol/cm$^2$ (TInAS). These numbers clearly indicate a reduced activity of the immobilized enzymes in comparison to the solution activity. As discussed above, different phenomena could contribute to a reduction of the catalytic activity upon immobilization of the enzymes on the glass surface. As the immobilization approach employed does not offer a control of the orientation of the enzyme, a simple explanation might be a hindered access of the active site of a fraction of enzymes, preventing proper substrate binding and therefore catalytic activity. Additionally, interactions of the support with the enzyme might reduce catalytic activity due to conformational changes induced in the enzyme. A quantification of different factors contributing to the reduction in catalytic activity was not attempted and might not be possible, as already the determination of the surface concentrations as performed here included certain assumptions, as discussed above. Nevertheless, the data presented here clearly confirm the successful immobilization of the two enzymes HRP and GOD on $SiO_2$ surfaces under retention of a good catalytic activity and with a good stability during storage in a wet state.

### 3.1.8 Enzymatic cascade reaction with *de*-PG2-BAH-HRP and *de*-PG2-BAH-GOD, or *de*-PG2-BAH-(GOD,HRP) in glass micropipettes

The possibility to immobilize the enzymes HRP and GOD on non-modified $SiO_2$ surfaces in an irreversible way, as demonstrated above, offers the potential for the preparation of enzymatic reactors using simple silicate glass supports and coating of the reactor by rinsing with a dilute solution of the denpol-enzyme conjugate carrying the enzyme of interest. To demonstrate the feasibility of such an approach, small glass reactors for a continuous flow operation were prepared. Commercially available glass micropipettes were used as support, offering a defined inner surface to volume ratio with a suitable geometry. A micropipette cut to a length of 7 cm had an inner volume of 140 µL and an inner surface of 3.5 $cm^2$. The inner surface of such glass micropipettes was readily coated with the enzymes simply by filling the micropipette with a dilute solution of the denpol-enzyme conjugate of the enzyme of interest using the immobilization protocol developed for the TInAS measurements and the adsorption on microscopy glass coverslips. After adsorption of the denpol-enzyme conjugate, the remaining solution was purged from the pipettes and the pipettes washed with buffer to remove remaining liquid containing non-adsorbed denpol-enzyme conjugate. The thus prepared micropipette reactors could be installed in a setup allowing operation under continuous flow conditions. The product formation was monitored online and in real time using a Z-flow cell for UV/vis spectrophotometric analysis of the solution after exit from the micropipette reactor. The substrate feed, the micropipette reactor, the Z-flow cell and a peristaltic pump were connected with PTFE tubing, allowing a control of the residence time of the substrate solution in the reactor area by adjusting the flow rate in the system (**Figure 3.1.17a**).

Two different setups were tested to run the enzymatic cascade reaction catalyzed by GOD and HRP in these reactors. In a first, sequential setup, two micropipettes, one containing immobilized GOD *via* adsorption of *de*-PG2-BAH-GOD and one containing immobilized HRP *via* adsorption of *de*-PG2-BAH-HRP, were connected in a way that the substrate entered the GOD containing pipette, and after exit from this micropipette immediately entered the HRP containing pipette. With a substrate feed containing D-glucose, dissolved $O_2$ and $ABTS^{2-}$, the GOD in the first tube catalyzed oxidation of D-glucose with $O_2$ yielding glucono-δ-lactone and $H_2O_2$. In the second tube, the $H_2O_2$ served as a substrate for the HRP catalyzed oxidation of two equivalents of $ABTS^{2-}$ yielding two equivalents of $ABTS^{\bullet-}$. The $ABTS^{\bullet-}$ chromophore was then detected online in the flow cell connected to a UV/vis spectrophotometer (**Figure 3.1.17a**). Monitoring of the level of $ABTS^{\bullet-}$ during continuous substrate flow in this setup allowed a measurement of the

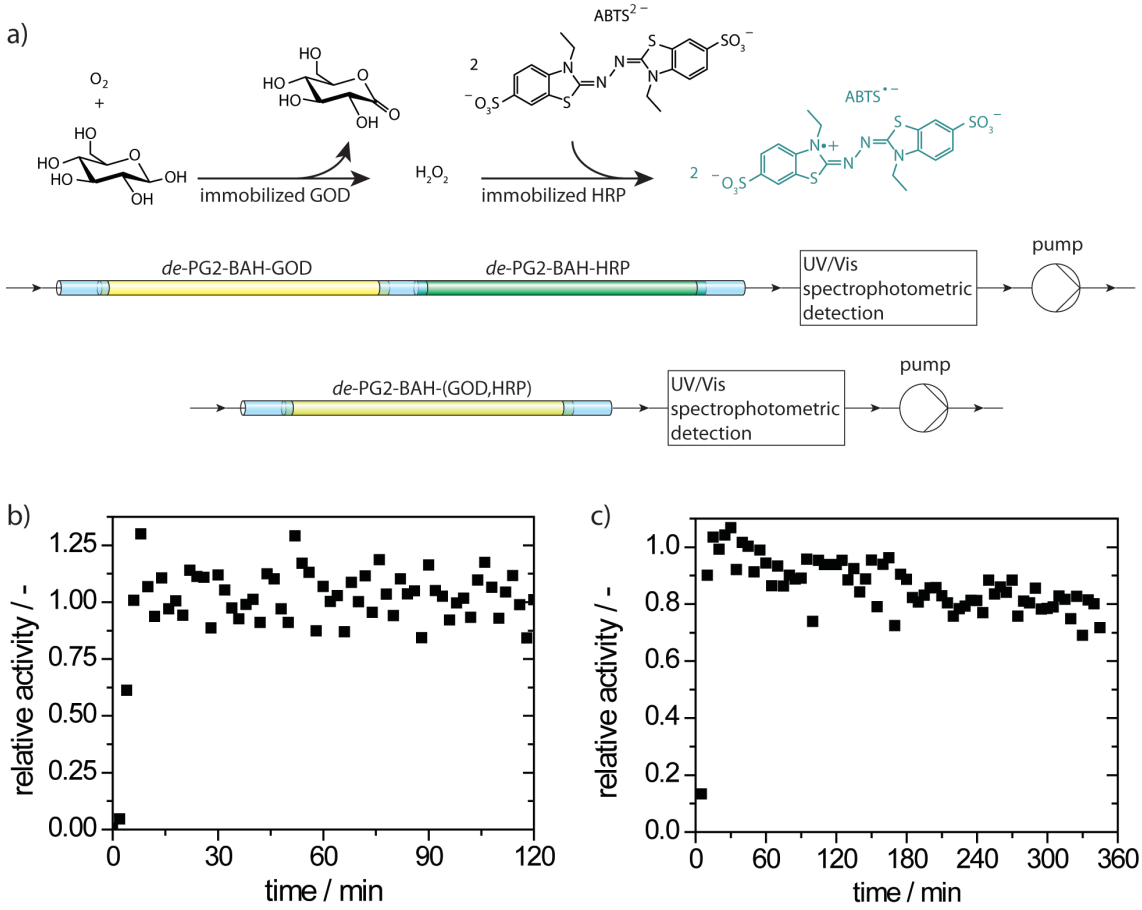


**Figure 3.1.17 a)** Setup for the test of the operational stability of the immobilized GOD and HRP in continuous flow reactors. A *sequential setup* was assembled by connecting a glass micropipette containing immobilized GOD and one containing immobilized HRP. The outlet of the second reactor was connected to a flow cell for online UV/vis spectrophotometric quantification of the produced $ABTS^{\bullet-}$. The setup for the *co-immobilized* GOD and HRP upon adsorption of *de*-PG2-BAH-(GOD,HRP) included only one micropipette reactor. **b)** The enzymatic activity of the sequential setup, as monitored by quantification of $ABTS^{\bullet-}$, the product of the enzymatic cascade reaction catalyzed by GOD and HRP, was stable under continuous flow operation at room temperature within two hours without a detectable decrease in activity. **c)** The enzymatic activity of the co-immobilized GOD and HRP decreased slightly to about 90 % within two hours of operation under continuous flow conditions. After six hours, there was still a remaining activity corresponding to about 80 % of the initial activity.

enzymes' stability under operating conditions. During an observation of 2 hours of continuous operation, no significant decrease in activity was measured for this system (**Figure 3.1.17b**).

For the second setup, a single micropipette containing both enzymes, GOD and HRP, was prepared by adsorption of the *de*-PG2-BAH-(GOD,HRP) conjugate. With this reactor incorporating co-immobilized GOD and HRP, the same enzymatic activity assay was performed as for the sequential setup. After 2 hours, a slight decrease in activity of about 10 % was observed, and after a total of 6 hours, a remaining activity of about 80 % was measured (**Figure 3.1.17c**). This indicated a good stability of the enzymes also under operating conditions.

### 3.1.9 Conclusions

The feasibility of the synthesis of denpol-enzyme conjugates carrying the enzymes GOD and HRP was demonstrated. Additionally, a conjugate carrying both types of enzymes on the same denpol chain was prepared. The composition of the conjugates was determined by quantification of the UV/vis signature of the BAH-bond formed during the conjugation. The obtained conjugates contained 108 molecules of HRP, about 50 molecules of GOD, or about 25 molecules of GOD and 78 molecules of HRP on an average denpol of 1400 repeating units. By AFM imaging, the increased thickness of single chains of the conjugate as compared to the free denpol was characterized.

The conjugates were successfully used for the immobilization of the attached enzymes on unmodified glass surfaces. Characterization of the adsorption process with the TInAS allowed determination of the adsorbed mass and indicated a good control of the adsorption process from solution. AFM imaging confirmed the presence of a layer corresponding to a thickness of about one conjugate chain on the surface.

The activity of the immobilized enzymes was demonstrated and the stability during storage and operation characterized. A simple enzymatic reactor was prepared by immobilization of the enzymes within glass micropipettes and shown to allow operation under continuous flow conditions.

## 3.2 Localized co-immobilization of GOD and HRP using denpol-enzyme conjugates and mesoporous silica nanoparticles

After the feasibility of a denpol mediated enzyme immobilization on silicate glass surfaces had been demonstrated (see **chapter 3.1**), it was investigated whether this approach could be combined with other, established enzyme immobilization procedures. The combination of different enzyme immobilization protocols for the fabrication of supports carrying different types of enzymes is of special interests if enzymatic cascade reactions are considered to be carried out with the immobilized enzymes. Focusing on enzyme immobilization techniques using non-modified silicate surfaces as support, which could allow a direct combination with the denpol mediated immobilization approach, mesoporous silica materials appeared promising. The immobilization of enzymes in mesoporous silica materials is based on a non-specific interaction of the enzymes with the surface of the silica support, which is maximized inside mesopores of a size comparable to the size of the enzyme molecules. This special feature of mesoporous materials has been exploited in numerous works for the immobilization of various different enzymes [44, 46, 48, 49, 127, 128].

In a recent report, Thörn *et al.* have demonstrated a novel method for the direct monitoring of the immobilization of enzymes in mesoporous silica particles using quartz crystal microbalance with dissipation monitoring (QCM-D) [129]. The mesoporous silica nanoparticles used in this system, (**Figure 3.2.1**, Hiroshima mesoporous materials, HMM [130, 131]), were in a first step adsorbed on a silanized QCM-D sensor with primary amines on the surface, and subsequent loading of the surface adsorbed HMM particles was studied with QCM-D. This procedure was chosen as a promising platform for a combination with the denpol-mediated enzyme immobilization approach developed for GOD and HRP as described above. After adsorption and loading of the HMM particles on a surface of interest, they form themselves a silica layer on the surface of the support facing the aqueous environment, which could be exploited for the adsorption of a second enzyme containing layer, this time formed by a denpol-enzyme conjugate deposited on the HMM particles. Such an approach was followed for a layered co-immobilization of two enzymes on a silicate surface.

### 3.2.1 Enzyme loading of surface adsorbed mesoporous silica particles studied with QCM-D

In a first step, the loading of HMM particles with the enzymes HRP or GOD was investigated using QCM-D. The HMM particles used had a diameter of about 40 nm and an average pore size around 9 nm (**Figure 3.2.1**). The $SiO_2$ surface of the QCM-D sensors used for these measurements was modified with (3-aminopropyl)trimethoxysilane (APTMS), forming a silane layer with terminal amino groups on the sensor surface. This modification allowed the *in situ* adsorption of silica nanoparticles on the QCM-D sensor as described by Thörn *et al*. [129]. For a determination of the extent of enzyme immobilization inside the mesopores of the HMM particles adsorbed on the amino terminated surface, a reference measurement using non-porous silica particles was carried out.

The adsorption of the silica particles applied as a suspension in 0.01 M HCl (*i.e.* pH 2) on the QCM-D sensor was observed as a shift in frequency and an increasing dissipation (**Figure 3.2.2**). While the shift in frequency was similar upon adsorption of the porous and the non-porous particles, the increase in dissipation was significantly higher in the case of the porous particles. This behavior could be rationalized by the fact that the non-porous particles formed a relatively dense layer, while the layer of the porous HMM particles contained a large amount of associated water inside the porous structure, increasing the dissipation of the adsorbed particles considerably [129].

The immobilization of the two enzymes GOD and HRP in the adsorbed HMM particles was monitored by the frequency change in the QCM-D measurement upon addition of a solution of either of the enzymes at pH 6.0 (**Figure 3.2.3**). For a comparison

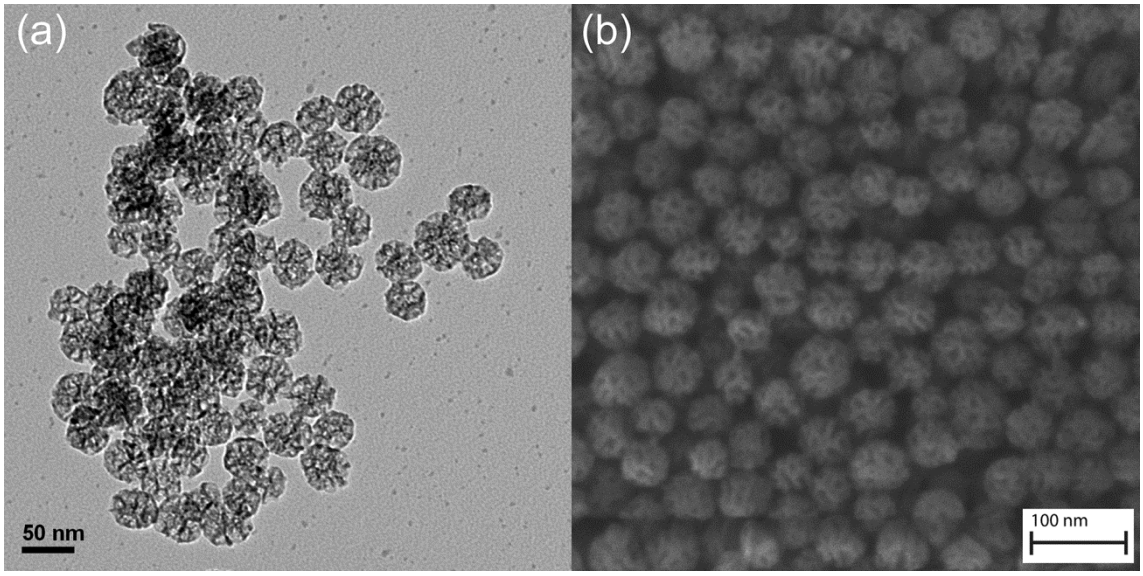


**Figure 3.2.1 a)** Transmission electron micrograph and **b)** scanning electron micrograph of HMM particles with a particle size of about 40 nm and an average pore size of about 9 nm.

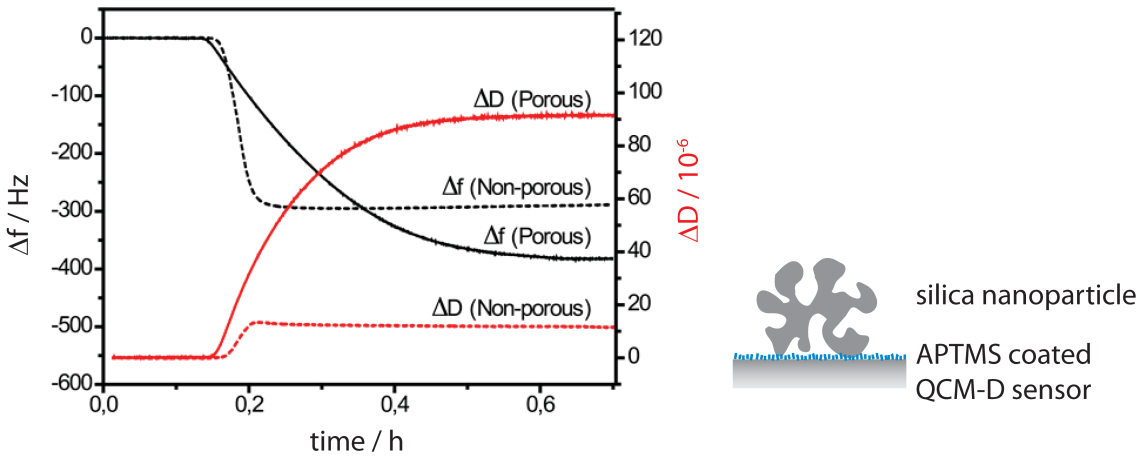


**Figure 3.2.2** QCM-D analysis of the adsorption of the mesoporous HMM particles on the amino-modified $SiO_2$ surface of the sensor after injection of a 0.4 % (w/v) suspension in 0.01 M HCl. As a control measurement, the adsorption of non-porous particles was performed under the same conditions.

with the enzyme adsorption on non-porous silica particles, the obtained frequency shifts were normalized according to the frequency shift during the particle adsorption, to account for the different efficiency of the particle adsorption to the surface [129]. In the case of GOD, the frequency shift during adsorption of the enzyme in the HMM particles indicated the immobilization of more than three times the amount as compared to the non-porous particles. In the case of HRP, the adsorbed amount was more than four times as high as in the case of the non-porous particles. Apart from the higher frequency shift during the adsorption of the enzymes GOD and HRP in the HMM particles compared to the adsorption on the non-porous particles, the desorption during a subsequent rinsing with buffer was significantly smaller in the case of the mesoporous particles. In the case of GOD, a desorption of 5% was observed for the HMM particles, while 20 % of the GOD adsorbed on the non-porous particles desorbed according to the frequency shift. For HRP, the situation was even more pronounced, with a desorption of 7 % from the HMM particles as compared to a desorption of 45 % from the non-porous particles. These differences indicated that the enzymes were stably adsorbed in the mesoporous particles, while the adsorption at the non-porous particles was of a relatively weak nature and subsequent desorption during rinsing resulted in a significant loss of enzyme from the surface. The combination of the increased adsorption and the decreased desorption in the case of the mesoporous particles clearly indicated that the majority of the enzymes were immobilized inside the porous structure of the HMM particles, and only a minor part on the outer surface.

In a second step, the influence of the pH on the immobilization of the two enzymes GOD and HRP inside the HMM particles was investigated. Upon a decrease of the pH of the applied enzyme solutions from pH 6.0 to pH 5.0, an increase in the amount of immobilized

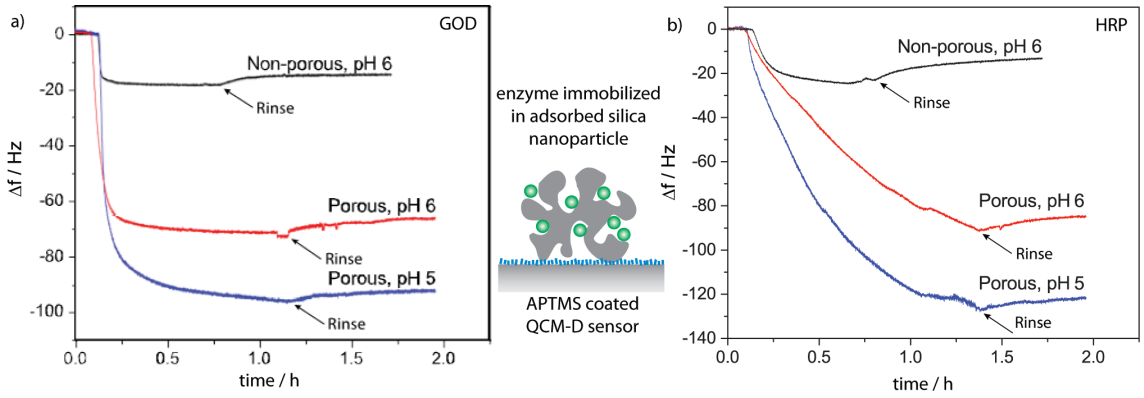


**Figure 3.2.3** QCM-D analysis of the immobilization of **a)** GOD and **b)** HRP in adsorbed HMM particles (blue and red curves) and on adsorbed non-porous particles (black curves). After the enzyme loading, the QCM-D flow cell was rinsed with buffer to monitor possible enzyme desorption.

enzymes was observed for both, GOD and HRP (**Figure 3.2.3**). Additionally, during a rinsing step following the adsorption of the enzymes in the HMM particles, the desorption was further decreased as compared to the results obtained at pH 6.0. For GOD, the decreased pH during adsorption and rinsing resulted in a decrease in desorption from about 5 % to about 2 %, and for HRP, the desorption was reduced from about 7 % to about 4 %.

The increased efficiency of the enzyme immobilization upon a decrease of pH from 6.0 to 5.0 indicated an improved interaction of the enzymes with the mesoporous silica material. This might be explained by the pH dependency of the surface localized charged areas of the enzymes. While the point of zero charge of mesoporous silica materials is around 2-3 [132], the isoelectric points of GOD and HRP are 4.2 [89] and about 9 [76], respectively. Therefore, for the silica material a negative surface charge is expected, with no big changes upon a change of pH from 6.0 to 5.0. On the other hand, protein structures

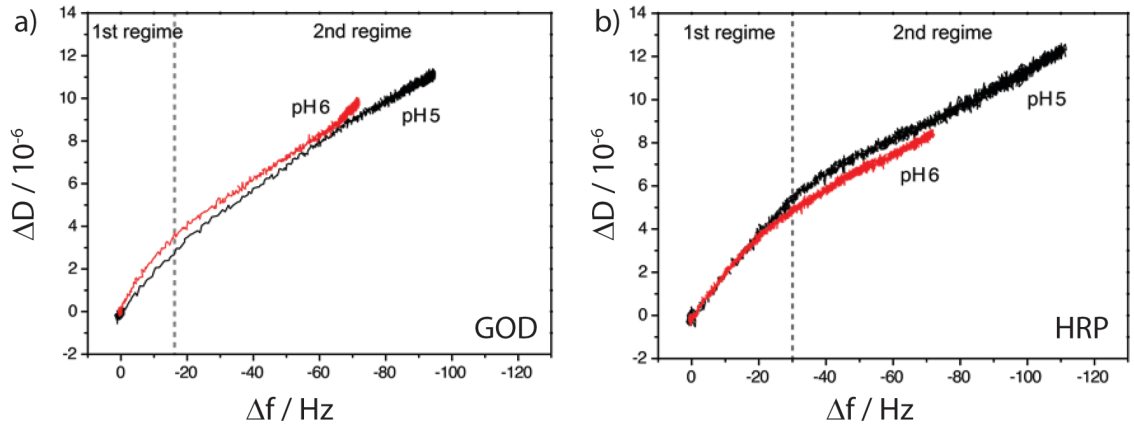


**Figure 3.2.4** Dissipation versus frequency plot for the immobilization of **a)** GOD and **b)** HRP in the adsorbed HMM particles. The fast increase of dissipation during the first phase can be correlated to an enzyme adsorption mainly on the outer surface of the particles, while the slower increase of dissipation during the second phase can be correlated with an adsorption of the enzyme mainly inside the mesopores.

include, due to the presence of different functional groups, both positively and negatively charged areas on their surface. While the isoelectric point (pI) indicates the overall charge of the protein structure, the electrostatic interactions contributing to the adsorption properties can be governed by the areas of positive or negative charge on the surface, and therefore change even upon pH changes far from the pI of the enzyme. This feature of protein structures also explains the good adsorption of GOD which, according to a pI of 4.2, exhibits an overall negative charge at pH 6.0 and 5.0, but still exhibits a good adsorption in the negatively charged silica particles. Apart from the interactions of positively charged areas of the GOD with the negatively charged silica surface, other interactions such as hydrophobic interactions might also contribute to the stable adsorption.

Additional information on the details of the adsorption processes of the two enzymes GOD and HRP inside the mesopores of the HMM particles was obtained by further evaluation of the frequency and dissipation shifts during the adsorption processes. This analysis indicated two different phases of the adsorption process, where in a first regime the relative fast increasing dissipation indicated a loose adsorption of the enzyme, which was attributed to an adsorption of enzyme on the outer surface of the particles, while in the second regime, the dissipation increase was considerably slower. This second regime was ascribed to an adsorption of enzyme mainly inside the mesopores (**Figure 3.2.4**) [129].

### 3.2.2 QCM-D monitoring of GOD/HRP co-immobilization on $SiO_2$ surfaces

After the successful immobilization of GOD and HRP inside surface adsorbed HMM particles, the combination of this enzyme immobilization procedure with the developed denpol-mediated enzyme immobilization approach *via* the adsorption of denpol-enzyme conjugates was investigated. In a first step, the HMM adsorption process was modified by eliminating the previously necessary modification of the surface used for the immobilization with APTMS to obtain a positively charged, amino functionalized surface. This step, performed by *ex situ* modification of the QCM-D sensors in the previous experiments, was replaced by a simple *in situ* adsorption of the denpol *de*-PG2 from a buffered solution at pH 5.0 on the $SiO_2$ surface of the sensor, yielding a stable layer of *de*-PG2 with exposed amines and ammonium groups.

Interestingly, the QCM-D analysis of the adsorption of *de*-PG2 on the $SiO_2$ coated sensor surface suggested different phases of the adsorption process. While the frequency shift indicated a relatively constant adsorption process forming a stable layer also during

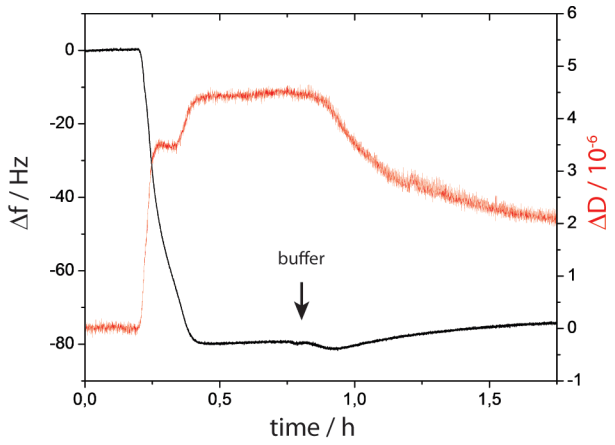


**Figure 3.2.5** QCM-D analysis of the adsorption process of *de*-PG2 on the $SiO_2$ surface of the QCM-D sensor. Different phases for the adsorption process are observed, exhibiting an intermediate plateau in the dissipation curve during the adsoption. During rinsing with buffer, the decreasing dissipation signal and almost stable frequency indicated a compaction of the adsorbed *de*-PG2 layer.

the subsequent rinsing step, the change in dissipation indicated major rearrangements occurring in the adsorbed denpol layer during the adsorption process as well as during the subsequent rinsing step (**Figure 3.2.5**). A possible explanation for such a behavior might be a stepwise process, with a first adsorption of the denpol chains forming loops on the surface, which in a later phase come into closer contact with the surface as well, resulting in a compaction of the adsorbed layer.

After establishing the adsorption of the denpol *de*-PG2 for the formation of a positively charged surface, the immobilization of the HMM particles was performed on this surface. Using a suspension of the HMM particles in a solution buffered at pH 5.0, the adsorption of the particles on the *de*-PG2 coated surface was more efficient than in the previous setup using the APTMS modified surface, as indicated from the frequency shift observed in the QCM-D analysis of the adsorption process. This means that a larger amount of particles adsorbed if *de*-PG2 was used as compared to the APTMS treated surface. A SEM analysis of the surfaces of QCM-D sensors after the adsorption of HMM

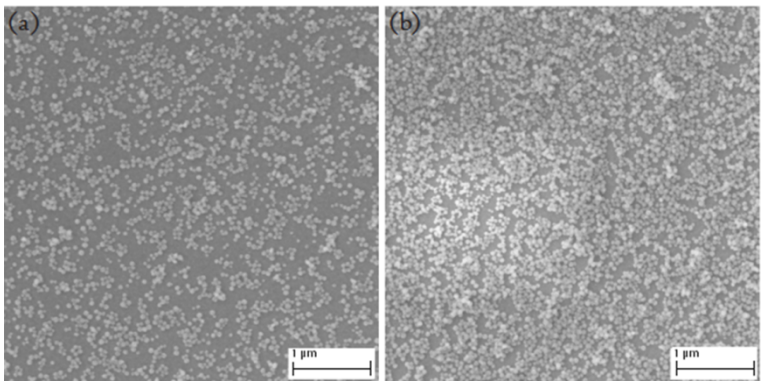


**Figure 3.2.6** SEM images of the $SiO_2$ surfaces of QCM-D sensors after adsorption of HMM particles on **a)** an APTMS modified sensor and **b)** a sensor with *in situ* adsorbed *de*-PG2 for the preparation of a positively charged surface before silica particle adsorption.

particles on APTMS modified and *de*-PG2 coated sensors indicated as well an increased surface coverage in the case of the *de*-PG2 coating (**Figure 3.2.6**). Therefore, the optimized system using the *de*-PG2 layer instead of the APTMS surface modification was used for the further enzyme immobilization experiments.

After adsorption of the HMM particles on the *de*-PG2 coated surface, the mesoporous particles were loaded with enzymes according to the conditions elaborated in the loading studies of the HMM particles described above. Two setups for the co-immobilization of GOD and HRP were investigated, one containing the GOD inside the HMM particles, coated with an additional layer of adsorbed *de*-PG2-BAH-HRP as the second enzyme containing layer, and a reversed system containing the HRP inside the HMM layer, coated with a subsequently adsorbed *de*-PG2-BAH-GOD layer.

Observation of the QCM-D signal during the adsorption of *GOD inside the HMM particles* on the *de*-PG2 layer indicated a good loading of the mesoporous particles with the enzyme as observed from the frequency shift during the adsorption process, while the increase in dissipation was relatively small, again attributed to the fact that the enzyme mainly adsorbed inside the porous structures, which reduced the contribution of the adsorbed GOD to the dissipation shift (**Figure 3.2.7**). In a last step, *de*-PG2-BAH-HRP was adsorbed as a covering layer, resulting in a distinct increase in dissipation as well as a

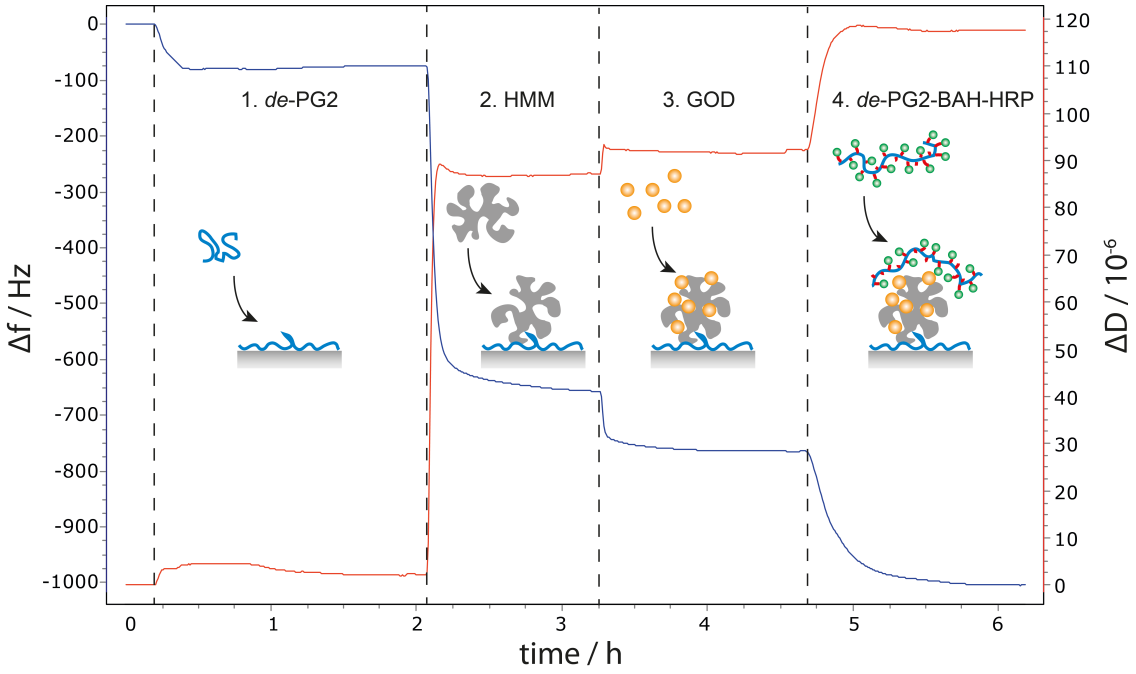


**Figure 3.2.7** QCM-D analysis of the co-immobilization of GOD and HRP. At pH 5.0, *de*-PG2 was adsorbed on the $SiO_2$ surface of the QCM-D sensor in order to render the surface positively charged. After subsequent adsorption of HMM particles on the surface, the particles were loaded with GOD. At this stage, the buffer was changed to a pH of 7.0, and the last step of the assembly, the adsorption of *de*-PG2-BAH-HRP, was carried out at pH 7.0. Each adsorption step was followed by a rinsing step with buffer in order to remove excess of material from the QCM-D flow cell.

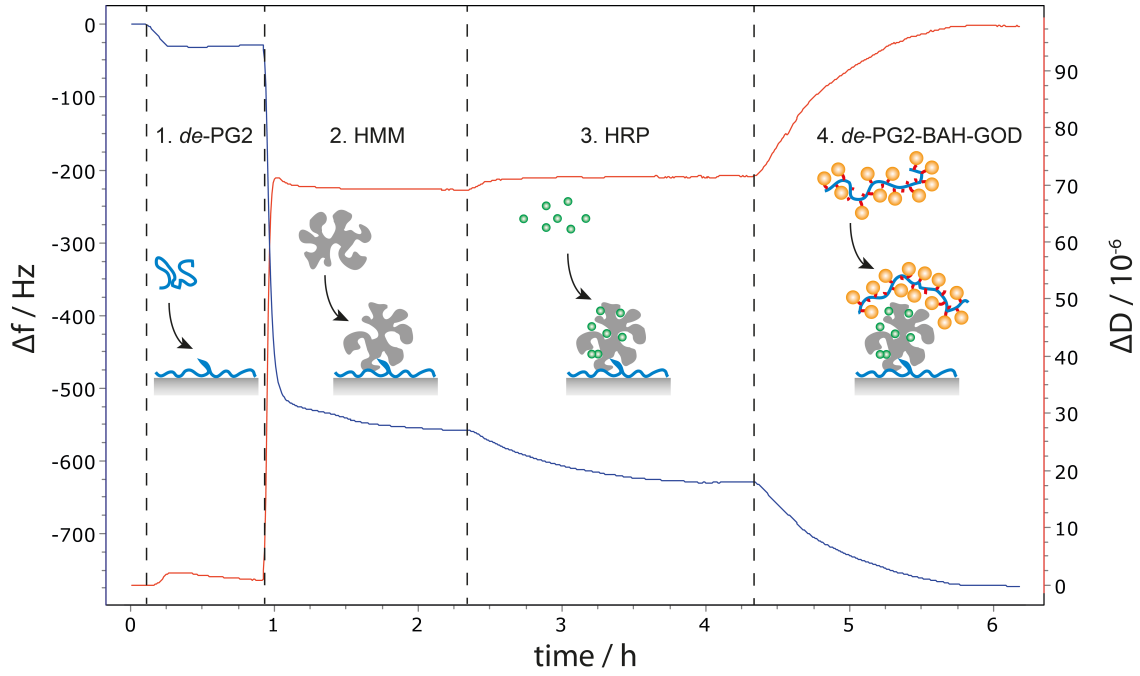


**Figure 3.2.8** QCM-D analysis of the co-immobilization of HRP and GOD. *De*-PG2 was adsorbed on the $SiO_2$ surface of the QCM-D sensor, followed by adsorption of the HMM particles, loading of the particles with HRP and adsorption of *de*-PG2-BAH-GOD as a covering layer. All adsorption steps were carried out at pH 5.0 and each adsorption step was followed by a rinsing step with buffer in order to remove excess of material from the QCM-D flow cell.

decrease in the frequency. This step was found to proceed more efficient when the pH of the solution was increased from 5.0 to 7.0. Adsorption of the denpol-enzyme conjugate on top of the structure presented by the adsorbed HMM particles is expected to result in a rough surface morphology, consistent with the large increase in dissipation observed during the adsorption process. Even though this would suggest that, at least to some extent, flexible parts of the denpol-enzyme conjugate chains exist which are not directly adsorbed on the HMM particles, no desorption during the following rinsing with buffer was observed, indicating a stable adsorption of the *de*-PG2-BAH-HRP layer without significant desorption. The increased amount of adsorbed *de*-PG2-BAH-HRP when the adsorption was performed at pH 7.0 instead of 5.0 might be caused by the fact that the surface of the HMM accessible for *de*-PG2-BAH-HRP adsorption was partially covered with GOD, which presents only a small negative charge at pH 5.0 (pI = 4.2). Upon an increase of the solution pH to 7.0, the GOD should hold a more distinct negative charge, contributing to the overall negative charge of the surface of the GOD loaded HMM particles, and therefore promoting efficient adsorption of the *de*-PG2-BAH-HRP conjugate.

The corresponding setup containing *HRP inside the HMM particles* and a covering layer of *de*-PG2-BAH-GOD was prepared in an analogous way (**Figure 3.2.8**). Upon adsorption of a *de*-PG2 layer rendering the $SiO_2$ surface positively charged, the HMM particles were adsorbed and loaded with HRP, followed by an adsorption of a *de*-PG2-

BAH-GOD layer. In this setup, all the adsorption steps were carried out at pH 5.0, without a buffer exchange to pH 7.0 as needed in the case of the system featuring the HRP in the top layer formed by the denpol-enzyme conjugate. As seen for GOD before, the HRP adsorption inside the mesoporous HMM particles resulted only in a small increase in dissipation as monitored by QCM-D, while in the subsequent step of *de*-PG2-BAH-GOD adsorption, the increase in dissipation was considerable. This indicted again an immobilization of the HRP molecules mainly inside the pores of the mesoporous particles, while the adsorption of the denpol-enzyme conjugate forming the top layer resulted in a structure with considerable flexibility, resulting in a high contribution to the dissipation measured by QCM-D.

The results of the QCM-D analysis of the co-immobilization procedure for GOD and HRP indicated a successful enzyme immobilization in two different setups. The buildup of the layered structure consisting of a deposition of *de*-PG2 on the $SiO_2$ surface of the QCM-D sensor, followed by adsorption of HMM particles, loading of the particles with a first type of enzyme, and subsequent formation of an additional layer containing the second type of enzyme by deposition of the corresponding denpol-enzyme conjugate was demonstrated for the arrangement containing GOD inside the mesoporous layer and HRP in the denpol-enzyme conjugate layer as well as the reverse system containing HRP inside the mesoporous layer and GOD in the denpol-enzyme conjugate layer.

### 3.2.3 Activity and stability of co-immobilized GOD and HRP using mesoporous silicates and denpol-BAH-enzyme conjugates

After the successful preparation of the two systems containing co-immobilized GOD and HRP as demonstrated by QCM-D, the catalytic activity of the systems produced upon use of this methodology was investigated. For this, clean, round silicate glass microscopy coverslips with a diameter of 8 mm were used as substrate for the immobilization. The immobilization protocol as elaborated in the QCM-D studies of the co-immobilization system was applied for the adsorption on the glass surfaces. For the stepwise coating of the microscopy glass coverslips, a polypropylene tube containing the glass coverslip was filled with the corresponding solutions containing the individual components necessary for the buildup of the adsorbed layers. After the adsorption, the solutions were removed from the tube and the coverslips washed with buffer to remove remaining non-bound material from the storage tubes. Finally, the glass coverslips were stored in buffer at pH 7.0 at 4 °C in the tubes until further use.

For the measurement of the enzymatic activity, the storage buffer solution was removed from the tubes containing the glass coverslips with the immobilized enzymes, and a solution containing a chromogenic substrate was added. After a defined incubation time, the substrate solutions were removed and the conversion of substrate to product was measured by UV/vis spectrophotometry. The glass coverslips with the adsorbed enzymes were washed and stored in buffer at pH 7.0 at 4 °C until further use.

For a quantitative analysis of the activity of the immobilized enzymes, the values obtained from the activity assays were compared to a calibration curve obtained from enzymatic activities measured for known concentrations of native enzyme in bulk solution. Considering the geometry of the round glass coverslips with a diameter of 8 mm, the total surface of such a glass coverslip was calculated to be 1 $cm^2$. Adjusting the volume of the substrate solution added to the glass coverslip to 1 mL, the measured product formation could be correlated to an apparent concentration of enzyme in this volume. The amount of active enzyme measured in this volume corresponded to the amount of active enzyme on the 1 $cm^2$ surface exposed to the solution, resulting in an apparent surface concentration of the enzyme assayed. This methodology includes, as already discussed in the case of the denpol-enzyme conjugates adsorbed directly on the microscopy glass coverslips, the assumption of similar catalytic constants for the immobilized enzymes as compared to the dissolved enzyme. Even though this assumption might not be valid in all cases, the obtained values for an apparent surface concentration of the enzymes are of interest for comparing the efficiency of such an enzyme immobilization methodology with other immobilization procedures.

For the determination of the activity of immobilized HRP on the glass surfaces, a substrate mixture containing 0.2 mM $H_2O_2$ and 1 mM $ABTS^{2-}$ was used. HRP catalyzed the oxidation of the chromogenic substrate $ABTS^{2-}$ to the chromophore $ABTS^{\bullet-}$. The conversion was monitored by UV/vis spectrophotometry, quantifying the emergent absorption band at 414 nm ($\varepsilon_{414nm}$ = 36000 $M^{-1}cm^{-1}$ [85]). For low apparent surface concentrations of HRP as observed in the setup where HRP was immobilized inside the HMM particles, OPD (3.14 mM) was used as an alternative chromogenic substrate in combination with 80 µM $H_2O_2$. In contrast to the $ABTS^{\bullet-}$ radical formed upon oxidation of $ABTS^{2-}$, the oxidation product of OPD undergoes further dimerization and non-enzymatic oxidation, yielding the stable DAP as product ($\varepsilon_{418nm}$ = 16700 $M^{-1}cm^{-1}$ [133]). This allowed for elongated reaction times during the activity assay and therefore for a significantly lower detection limit as compared to the standard assay with $ABTS^{2-}$ (about 10 pM HRP with OPD *vs.* about 0.25 nM HRP with $ABTS^{2-}$).

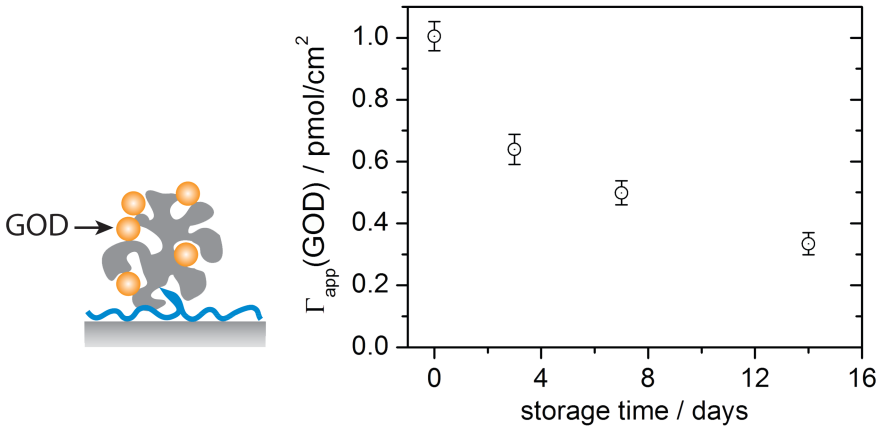


**Figure 3.2.9** Stability of GOD immobilized in HMM particles adsorbed on a *de*-PG2 coated surface. The apparent surface concentration of GOD was determined by comparison of the activity of a defined surface with the activity of known amounts of GOD in solution. The samples were stored at pH 7.0 at 4 °C.

For the determination of the GOD activity, the same coupled assay system as already used for the determination of the GOD activity of *de*-PG2-BAH-GOD adsorbed directly on the glass surface was exploited. A solution containing 3.45 mM D-glucose, dissolved $O_2$ (approximately 0.25 mM [126]), 3.14 mM OPD and 2 nM HRP was used as assay mixture. In this setup, GOD catalyzed the oxidation of D-glucose by $O_2$, yielding glucono-δ-lactone and $H_2O_2$. In a subsequent step, the $H_2O_2$ produced was quantified by the HRP catalyzed oxidation of OPD yielding the chromophore DAP. For all determinations of the apparent surface concentrations, the macroscopic surface area of the coverslips was considered, and not the microscopic surface area of the mesoporous particles.

In a first step, the activity of the GOD adsorbed inside the HMM particles was measured before the adsorption of the covering *de*-PG2-BAH-HRP layer. Comparison with the activity of native enzyme in solution indicated an apparent surface concentration of

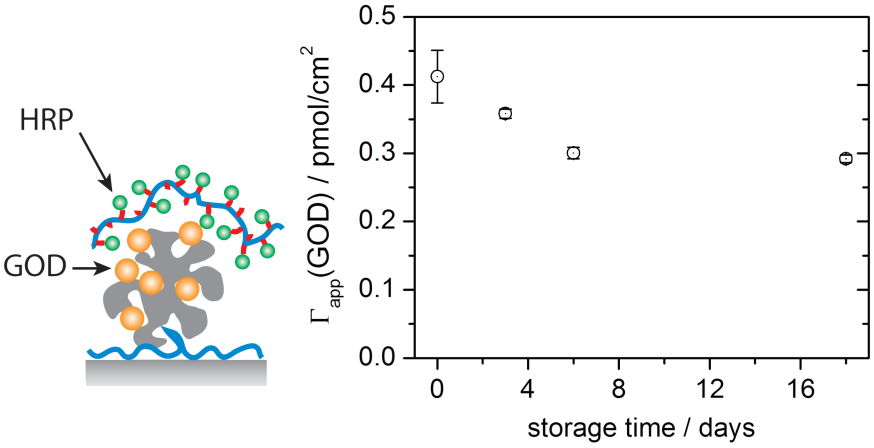


**Figure 3.2.10** Stability of the GOD immobilized in HMM particles adsorbed on *de*-PG2 after deposition of a covering layer of *de*-PG2-BAH-HRP. Presence of additional HRP in the assay solution did not result in an increase in product formation, indicating efficient conversion of the intermediate $H_2O_2$ by the immobilized HRP. The samples were stored at pH 7.0 at 4 °C.

GOD of 1.0 pmol/cm² (**Figure 3.2.9**). Upon storage of the glass coverslips in buffer at pH 7.0 at 4 °C, the activity decreased to about 30 % of the initial activity within 14 days, as determined by repeated measurements of the remaining activity. The reduction of the enzymatic activity detected was attributed to a leakage of GOD from the porous structure of the HMM particles on the surface, which resulted in loss of enzyme during storage and the rinsing steps performed before and after the activity measurements.

After the determination of the apparent surface concentration of the GOD loaded HMM layer, the corresponding glass slides decorated with the complete setup for the co-immobilization, including as well the coating layer of *de*-PG2-BAH-HRP, were analyzed for enzymatic activity. Determination of the HRP activity of the top layer indicated a high apparent surface concentration of HRP corresponding to 8 pmol/cm². The GOD activity measured for the *de*-PG2-BAH-HRP covered layer of GOD loaded HMM particles was determined as 0.4 pmol/cm². This indicated a reduced GOD activity as compared to the non-covered GOD loaded HMM particles. Interestingly, in a measurement determining the activity of the surface localized cascade reaction, *i.e.* an activity assay as performed for the determination of the GOD activity but without additional HRP in the assay solution, resulted in the same amount of product formation as in the case where additional HRP was added to the assay solution. This indicated that the covering layer of *de*-PG2-BAH-HRP was efficient for the conversion of the $H_2O_2$ produced in the lower GOD layer. Therefore, these measurements demonstrate a good efficiency of the cascade reaction in this setup, but a reduced overall activity of GOD as indicated by the apparent surface concentration of 0.4 pmol/cm² as compared to the 1.0 pmol/cm² for the GOD loaded HMM particles without the *de*-PG2-BAH-HRP covering layer.

In a further investigation of the storage stability of the co-immobilized enzymes, the covering of the GOD loaded HMM particles with the *de*-PG2-BAH-HRP layer was shown to result in an increased retention of enzymatic activity of GOD during storage, with a decrease of only about 30 % during 18 days of storage (**Figure 3.2.10**) as compared to about 70 % within 14 days in the case of the non-covered GOD loaded HMM particles. This increased storage stability seen for the GOD activity was attributed to a reduced desorption and leakage of GOD from the mesoporous HMM particles due to the covering of their surface with *de*-PG2-BAH-HRP. A similar effect of decreased leakage of immobilized enzymes from mesoporous structures upon coating of the mesoporous particles with polyelectrolytes has been described by Wang and Caruso [134, 135].

After demonstrating the good activity of both enzymes in a setup with GOD loaded HMM covered with the *de*-PG2-BAH-HRP conjugate, the reversed system featuring the

HRP in the mesoporous particles and GOD as part of the denpol-enzyme conjugate was investigated as well for activity. For the as adsorbed HRP loaded HMM layer not covered with *de*-PG2-BAH-GOD, an HRP activity corresponding to an apparent surface concentration of 0.05 pmol/cm$^2$ was measured. While the frequency shifts measured by QCM-D during the loading of HRP or GOD in the HMM particles were comparable for both enzymes, the apparent surface concentrations determined by the catalytic activity of the enzyme indicated large differences. The value of 0.05 pmol/cm$^2$ obtained for HRP was drastically lower than the values measured before in the case of GOD inside the HMM particles. This low activity of the immobilized HRP might be caused by different effects: i) A hindered access to the active site of HRP inside the mesopores, preventing proper substrate binding, ii) conformational changes in the HRP structure upon adsorption of the enzyme within the mesopore resulting in an inactivation, or iii) the different local microenvironment within the mesopores. Such effects, which are governed by the intrinsic properties of the mesoporous materials used, have been shown to have a strong influence on the success of HRP immobilization approaches using mesoporous silicates [136, 137].

After adsorption of the covering *de*-PG2-BAH-GOD layer on the HRP loaded HMM particles, the measured HRP activity was reduced from 0.05 pmol/cm$^2$ to an apparent surface concentration of 0.03 pmol/cm$^2$. At the same time, the GOD activity measured in this system corresponded to 0.9 pmol/cm$^2$. In an assay for the surface localized cascade reaction catalyzed by the denpol conjugated GOD present as a covering layer on the HMM particles, and HRP inside the pores of the particles – without addition of HRP in the assay solution – no product formation was detected. This observation was in strong contrast to the situation when GOD was immobilized in the HMM and HRP as the denpol-enzyme conjugate, where the rate of product formation was dominated by the GOD concentration and addition of HRP in solution did not change the overall rate of the reaction.

Considering the large excess of GOD activity compared to HRP activity in this system, a situation where the HRP activity dominates the rate of the cascade reaction might have been expected. Instead, the absence of any detectable product formation from a cascade reaction catalyzed by the two co-immobilized enzymes in this setup indicated a more complex situation as in the case when GOD was immobilized in the lower HMM layer and HRP in the covering denpol-enzyme conjugate layer. A possible reason for this observation could be the loss of the intermediate $H_2O_2$ to the bulk solution, which might be favored in an arrangement including the GOD producing the intermediate in the covering layer and the HRP converting the intermediate in the lower layer and in an environment

disfavoring an efficient HRP reaction as observed from the low apparent surface concentration determined *via* the catalytic activity.

Focusing on the setup with GOD loaded HMM particles and the *de*-PG2-BAH-HRP conjugate which showed a good enzymatic activity and an efficient surface localized cascade reaction, the role of GOD adsorption inside the mesoporous particles was further investigated. As the stepwise adsorption of the HMM particles and subsequent loading of the adsorbed HMM with GOD was prone to additional non-specific adsorption of GOD on the *de*-PG2 coated surface, GOD loaded HMM was first prepared in solution and purified by repeated sedimentation and buffer exchange to remove non-bound GOD from the solution. Such preloaded HMM was then used for the adsorption on a *de*-PG2 coated surface, and enzymatic activity measurements indicated a decreased GOD activity corresponding to an apparent surface concentration of about 0.5 pmol/cm² (**Figure 3.2.11**) as compared to 1.0 pmol/cm² in the stepwise buildup on the surface with *in situ* loading of the HMM particles with GOD. Upon addition of the covering de-PG2-BAH-HRP layer on these adsorbed, preloaded HMM particles, the GOD activity decreased to an apparent surface concentration of 0.25 pmol/cm² (**Figure 3.2.12**). Therefore, this approach using GOD preloaded HMM particles allowed a more defined buildup of the layered system for the co-immobilization of GOD and HRP with a minimized non-specific adsorption of GOD on the supporting *de*-PG2 layer. On the other hand, the activity and stability of this system was reduced as compared to the corresponding setup formed by in situ loading of the HMM particles.

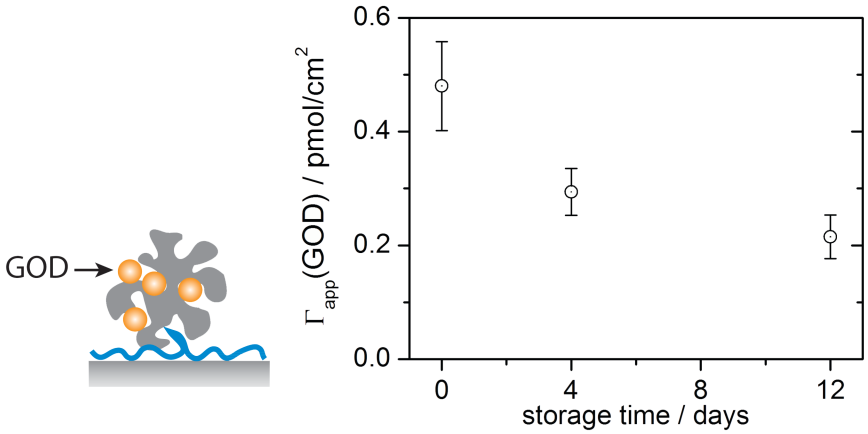


**Figure 3.2.11** Stability of GOD immobilized by adsorption of GOD loaded HMM particles on *de*-PG2. The apparent surface concentration of GOD was determined by comparison of the activity of a defined surface with the activity of known amounts of GOD in solution. The samples were stored at pH 7.0 at 4 °C.

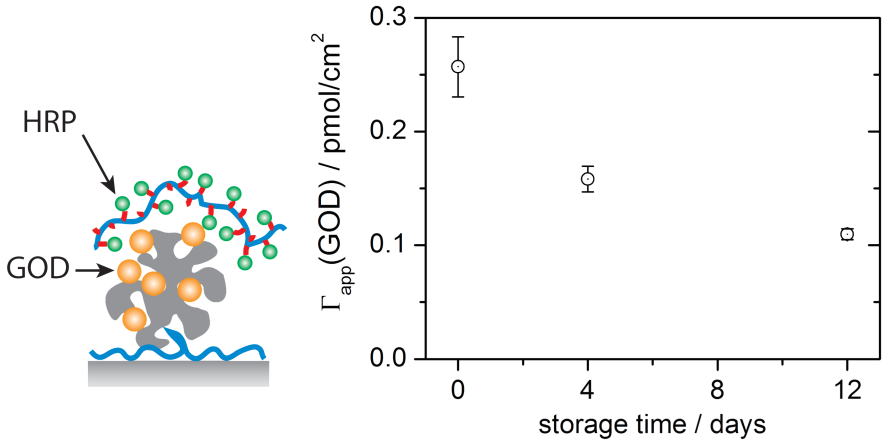


**Figure 3.2.12** Stability of GOD immobilized by adsorption of GOD loaded HMM particles on *de*-PG2 after deposition of a covering layer of *de*-PG2-BAH-HRP. The samples were stored at pH 7.0 at 4 °C.

### 3.2.4 Conclusions

The combination of the two different enzyme immobilization techniques, adsorption in mesoporous silica particles and the denpol-mediated immobilization on silicate surfaces, allowed the development of a system for a localized co-immobilization of two different types of enzymes. The adsorption of a layer of *de*-PG2 on a $SiO_2$ surface was demonstrated to allow simple adsorption of HMM particles on this surface. This layer of adsorbed mesoporous particles was used for the immobilization of a first type of enzyme, GOD or HRP, within the mesoporous structures. The addition of the second enzyme as a covering layer formed by adsorption of the corresponding denpol-enzyme conjugate on top of the first layer was successful. All the adsorption processes could be characterized *in situ* by QCM-D.

It was found that the order in which the two enzymes were immobilized in the layered structure is of great importance. If the GOD was immobilized inside the HMM particles and the HRP as the covering *de*-PG2-BAH-HRP layer, a good enzymatic activity and an efficient cascade reaction catalyzed by the two co-immobilized enzymes was observed. In the case of HRP immobilization within the HMM particles and a covering layer of *de*-PG2-BAH-GOD, the activity of HRP inside the particles was poor and the cascade reaction did not occur. These findings indicate the importance of a proper choice for the immobilization protocol and setup for the successful co-immobilization of enzymes to enable catalytic cascade reactions.

## 3.3 Immobilization of proK with *de*-PG2-BAH-proK on $SiO_2$ surfaces

Complementary to the advantages of denpol-enzyme hybrid structures for the controlled co-immobilization of enzymes for cascade reaction systems as demonstrated above (**chapters 3.1 & 3.2**)in the case of GOD and HRP, such conjugates offer further promising properties. The propensity of the polycationic denpol to adsorb on supports exhibiting a negative surface charge combined with a multiplication of the adsorption forces acting between a single enzyme and a solid support through the formation of hybrid structures carrying multiple copies of the enzyme on the denpol chain also exploited the intrinsic property of many enzymes to adsorb on silicate surfaces. While the adsorption of a single enzyme on a $SiO_2$ surface is often transient and therefore enzyme immobilization via non-covalent adsorption is accompanied by considerable enzyme desorption during storage and operation [138], the non-covalent adsorption of the denpol-enzyme conjugates allowed a stable enzyme immobilization without the necessity of any chemical surface modification.

A case of special interest for the use of immobilized enzymes is in the area of miniaturized devices for the enzymatic degradation of compounds for analytical purposes. In order to exploit the advantages of miniaturization possible in the field of microchip fabrication for proteomic studies, various approaches for on chip immobilization of proteases have been undertaken [139-143]. One of the key approaches for the immobilization of enzymes in microfluidic channels is based on the use of magnetic nanoparticles as support, and subsequent immobilization of the enzyme coated magnetic nanoparticles within the microfluidic channels [139, 144, 145]. Such approaches have shown to allow a good enzyme loading in the channel, but are often accompanied by leakage of the particles from the chip [146]. Other approaches such as direct covalent linkage of the enzyme require multistep chemical immobilization procedures to be performed on chip [147, 148]. Therefore, da Costa *et al.* clearly pointed out the challenge of developing protease immobilization systems avoiding possible leaking of particles or beads for downstream application, and devoid of extensive chemical modifications of the microchannels [146].

### 3.3.1 Preparation of *de*-PG2-BAH-proK

In order to investigate the possible use of a denpol-enzyme conjugate for the stable immobilization of a protease, the serine protease proteinase K (proK) was selected for further studies. In a first step, the modification of proK with a 4FB linker moiety was performed in order to allow further linking to the modified denpol *de*-PG2-HyNic. Reaction

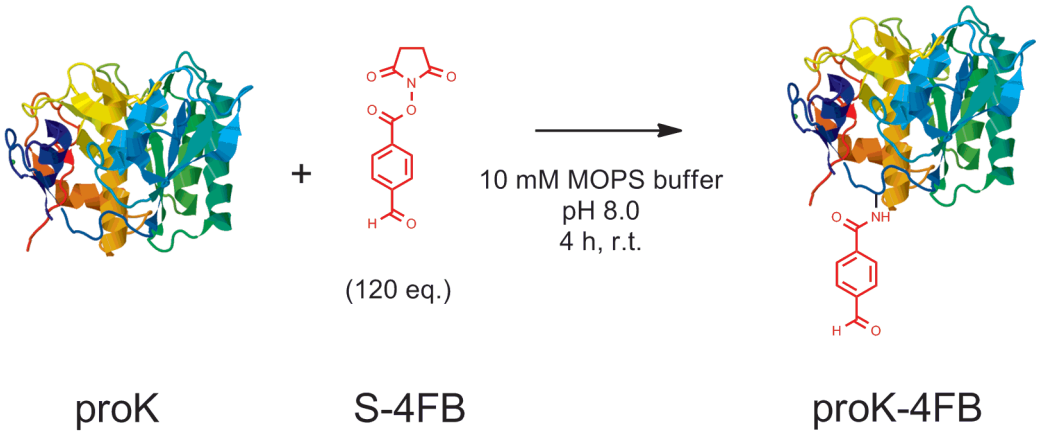


**Figure 3.3.1** Modification of proK with the 4FB linker. The activated S-4FB linker was reacted with nucleophiles present on the surface of proK, presumably amino groups of lysine side chains or the N-terminal amine. A large excess of S-4FB had to be used in order to obtain a reasonable modification ratio of approximately 1 linker/proK, likely due to a hydrolytic activity of the proteins active site towards the linker reagent.

of proK with S-4FB proceeded only with a considerable higher excess of reactive linker species as compared to the cases of HRP and GOD described above. This was attributed to a preferred hydrolysis, which was ascribed to the hydrolytic activity of proK. The residual hydrolytic activity of proK towards S-4FB, even though far from a natural substrate, combined with the ease of hydrolysis for this activated ester, was expected to result in a considerable loss of linker reagent in the reaction mixture. An increase of the pH to 8.0 instead of 7.2 as used in the case of HRP and GOD resulted in an increased modification of proK. This was attributed to the availability of more neutral amino groups on the protein surface at higher pH, and therefore a more efficient reaction of such amino groups as nucleophiles for the aminolysis of the S-4FB linker yielding the modified proK-4FB (**Figure 3.3.1**).

Optimizing the S-4FB/proK ratio for a modification of proK with a 4FB linker moiety, the same considerations as in the case of the corresponding modification of HRP and GOD had to be made. The presence of proK molecules modified with more than one linker moiety needed to be reduced to a minimum in order to avoid crosslinking of the denpol chains during the conjugation reaction. In the case of proteinase K, the moderate size of 28930 Da allowed a mass spectrometric (MS) analysis of the modified proK-4FB. A removal of non-modified proK from proK-4FB was not attempted and might not be feasible due to the small differences between the two species. The MS analysis of proK-4FB prepared with 100, 120 and 200 equivalents of S-4FB indicated the modification of proK with the 4FB moiety by appearance of an additional peak at 29062 Da in the deconvoluted spectrum (**Figure 3.3.2**). Additionally, at higher S-4FB/proK ratios, a signal corresponding to a doubly modified proK (proK-$(4FB)_2$: 28930 Da + 2 x 132 Da = 29194 Da) was visible (**Figure 3.3.2f&h**).

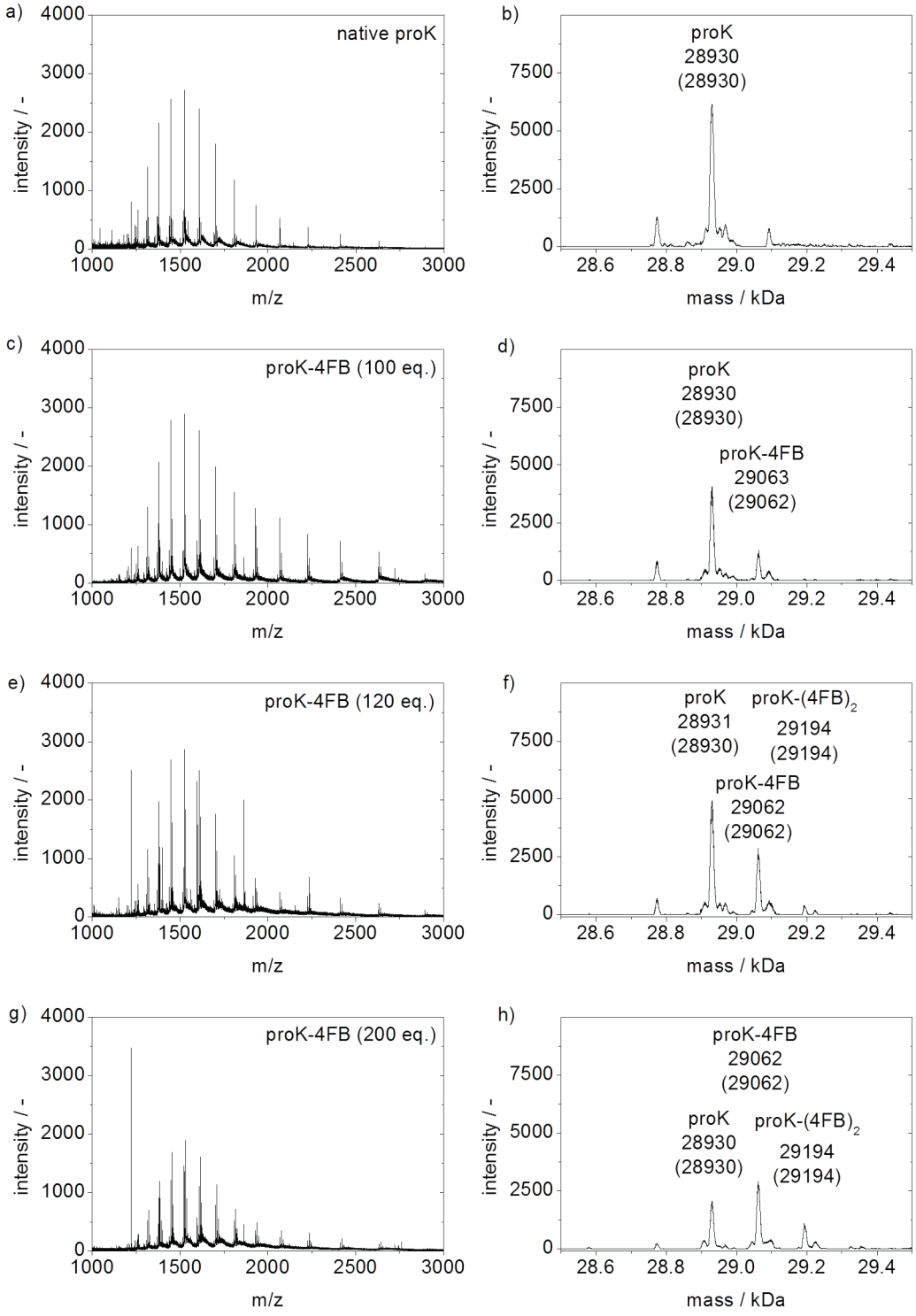


**Figure 3.3.2** MS analysis of the linker attachment to proK using different S-4FB/proK ratios in the modification reactions. Spectra of the multiply charged species and the corresponding deconvoluted spectra are given **a&b)** for native proK, and the S-4FB/proK ratios of **c&d)** 100/1, **e&f)** 120/1, and **g&h)** 200/1, respectively. The measured values are indicated in the deconvoluted spectra and the calculated values are given in parentheses.

Using 120 eq. of S-4FB for the synthesis of proK-4FB resulted in a tolerable small amount of proK-$(4FB)_2$ in order to use the obtained proK-4FB solution for the synthesis of

a *de*-PG2-BAH-proK conjugate. Even though a quantitative comparison of the different species according to the observed intensities could not be performed, it seemed evident that the presence of multiply modified species such as proK-$(4FB)_2$ became relevant at levels where there was still a considerable amount of native proK available. This could be explained by the fact that at pH 8.0 several similarly reactive neutral amino groups were present on the surface of a proK molecule, which leads to a statistical distribution of 4FB linkers on these modification sites. While a lower pH could enable the discrimination of different modification sites due to different $pK_A$ values of the involved amino groups according to their different environment, such an approach was excluded by the property of proK to hydrolyze the S-4FB reagent efficiently. Therefore, the conjugation experiments were performed using proK-4FB as obtained from a modification reaction using 120 eq. of S-4FB.

The denpol used for the synthesis of *de*-PG2-BAH-proK was similar to the one used for the synthesis of the denpol-enzyme conjugates containing HRP and GOD, featuring the same structure of the repeating unit but with a $P_n$ of 2000 and a PDI of 4.3 (it is therefore abbreviated here as *de*-$PG2_{2000}$). Upon modification of *de*-$PG2_{2000}$ with S-HyNic similar as described above (**chapter 3.1.2**), a denpol carrying about 500 HyNic moieties was obtained. As the solubility of proK was limited at high ionic strength, a modified

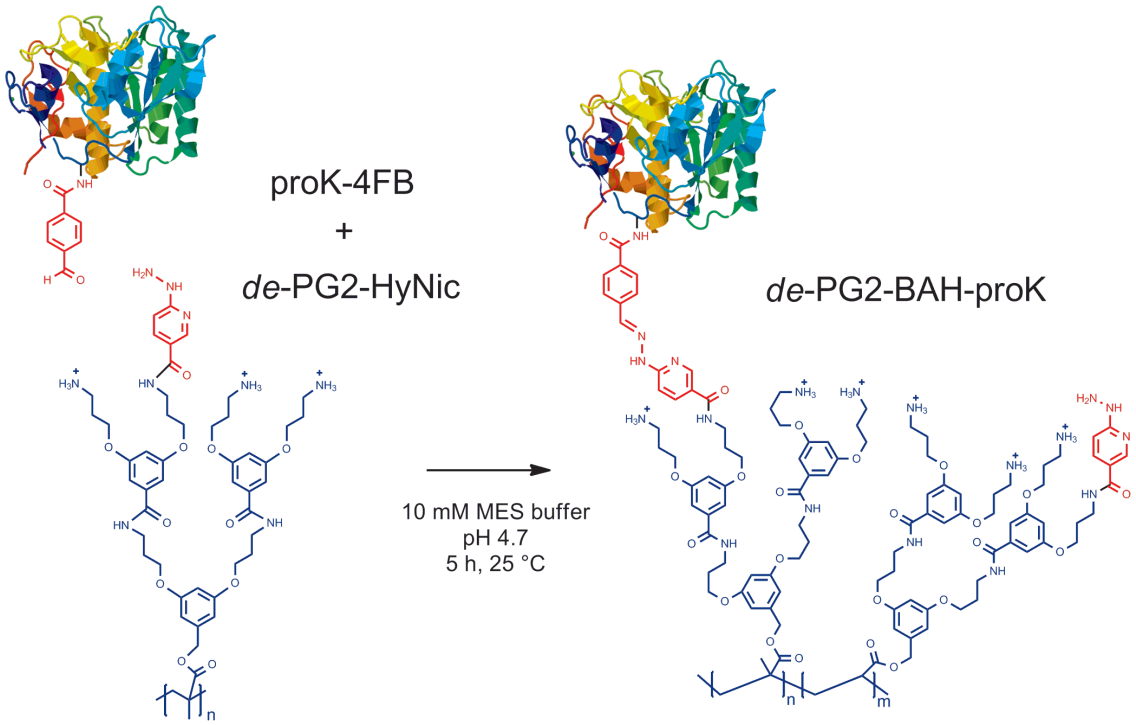


**Figure 3.3.3** Conjugation reaction of *de*-PG2-HyNic and proK-4FB. Upon reaction of the 4FB moiety on the proK and the HyNic moiety at the periphery of denpol, the enzyme is covalently linked to the denpol. Quantification of the concomitant emergence of the BAH absorption band by UV/vis spectrophotometry allowed a determination of the amount of enzyme bound in the *de*-PG2-BAH-proK conjugate.

conjugation buffer (10 mM MES, pH 4.7) was used to ensure solubility of all components during the conjugation reaction (**Figure 3.3.3**).

The conjugation reaction of *de*-PG2-HyNic and proK-4FB was performed at a ratio of 2/1 HyNic/4FB linkers, and monitored by UV/vis spectrophotometry, exploiting the characteristic BAH absorption band at 354 nm (**Figure 3.3.4**). Evaluation of the increasing absorption of the BAH bond indicated no further significant changes after about 5 h of reaction (**Figure 3.3.4c**). The increase in absorbance at 354 nm of 0.080 absorption units during this time indicated the formation of BAH bonds corresponding to a concentration of 28 µM ($\varepsilon_{354nm}$ = 29000 $M^{-1}cm^{-1}$, [113]), and assuming the binding of one proK molecule upon each BAH bond formation, the addition of the same amount of proK to the denpol chains. In a reaction mixture containing *de*-PG2-HyNic at a repeating unit concentration of about 400 µM, this corresponded to the attachment of about 140 molecules of proK on an average denpol chain of 2000 r.u. The obtained denpol-enzyme conjugate was therefore designated as *de*-$PG2_{2000}$-BAH-$proK_{140}$. To remove the remaining non-bound enzyme,

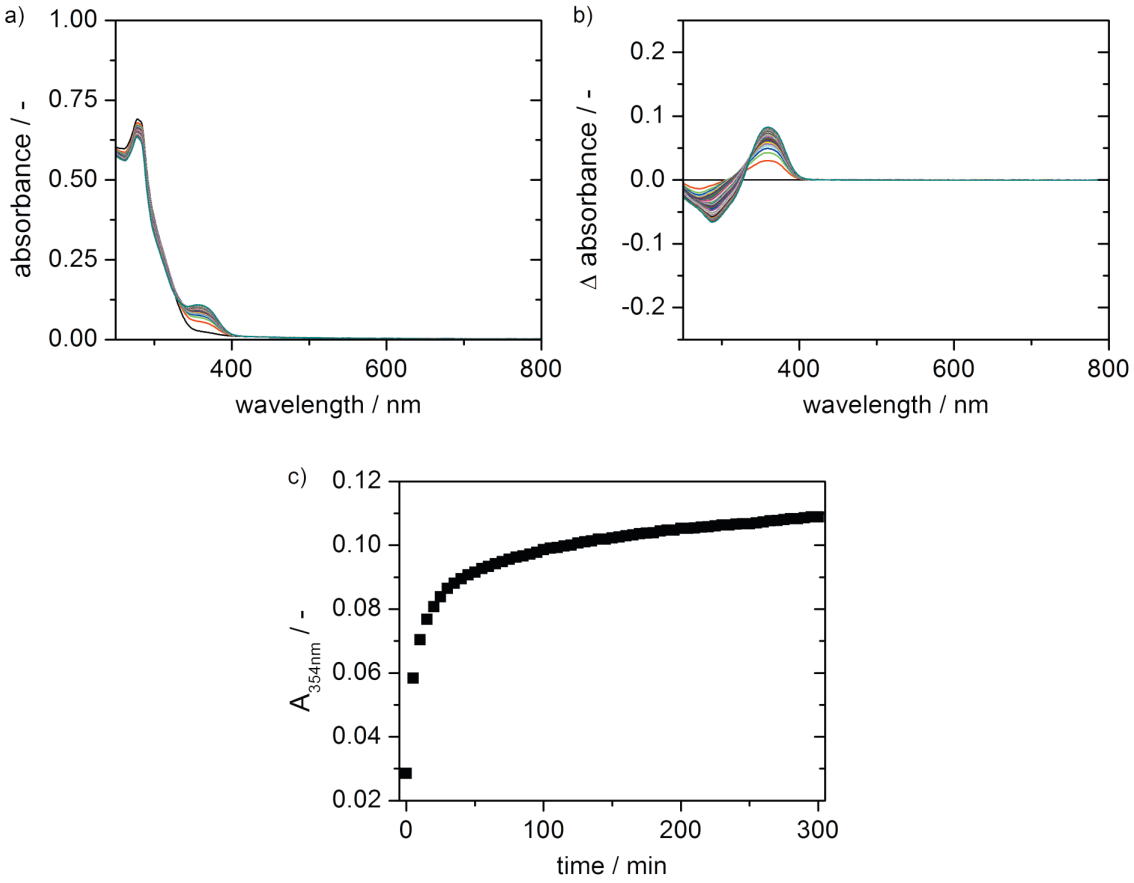


**Figure 3.3.4** *In situ* UV/vis spectrophotometric monitoring of the conjugation of *de*-PG2-HyNic and proK-4FB yielding *de*-PG2-BAH-proK. **a)** UV/vis spectra of the reaction solution recorded at intervals of 5 min. **b)** Difference spectra obtained by subtraction of the initial spectrum measured at t = 0 min. The emerging peak of the BAH bond at 354 nm could be quantified to determine the amount of bound proK on the *de*-PG2-BAH-proK. **c)** The increase in absorbance at 354 nm indicated no further significant increase after about 5 hours of reaction time.

comprising proK-4FB which did not react with the denpol, as well as native proK still available in the proK-4FB solution after the enzyme modification as discussed above, the reaction mixture was purified by repetitive ultrafiltration, yielding the *de*-PG2$_{2000}$-BAH-proK$_{140}$ conjugate in a buffered solution.

### 3.3.2 Enzymatic activity of *de*-PG2-BAH-proK in solution

After successful synthesis of the *de*-PG2-BAH-proK conjugate, the enzymatic activity of proK in this conjugate was investigated. In the previous cases of HRP and GOD, the UV/vis signature of the prosthetic heme and FAD group, respectiviely, interfered with the absorption band of the BAH linker and prevented an exact quantification of the enzyme concentration in a solution containing the conjugate. This hindered a quantitative evaluation of the catalytic properties of the enzymes in the corresponding denpol-enzyme conjugates. In the case of HRP, a fluorescent label on the denpol had been used in an earlier study to evaluate the kinetic parameters of a similar conjugate [64].

In the case of *de*-PG2-BAH-proK, the BAH bond was the only UV/vis active moiety at 354 nm and therefore a quantification of the BAH concentration in a solution of *de*-PG2-BAH-proK could be performed UV/vis spectrophotometrically. Under the assumption of each BAH bond corresponding to one proK molecule, the determined BAH concentration corresponded to the proK concentration of the *de*-PG2-BAH-proK solution. Such an exact determination of the enzyme concentration is essential for a meaningful investigation of the kinetic parameters of the enzyme according to Michaelis-Menten kinetics.

Enzymatic activity assays were performed in 10 mM MOPS buffer at pH 7.0 with

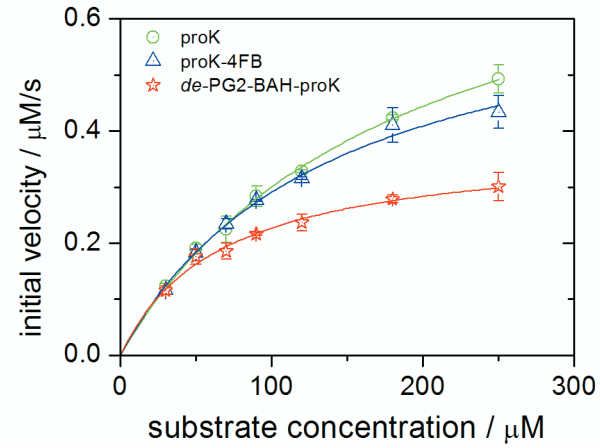


**Figure 3.3.5** Michaelis-Menten kinetics of the native proK, the modified proK-4FB and *de*-PG2-BAH-proK. The kinetic measurements were performed at room temperature at pH 7.0 using Suc-AAPF-pNA as substrate and with enzyme concentrations of 5 nM for proK and proK-4FB, and 16.5 nM for *de*-PG2-BAH-proK. The continuous lines indicate the fitted curve to the Michaelis-Menten equation.

substrate concentrations between 25 and 250 µM Suc-AAPF-pNA and the initial reaction velocities determined by UV/vis spectrophotometric quantification of the *p*-nitroaniline ($\varepsilon_{410nm}$ = 8800 $M^{-1}cm^{-1}$, [110]) released upon enzymatic hydrolysis (**Figure 3.3.5**). The obtained values corresponded well to the ideal Michaelis-Menten equation and the obtained kinetic parameters for native proK were in good agreement with the reported values obtained for the same substrate [112]. Comparing the turnover number $k_{cat}$ of the native proK with the modified proK-4FB and the conjugate *de*-PG2-BAH-proK (**Table 3.3.1**), a small decrease was observed upon the modification with the 4FB linker moiety, while a moderate decrease was observed upon conjugation of the enzyme to the denpol. As the Michaelis constants $K_m$ decreased as well upon modification of the proK with the 4FB linker and further upon conjugation with the denpol, the enzyme efficiency $k_{cat}/K_m$ was not significantly affected upon the modification of proK with the 4FB linker, and only a small decrease in efficiency was observed for the conjugate. These values indicated that even though the attachment of the proK molecules to the macromolecular scaffold formed by the denpol, the enzymatic activity was maintained. A certain decrease in activity was attributed to the fact that the modification of the enzyme was carried out without precise control of the modification site, which could result in a steric hindrance of the active site upon conjugation to the denpol and therefore to a decreased accessibility of a part of the active sites present on the denpol-enzyme conjugate.

**Table 3.3.1** Kinetic constants of proK, proK-4FB and *de*-PG2-BAH-proK obtained from the nonlinear fit of the initial velocities to the Michaelis-Menten equation (c.f. **Figure 3.3.5**). Literature values were from Georgieva *et al.*, measured in 0.1 M Tris/HCl buffer, pH 8.2, 5 % DMF, at 25 °C [112].

| | $K_m$ / µM | $k_{cat}$ / $s^{-1}$ | $k_{cat}/K_m$ / $\mu M^{-1}\cdot s^{-1}$ |
|---|---|---|---|
| proK | 185 ± 14 | 172 ± 8 | 0.93 ± 0.11 |
| proK-4FB | 138 ± 15 | 138 ± 8 | 1.00 ± 0.17 |
| *de*-PG2-BAH-proK | 66 ± 7 | 23.0 ± 0.6 | 0.35 ± 0.05 |
| proK (lit.) | 230 ± 20 | 178 ± 5 | 0.782 ± 0.090 |

Additionally to the determination of the kinetic constants of the modified enzyme proK-4FB and the conjugate *de*-PG2-BAH-proK, their storage stabilities were evaluated. The relative activity of a solution stored at 4 °C at pH 7.0 was assayed to monitor the remaining activity. While the concentration of proK and proK-4FB was set to 1 µM for the stored solution, the proK concentration of the *de*-PG2-BAH-proK solution was set to 10 µM as determined from the BAH concentration measured by UV/vis. This allowed the

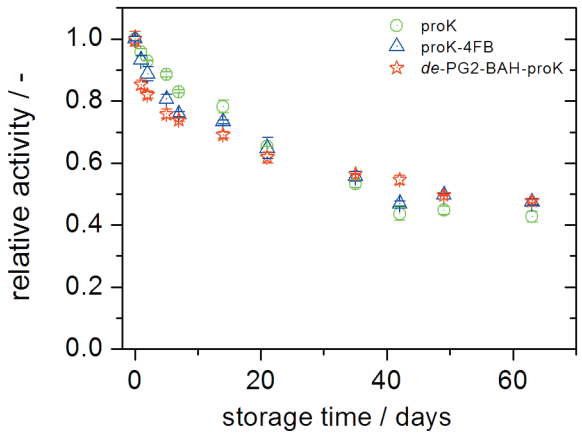


**Figure 3.3.6** Stability of the conjugate *de*-PG2-BAH-proK, the modified proK-4FB and native proK. Solutions at an enzyme concentration of 1 µM for proK and proK-4FB and 10 µM for *de*-PG2-BAH-proK (as determined from the BAH concentration) were stored in buffered solution at pH 7.0 at 4 °C. Repeated analysis of the remaining activity indicated no significant differences in the storage stability for the modified proK and the denpol-enzyme conjugate within 9 weeks.

comparison of the storage stability of solutions of comparable protease activity, compensating for the reduced hydrolytic activity of *de*-PG2-BAH-proK observed in the decreased $k_{cat}$ as determined above. In all three cases, proK, proK-4FB, and *de*-PG2-BAH-proK, a gradual decrease of the enzymatic activity under such storage conditions was observed (**Figure 3.3.6**). A remaining activity of about 70 % after two weeks and about 50 % after 9 weeks was observed, without significant differences between the proK, proK-4FB and *de*-PG2-BAH-proK.

### 3.3.3 Immobilization of *de*-PG2-BAH-proK on $SiO_2$ surfaces

After successful synthesis of the *de*-PG2-BAH-proK conjugate and the characterization of the catalytic constants of the conjugate in solution, the adsorption properties of the obtained conjugate on $SiO_2$ surfaces were investigated. The adsorption on a sputtered $SiO_2$ surface was characterized with the TInAS. The refractive index increment of *de*-$PG2_{2000}$-BAH-$proK_{140}$ was calculated as described above for the denpol-enzyme conjugates of GOD and HRP, as a linear combination of the contributions of the denpol (29 mass%, dn/dc = 0.140 $cm^3/g$, [30]) and proK (71 mass%, dn/dc = 0.186 $cm^3/g$, [120]), resulting in a value of dn/dc = 0.173 $cm^3/g$. A stable baseline was recorded for several minutes at a constant flow of buffer (pH 7.0) in the flow cell to ensure a stable measurement system. For the adsorption of the denpol-enzyme conjugate, a solution containing *de*-PG2-BAH-proK at a concentration of 1 µ proK (corresponding to a concentration of about 14 µM r.u.) was injected into the flow cell. The adsorption on the $SiO_2$ surface was monitored under a constant flow of 20 µL/min to maintain a constant concentration of *de*-PG2-BAH-proK in the solution in the flow cell. Adsorption of a layer of

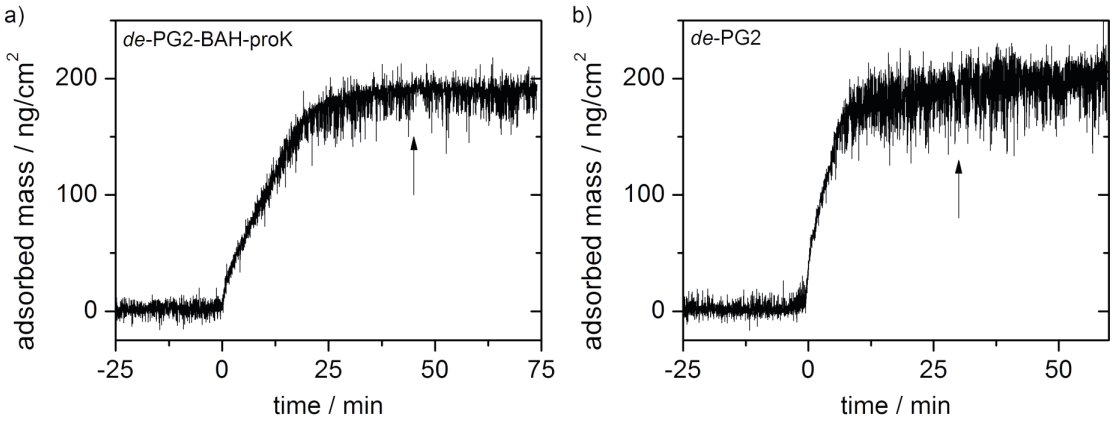


**Figure 3.3.7 a)** TInAS measurement of the adsorption of *de*-PG2-BAH-proK from buffered solution at pH 7.0. A baseline was recorded at constant flow of buffer, followed by injection of a solution of *de*-PG2-BAH-proK at an enzyme concentration of 1 µM (corresponding to a concentration of about 14 µM r.u.). After stabilization of the level of adsorbed mass, the buffer was injected into the flow cell (↑) to investigate the stability of the adsorbed layer. b) A solution of *de*-PG2 at a concentration of 20 µM r.u. was injected using the same setup as for the measurement of the adsorption of *de*-PG2-BAH-proK. The flow rate was kept at 20 µL/min except during solution changes, when it was raised to 0.4 mL/min to efficiently exchange the solution inside the flow cell.

about 200 ng/cm² was observed (**Figure 3.3.7a**). After reaching this level, no further increase of the adsorbed layer was detectable during further flow of the *de*-PG2-BAH-proK solution in the flow cell. After injection of buffer at a flow rate of 0.4 mL/min to remove the excess denpol-enzyme conjugate from the flow cell, the sensor was kept under a constant flow of buffer at a flow rate of 20µL/min. No desorption of the conjugate was observed during the rinsing of the flow cell, indicating a stable adsorption of the conjugate on the $SiO_2$ surface as seen for the free denpol and the conjugates of GOD and HRP above (**Figure 3.1.11**).

Knowing the mass fraction of proK in *de*-$PG2_{2000}$-BAH-$proK_{140}$ (71 mass%) and the molar mass of proK (28930 Da) allowed an estimation of the surface concentration of proK. The measured adsorbed mass of 200 ng/cm² therefore corresponded to a surface concentration proK of 4.9 pmol/cm².

Comparison of the adsorption of *de*-PG2-BAH-proK with a control measurement performed with *de*-PG2 indicated no significant differences between the adsorbed mass of *de*-PG2-BAH-proK and the non-modified denpol *de*-PG2 (**Figure 3.3.7b**). This indicated a less dense adsorption layer of the denpol-enzyme conjugate as compared to the free denpol. The similar amount of adsorbed mass for the non-modified denpol and the denpol-enzyme conjugate was in contrast to the results observed for the adsorption of the conjugates involving HRP and GOD discussed above. Considering the potentially large substrates of proK, oligopeptides or even native proteins, a less dense adsorption of the individual denpol-enzyme conjugates might even be of advantage in order to enable larger substrate molecules to come in contact with the enzyme's active site.

### 3.3.4 Enzymatic activity and stability of adsorbed *de*-PG2-BAH-proK

In order to characterize the catalytic activity of the immobilized proK, microscopy glass coverslips were used as supports and the *de*-PG2-BAH-proK conjugate adsorbed in a procedure as elaborated for the quantification of the adsorbed mass in the TInAS experiments. After adsorption of the denpol-enzyme conjugate on the coverslips, the reaction tubes containing the coverslips were washed with buffer to remove excess of the conjugate.

The activity of the obtained immobilized proK was quantified by comparison of the rate of product formation with the corresponding rates for known concentrations of native proK in solution. Such a comparison could be made under the assumption of similar kinetic constants for the immobilized enzyme as compared to the native enzyme in solution. As discussed in the case of GOD and HRP, and as already seen from the kinetic constants of *de*-PG2-BAH-proK in solution, this assumption might not be completely fulfilled. Nevertheless, such an estimation of an apparent surface concentration of enzyme allows a good description of the catalytic properties of the surface localized enzymes.

Using Suc-AAPF-pNA as substrate for the immobilized proK and a calibration curve obtained with proK in solution at concentrations between 0.1 nM and 2 nM, the apparent surface concentration of proK on a glass coverslip was determined as 2.0 pmol/cm² (**Figure 3.3.8**). Comparison of this value with the result obtained from the TInAS measurement, indicating a surface concentration of 4.9 pmol/cm², allowed an estimation of the decrease of catalytic activity upon immobilization of proK.

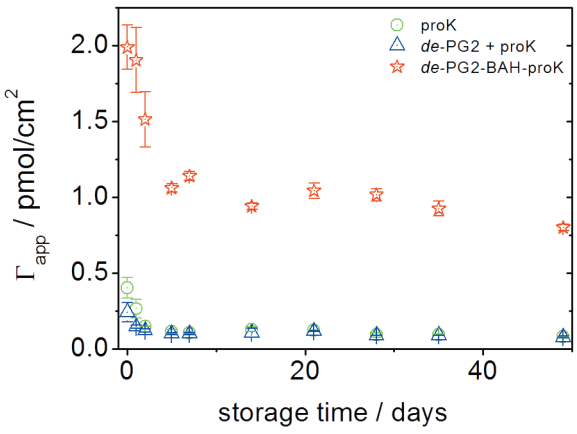


**Figure 3.3.8** Stability of *de*-PG2-BAH-proK adsorbed on a silicate glass coverslip. The apparent surface concentration was measured by comparison of the catalytic activity measured for a glass coverslip immersed in a solution of Suc-AAPF-pNA as substrate by comparison with a calibration performed with known amounts of native proK in solution.

Additional to the determination of the catalytic activity of the immobilized proK, the stability of the enzyme during storage was investigated. The glass coverslips were stored in buffered solution at pH 7.0 at 4 °C and the residual activity was determined by repeated activity measurements. In an initial phase, the activity dropped to an apparent surface concentration of proK of about 1 pmol/cm$^2$, corresponding to about 50 % of the initial activity,within 5 days. During further storage, the proK activity remained remarkably constant with a minor reduction to a level corresponding to an apparent surface activity of 0.8 pmol/cm$^2$ after a total storage time of 7 weeks (**Figure 3.3.8**). In control experiments using glass coverslips exposed to a solution containing proK or a mixture of proK and *de*-PG2 instead of the *de*-PG2-BAH-proK, low levels of adsorbed proK were detected in the initial activity measurements. During storage, these levels dropped within two days to the background level of the enzymatic activity assay.

These results for the determination of the stability of the adsorbed *de*-PG2-BAH-proK conjugate clearly demonstrated the suitability of this enzyme immobilization approach for the preparation of devices based on the proteolytic activity of the immobilized proK. Even though the initial decrease of the apparent surface concentration was considerable, the subsequent very slow loss of activity during 7 weeks of storage of the glass coverslips in solution indicated the potential to store devices prepared by adsorption of *de*-PG2-BAH-proK in a wet state.

### 3.3.5 Enzymatic flow reactor with *de*-PG2-BAH-proK in glass micropipettes

In order to apply the developed immobilization system for proK in a simple device for operation under continuous flow conditions, glass micropipettes were used as support for the adsorption of *de*-PG2-BAH-proK. The inner surface of the glass micropipettes was coated with *de*-PG2-BAH-proK by filling the pipette with a dilute solution of the denpol-enzyme conjugate as used for the adsorption measurements with the TInAS and the coating of the glass coverslips before. After rinsing of the glass micropipette with buffer to remove the excess *de*-PG2-BAH-proK, the prepared flow reactor was installed in a setup for online quantification of the enzyme activity by UV/vis spectrophotometry. One end of the micropipette was connected with PTFE tubing to a reservoir containing the chromogenic proK substrate Suc-AAPF-pNA, while the other end was connected to a Z-flow cell of the UV/vis spectrophotometer and a peristaltic pump installed after the flow cell (**Figure 3.3.9**). At a constant flow rate controlled with the peristaltic pump, the product level measured in the Z-flow cell exhibited a steady state.

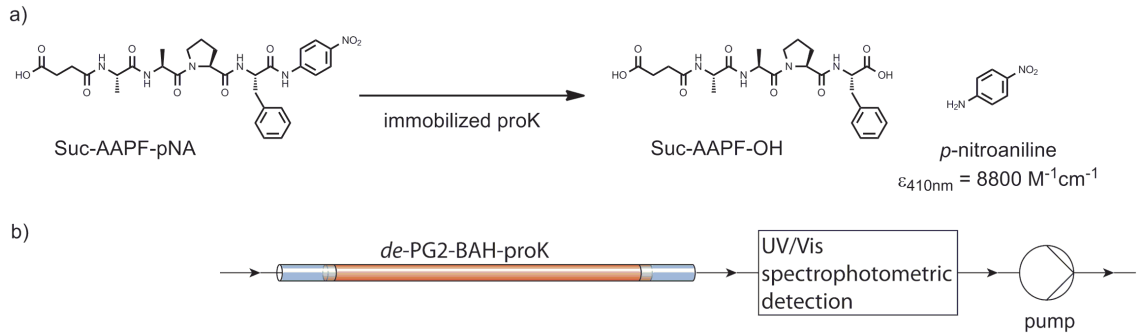


**Figure 3.3.9** Setup for the analysis of the operational stability of the immobilized proK. **a)** Hydrolysis of the chromogenic substrate Suc-AAPF-pNA by the immobilized proK yields the tetrapeptide Suc-AAPF-OH and the chromophore *p*-nitroaniline. **b)** The inlet of the glass micropipette with adsorbed *de*-PG2-BAH-proK was fitted with PTFE tubing to a substrate feed. The outlet was connected to a Z-flow cell for online UV/vis detection and a peristaltic pump to control the flow rate in the system.

In order to investigate the stability of the immobilized proK under operating conditions in the continuous flow setup, the system was run at room temperature at a constant flow rate of 35 µL/min for 33 h and the enzyme activity monitored. UV/vis spectra recorded at intervals of 10 min indicated an excellent stability of proK under these continuous flow conditions with a decrease of the rate of product formation of only about 5 % within 30 hours (**Figure 3.3.10**).

The remarkably low level of activity loss during operation was attributed to the very stable adsorption of the denpol-enzyme conjugate with no loss of enzyme from the surface. In comparison, Slováková *et al.* determined the operational stability of a proK reactor prepared by covalent attachment of proK to magnetic particles. In this setup, a decrease of activity to 50 % of the initial activity was determined after 8 batch experiments of 15 min [149].

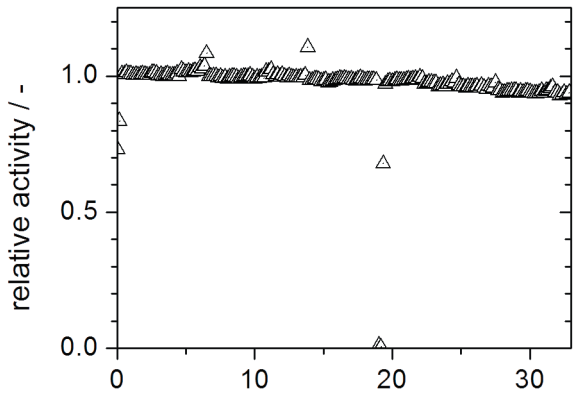


**Figure 3.3.10** Operational stability of proK immobilized in a glass micropipette by adsorption of *de*-PG2-BAH-proK. Product formation was quantified under continuous flow steady state conditions by online UV/vis spectrophotometry, using a substrate solution of 100 µM Suc-AAPF-pNA at pH 7.0 at room temperature. The outliers were caused by the formation of bubbles in the light path of the UV/vis Z-flow cell.

### 3.3.6 Enzymatic flow reactor with *de*-PG2-BAH-proK in a microfluidic device

After the promising results obtained from the immobilization of proK in glass micropipettes, the possibility of an application of the same *de*-PG2-BAH-proK conjugate for the immobilization of proK in microfluidic devices was investigated. A PDMS chip with a serpentine channel geometry was prepared and bonded on a glass coverslip. The channel was prepared such that it was connected to two inlets, one at the beginning and one in the mid of the serpentine (**Figure 3.3.11a**). Injection of a solution containing the *de*-PG2-BAH-proK conjugate through the second inlet was used for immobilization of proK on the glass coverslip in the area of the channel between second inlet and outlet. After adsorption, excess of *de*-PG2-BAH-proK was removed from the channel by injection of a buffer plug through the front inlet.

To monitor the proteolytic activity of proK, the fluorogenic substrate BODIPY-FL-casein was used. This casein derivative is multiply labelled with fluorescent BODIPY-FL tags. In the native casein, the fluorescence is quenched due to the spatial proximity of the substrates. Upon proteolytic digestion, the fragmentation of casein is accompanied by a

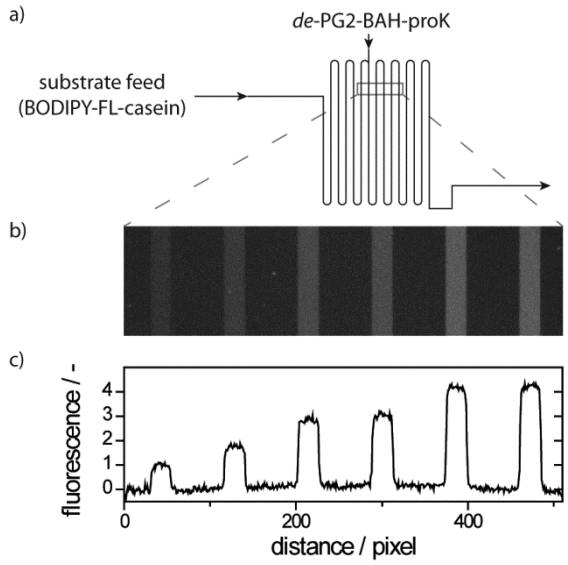


**Figure 3.3.11 a)** Design of the microfluidic chip used for the fabrication of the proteolytic micro-reactor. The first part of the channel between front and side inlet was used for the determination of the background fluorescence. In the second part, *de*-PG2-BAH-proK was deposited for the digestion of the fluorogenic substrate BODIPY-FL-casein (20 µg/mL, pH 7.0, room temperature). **b)** Image of the fluorescence detected in the area indicated in a). The first lane on the left is the channel before the turn with the second inlet and was used for the estimation of the background fluorescence. Subsequent lanes indicate an increasing fluorescence with increasing residence time of the substrate solution in the proK containing part of the channel under continuous flow steady state conditions. **c)** Evaluation of the fluorescence levels of the lanes depicted in b). The background fluorescence of the chip between the lanes was set to zero, the background fluorescence of the substrate solution as measured in the channel before the proK inlet was set to 1.

corresponding increase in fluorescence [150]. After injection of BODIPY-FL-casein into the front inlet at a continuous flow rate of 14 nL/min, a constant background fluorescence was detected in the channel between the first and the second inlet. In contrast to this, in the area of the channel containing adsorbed *de*-PG2-BAH-proK after the second inlet, an increasing fluorescence was detected. Under steady state conditions, the fluorescence level increased with increasing distance from the second inlet, indicating a proteolytic digestion of the BODIPY-FL-casein (**Figure 3.3.11b&c**). At an elevated flow rate of 1 µL/min, no increase in fluorescence was observed in the proK containing part of the channel.

Together with the results of a control measurement obtained on a microfluidic chip with adsorbed unmodified *de*-PG2 instead of *de*-PG2-BAH-proK, where no increase in fluorescence was observed after the second inlet, these results clearly demonstrated the successful preparation of a proK microreactor in a very simple design by a single adsorption step of the denpol-enzyme conjugate containing proK for the modification of the microchannel.

### 3.3.7 Conclusions

The synthesis of *de*-PG2-BAH-proK allowed a characterization of the obtained denpol-enzyme conjugate including the catalytic constants of the enzyme according to the Michaelis-Menten formalism. Such a characterization was possible due to the fact that the UV/vis absorbance of the BAH bond formed upon conjugation could be used for a quantification of proK in a *de*-PG2-BAH-proK solution. Such a concentration determination was interfered by overlapping absorption spectra of the enzymes' prosthetic groups in the cases of HRP and GOD, where an indirect method for the exact quantification of the conjugates would be necessary [56]. Additionally, the catalytic cycle of proK correlates adequately with the Michaelis-Menten formalism, while HRP and GOD both involve more complex cycles.

The successful immobilization of proK by adsorption of the denpol-enzyme conjugate was characterized with the TInAS and the catalytic activity of the enzyme was investigated. An excellent stability of the protease under operating conditions was observed in a small reactor run under continuous flow conditions. Additionally, the feasibility of an application of this enzyme immobilization approach in the production of microfluidic chips containing immobilized enzymes was demonstrated. The digestion of a native protein in such a device proved the possibility to not only process small peptidic model substrates, but also large macromolecular structures.

# 4 SUMMARY AND OUTLOOK

In the present work, dendronized polymer-enzyme hybrid structures were synthesized with the aim of using these hybrid structures for the immobilization of enzymes. The work was based on the idea of using molecularly dissolved chains of a polymer as a scaffold for the attachment of a multitude of copies of an enzyme along the polymer chain. To enable this, the water soluble, polycationic dendronized polymer *de*-PG2 was used (**Figure 4.1.1a**). The structural features and the properties of this denpol nicely comply with the requirements of a polymer to be used in such an approach. The dendritic structure of the repeating units results in a relatively rigid structure, with longer persistence length than traditional linear polymers. This feature is important for the possibility of an efficient attachment of enzymes along the polymer chain, which was expected to be hindered in the case of a condensed random coil conformation. Furthermore, the presence of the peripheral amino groups on the dendrons not only mediates water solubility, but also offers the possibility of functionalization of the denpol with amine-reactive reagents.

The feasibility of using a denpol in a stepwise procedure for a non-covalent enzyme immobilization in combination with the biotin-avidin linking system has been demonstrated earlier [30]. In another work, the synthesis of water soluble denpol-enzyme conjugates was performed [56]. In this work, these two approaches were combined to develop a non-covalent, stable, single step enzyme immobilization protocol using unmodified silicate glass as solid support.

The denpol-enzyme conjugates were synthesized in aqueous solution using the selective and quantifiable bis-aryl hydrazone (BAH, **Figure 4.1.1c**) linker chemistry. Modification of the denpol was obtained by reaction with an amino reactive linker moiety, yielding a denpol with attached 6-hydrazinonicotinamide moieties. The modification with these linker moieties was carried out in a statistical way. While the exact location and spacing of individual linker moieties on the polymer chain was not known, the overall modification ratio could be determined. This was used to estimate the average spacing between the linkers in order to ensure the possibility of linking the enzymes densely along the denpol chains. During the modification of the enzymes, special care had to be taken to avoid the presence of enzymes with several linker moieties attached to the same molecule, in order to avoid crosslinking of the dissolved denpol chains.

In the first parts of the thesis, the two glycosylated, redox active enzymes HRP and GOD (**Figure 4.1.1b**) were successfully used to prepare denpol-enzyme conjugates (**Figure 4.1.1d**). Light absorption at $\lambda_{max} \approx 350$ nm by the BAH bond formed during conjugation allowed the quantification of the amount of bound enzyme, and therefore the

determination of the number of enzyme molecules per denpol chain. This is unique and difficult to achieve with other linker chemistries. For HRP, a composition of the conjugate corresponding to 108 molecules of HRP per 1400 r.u. long denpol chain was measured. In the case of GOD, however, the quantification of the amount of bound GOD was hampered by the occurrence of turbidity in the conjugation mixture, due to the large size of the conjugates prepared. Therefore, the determined ratio of about 50 GOD molecules per 1400 r.u. long denpol chain was calculated with an according correction of the measured value and considered as an approximate value.

Additional to the two conjugates containing either HPR or GOD, a third conjugate carrying several copies of both of the two enzymes on the same denpol chain was prepared (**Figure 4.1.1d**). This was possible by consecutive attachment of GOD and HRP to the denpol chain. Attaching GOD, with a molar mass of about 153 kDa the considerably larger of the two enzymes, in a first step, and HRP, with a molar mass of about 44 kDa, in a second step was considered as the key approach enabling the attachment of the smaller enzyme to the denpol chain in free areas in-between the larger GOD molecules. Using such a procedure, a conjugate combining about 25 molecules of GOD and about 78 molecules of HRP on a 1400 r.u. long denpol chain was synthesized. As in the case of the conjugate containing GOD only, the appearance of turbidity during the attachment of GOD to the denpol resulted again in a given uncertainty, and the obtained values were taken as approximate numbers.

Apart from the two enzymes GOD and HRP, which catalyze two consecutive steps in an enzymatic cascade reaction, a third enzyme was used for the preparation of a denpol-enzyme conjugate. This conjugate carried proK (**Figure 4.1.1b**) along the denpol chain. It was synthesized by the same procedure, *i.e.* again with the BAH linker chemistry. Additionally, the relatively small molar mass of proK (28.9 kDa) and the non-glycosylated nature of this enzyme allowed a characterization of the proK modified with the 4FB linker moiety by mass spectrometry, assuring the absence of proK molecules carrying more than one linker moiety. The composition of the obtained conjugate was determined to include on average 140 molecules of proK per 2000 r.u. long denpol chain (**Figure 4.1.1d**).

The role of the denpol as a scaffold for the connection and spatial arrangement of the enzymes along this scaffold was illustrated considering the compositions of the denpol-enzyme conjugates. In all conjugates, the contribution of the denpol to the total mass of the conjugate was considerably lower than the contribution of the enzymes. This was also evident upon AFM visualization of single chains of the denpol-enzyme conjugates of HRP and GOD and the conjugate containing both of these enzymes on the same denpol

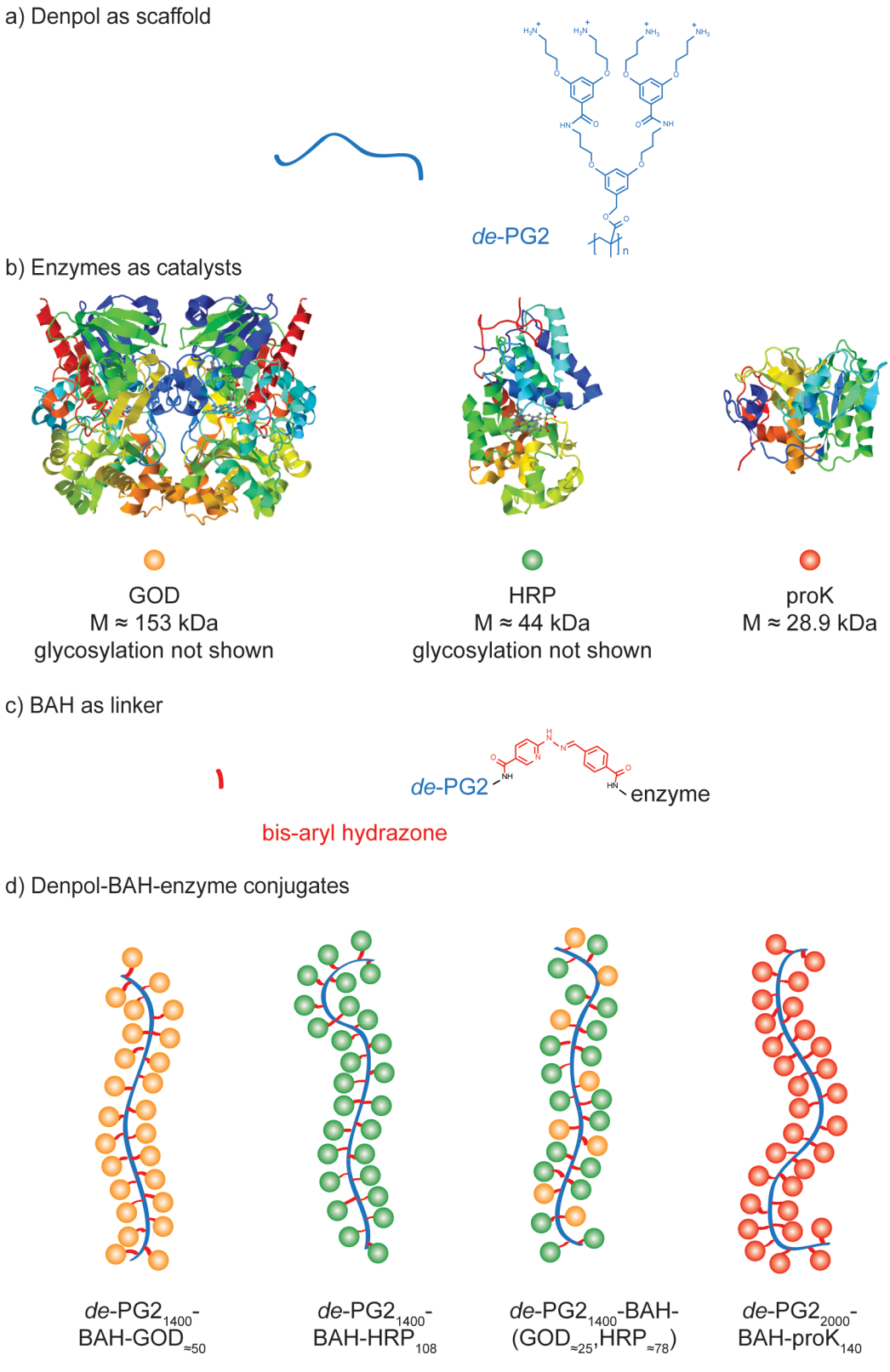


**Figure 4.1.1 a)** Schematic and chemical structure of the second generation dendronized polymer *de*-PG2 used as scaffold and **b)** cartoon representation of the enzymes attached (PDB-entry codes: 3QVP (GOD), 1H5A (HRP), and 1IC6 (proK) and symbols used for their representation in the conjugates. **c)** Schematic and chemical structure of the UV/vis traceable bis-aryl hydrazone linker used for the attachment of the enzymes to the *de*-PG2 scaffold and **d)** schematic representation of the conjugates synthesized in this work, featuring a multitude of copies of one or two types of enzymes along a denpol chain.

chain. After deposition and drying of such conjugates on mica, the measured heights were considerably higher than the values obtained for a *de*-PG2 chain.

After synthesis and characterization of the denpol-enzyme conjugates, the possibility of an application of these conjugates for the immobilization of enzymes on silicate supports was investigated. For this approach, the property of the unmodified denpol, *de*-PG2, to stably adsorb on negatively charged surfaces, such as $SiO_2$, was exploited. Additionally to this intrinsic adsorption characteristic of *de*-PG2, mediated by the positive charges of the peripheral amino groups present in the dendrons, there are also additional interactions between the denpol bound enzymes and the surface expected in the case of the denpol-enzyme conjugates. Native proteins interact with silicate surfaces via charged patches on the surface of the enzyme molecules. In the denpol-enzyme conjugates, such interactions were expected to be multiplied due to the connection of a multitude of enzymes to form the conjugates. Therefore, such interactions might contribute to a significant amount to the stable binding of the conjugates on the silicate surface, even though a dissection of the different contributions was not possible and not attempted in this work. The adsorption process of the denpol-enzyme conjugates was characterized with the transmission interferometric adsorption sensor, indicating a stable adsorption on a sputtered $SiO_2$ surface. The measurements indicated the formation of a rather defined layer of denpol-enzyme conjugate on the silica surface after exposition to a solution containing the conjugates. The adsorbed layer did not accumulate more conjugate from the solution during further exposition to a conjugate solution, nor was any desorption detectable after rinsing of the surface with buffer solution to probe the stability of the adsorbed layer. AFM imaging of microscopy glass coverslips coated with the denpol-enzyme conjugates by adsorption from solution confirmed the presence of a defined layer of conjugate on the surface. A homogeneous surface coverage was observed, and the thickness of the adsorbed layers corresponded to about the thickness of individual conjugate chains. These findings confirmed the applicability of these denpol-enzyme conjugates for a defined enzyme immobilization on non-modified glass surfaces.

Besides the direct adsorption of the denpol-enzyme conjugates on silicate glass surfaces, an additional system for a localized co-immobilization of the two enzymes GOD and HRP was developed. In a combination of the immobilization of one type of enzyme within mesoporous silica nanoparticles and the immobilization of the second type of enzyme using a denpol-enzyme conjugate, the two enzymes were co-immobilized on silicate glass surfaces in a layered structure. The adsorption processes of the HMM particles and the subsequent loading of the particles with enzyme and covering with

denpol-enzyme conjugate were investigated by quartz crystal microbalance with dissipation monitoring.

After successful fabrication of these different systems with immobilized enzymes, the catalytic activities and the stabilities of the enzymes were determined. The activity of the enzymes could be correlated to an apparent surface concentration of the enzymes by quantification of the activity measured per surface area and comparison with the values measured for the native enzymes in solution. Additionally, the possibility of the co-localized GOD and HRP to catalyze a sequential two step cascade reaction was investigated. Interestingly, the approach for the localized co-immobilization using adsorption in HMM particles for one type of enzyme and deposition of the denpol-enzyme conjugate for the second type of enzyme produced very different results for the measured cascade reaction, depending on which type of enzyme was immobilized in the HMM particles and which type of enzyme was added as the covering denpol-enzyme layer. In the case where GOD, the enzyme catalyzing the first step in the cascade reaction, was immobilized in the lower HMM layer and the covering denpol-enzyme layer contained the HRP, catalyzing the second step of the cascade reaction, a high efficiency of the cascade catalyzed by the two co-immobilized enzymes, was detected. In contrast, if HRP was immobilized in the HMM particles, a very low activity of the immobilized HRP was measured. After addition of the GOD by adsorption of the covering denpol-enzyme layer, the cascade reaction was inefficient. A possible reason leading to this phenomenon was considered to be the loss of the intermediate into the bulk solution due to the inefficient catalysis of the second reaction step by the HRP immobilized inside the mesoporous particles. Apart from the better enzymatic activity in the case of GOD in the lower HMM layer and HRP in the top denpol-enzyme layer, this arrangement also necessarily includes diffusion of the intermediate through the covering HRP layer before release to the bulk solution.

The stabilities of the immobilized enzymes during storage were investigated by repeated activity measurements over several weeks. While the adsorbed GOD conjugate showed excellent storage stability, the adsorbed HRP conjugate and proK conjugate displayed an initial decrease in activity, but then stabilized as well at a reduced level during prolonged storage. Measurement of the stability under operating conditions was performed using a continuous flow system, and showed very good stability for two systems featuring the two step cascade reaction catalyzed by GOD and HRP either in a sequential setup with a first reactor with immobilized GOD and a second reactor with immobilized HRP, or in a system with co-immobilized GOD and HRP in a single reactor.

An excellent stability under operating conditions was also detected for the immobilized proK. An application of the immobilization procedure developed for proK *via* adsorption of the *de*-PG2-BAH-proK conjugate was also tested by incorporation of proK in a microfluidic chip. On chip enzyme immobilization was possible in a single step by introduction of a solution of the conjugate into the microchannel. The activity of the immobilized proK in the microchannel towards a native protein substrate was demonstrated with a fluorescently labelled casein substrate.

Combined, these findings demonstrate the feasibility of the preparation of denpol-enzyme conjugates carrying several copies of one or two types of enzyme molecules on the denpol chain, and their application in a simple, single step enzyme immobilization procedure. The property of the conjugates to readily and stably adsorb on unmodified glass surfaces from dilute aqueous solutions is a key feature enabling this approach. This is of special importance if straightforward enzyme immobilization is needed, and contaminations from desorbing enzymes need to be excluded for downstream processing.

Furthermore, the nature of the conjugates, presenting enzymes surrounding a denpol backbone, results in the localization of enzymes at different distances from the surface upon adsorption. This might result in interesting differences of the catalytic behavior between these enzyme molecules. Such observations could be of special interest in the area of bioelectrodes fabrication, where properties such as substrate accessibility, but also the efficiency of the electron transport from the enzymes to the electrode are of crucial importance [151].

The demonstration of the feasibility of the digestion of native casein by the immobilized proK also indicates promising possibilities towards the enzymatic transformation of macromolecules. Such processes might not be trivial in all cases, as the access of macromolecules to the active site of immobilized enzymes is restricted upon immobilization of the enzyme. Enzymatic modifications of macromolecules are of a special interest not only in analytical areas such as limited proteolysis for proteomics applications [146], but also for life science applications such as the detection of prion proteins [108]. A developing field for such systems lies also in the synthetic area, where a special focus recently was laid on the selective, enzymatic or chemo-enzymatic formation of antibody-drug conjugates [152].

Overall, the enzyme immobilization methodology developed in this thesis on the basis of *de*-PG2 as a convenient scaffold is not only a scientifically interesting approach but is also promising for real applications.

# 5 EXPERIMENTAL PART

## 5.1 Chemicals and buffer solutions

*Aspergillus* sp. glucose oxidase (GOD, EC 1.1.3.4, product code GLO-2022, lot 9448520002, 242 U/mg, M ≈ 153 kDa) and horseradish peroxidase (HRP, EC 1.11.1.7, product code PEO-131, lot 2131616000, 278 U/mg, M ≈ 44 kDa) were from Toyobo Enzymes (Japan). *Engyodontium album* proteinase K (proK, recombinant from *Pichia pastoris*, EC 3.4.21.64, catalog number 03115879001, lot 14321500 (46.0 U/mg) and lot 1016630 (48.2 U/mg), M = 28.9 kDa) was obtained from Roche Applied Science (Switzerland). *De*-PG2$_{1400}$ ($P_n$ ≈ 1400, PDI ≈ 4.7) was synthesized by Dr. Baozhong Zhang (Polymer Chemistry, ETH Zürich) and *de*-PG2$_{2000}$ ($P_n$ ≈ 2000, PDI ≈ 4.3) by Dr. Andrea Grotzky (Polymer Chemistry, ETH Zürich) as described earlier [55]. *N*-Succinimidyl 6-hydrazinonicotinate acetone hydrazone (S-HyNic) and *N*-succinimidyl 4-formylbenzoate (S-4FB) were synthesized by Dr. Andrea Grotzky as described earlier [56]. Hiroshima mesoporous material (HMM) particles were synthesized by Dr. Hanna Gustafsson as described before [131]. Non-porous silica particles (Bindzil 50/80) were a gift from AkzoNobel Pulp and Performance Chemicals AB (Sweden). 3(*N*-morpholino)propanesulfonic acid (MOPS), 2(*N*-morpholino)ethanesulfonic acid (MES), and ammonium sulfate were obtained from AppliChem (Germany). Sodium dihydrogenphosphate, 2,2'-azino-bis(3-ethylbenzothiazoline-6-sulfonic acid) diammonium salt ($ABTS^{2-}$), *o*-phenylenediamine (OPD), D-glucose, and 2-hydrazinopyridine were obtained from Sigma-Aldrich (Switzerland). 4-nitrobenzaldehyde was obtained from Fluka (Switzerland). Dry *N*,*N*-dimethylformamide (DMF) and trypan blue were obtained from Acros Organics (Switzerland). Sodium hydroxide (NaOH) was obtained from Brenntag Schweizerhall AG (Switzerland). Succinyl-L-alanyl-L-alanyl-L-prolyl-L-phenylalanyl-*para*-nitroanilide (Suc-AAPF-pNA) was obtained from Bachem (Switzerland). BODIPY-FL-casein was purchased from Life Technologies (Switzerland).

Amicon ultrafiltration devices (0.5 mL, 4 mL and 15 mL, 10 kDa, 50 kDa and 100 kDa NMWL) were purchased from Merck Millipore or Sigma Aldrich, Centrisart I ultrafiltration devices (300 kDa MWCO) were obtained from Sartorius (Switzerland). Round glass coverslips 8 mm diameter were obtained from Science Services (Germany), rectangular glass coverslips were obtained from Knittel Gläser (Germany), and glass micropipettes (intraMARK, 200 µL) were from Brand (Germany).

The following buffer solutions were prepared at room temperature using a pH-Meter (Mettler-Toledo FE20) and a solution of 2 M NaOH to adjust the pH:
Buffer-1: 100 mM MOPS, 150 mM NaCl, pH = 7.6
Buffer-2: 100 mM MES, 150 mM NaCl, pH = 4.7

Buffer-3: 100 mM MES, pH = 5.0

Buffer-4: 10 mM sodium dihydrogenphosphate, 150 mM NaCl, pH = 7.2

Buffer-5: 10 mM sodium dihydrogenphosphate, 150 mM NaCl, pH = 5.0

Buffer-6: 100 mM MES, 1.15 M NaCl, pH = 4.7

Buffer-7: 10 mM sodium dihydrogenphosphate, 150 mM NaCl, pH = 7.0

Buffer-8: 10 mM sodium dihydrogenphosphate, 150 mM NaCl, pH = 6.0

Buffer-9: 10 mM MOPS, pH 8.0

Buffer-10: 10 mM MES, pH 4.7

Buffer-11: 10 mM MOPS, pH 7.0

## 5.2 Intruments

A Hermle Z 320 K centrifuge and a Eppendorf Centrifuge 5415 D were used for ultrafiltrations. A Mettler AE 163 balance was used for weighting.

A Jasco V670 spectrophotometer equipped with a water cooled peltier cuvette holder was used for high resolution UV/vis spectrophotometry and an Analytik Jena Specord S 600 photodiodearray spectrophotometer equipped with a water cooled peltier cuvette holder was used for enzymatic activity measurements. A Nanodrop ND-1000 was used for concentrations determinations. A USB2000+ photodiodearray spectrophotometer (350-1100 nm, OCOUSB2000+VIS-NIR) connected with 400 µm optical fibers (OCOQP400-2-UV-BX) to a Z-flow cell (OCOFIA-Z-SMA-ML-TE) and a tungsten halogen light source (OCOHL-2000-HP-FHSA), all from Ocean Optics , obtained via GMP SA (Switzerland), was used for continuous flow online UV/vis analysis. A Pharmacia LKB pump P-1 was used to control the flow of the continuous flow of the micropipette reactor systems. The cuvettes used for UV/vis spectroscopy were: 1.4 mL, 1 cm (114-QS), 350 µL, 1 mm (110-QS, with spacer 013.101), and 50 µL, 10 mm (105.202-QS), all from Hellma Analytics, and disposable cuvettes semi-micro, PS, from Brand.

The transmission interferometric adsorption sensor (TInAS), courtesy of the Surface Science and Technology Group, D-MATL, ETH Zürich, was a custom built instrument as described by Heuberger and Balmer [117].

Atomic force microscopy (AFM) measurements were performed by Dr. Jozef Adamcik at the Laboratory of Food and Soft Materials, D-HEST, ETH Zürich, on a MultiMode VIII Scanning Probe Microscope (Bruker, USA) covered with an acoustic hood and operated in intermittent mode under ambient conditions and using AFM cantilevers (Bruker, USA) for tapping mode in soft tapping conditions at a vibrating frequency of 150 kHz.

Scanning electron microscopy (SEM) images were recorded by Dr. Hanna Gustafsson (Applied Surface Chemistry, Chalmers University of Technology, Gothenburg, Sweden) with a Leo Ultra 55 FEG SEM operated at 2 kV and a working distance of 1.7-2.2 mm. Transmission electron microscopy images were recorded by Dr. Hanna Gustafsson with a FEI Tecnai T20 LaB6 TEM operated at 200 kV.

## 5.3 Preparation and characterization of denpol-BAH-enzyme conjugates of GOD, HRP and proK

### 5.3.1 Preparation of *de*-PG2-HyNic

The modification of the deprotected denpol *de*-$PG2_{1400}$ with the linker moiety 6-hydrazinonicotinamide (HyNic) was carried out as described earlier [56], with slight modifications. *De*-$PG2_{1400}$ was dissolved at 2 mg/mL in buffer-1. The exact repeating unit concentration was determined by UV/vis spectrophotometry on a NanoDrop ND-1000 ($\varepsilon_{285nm}$ = 5000 $M^{-1}cm^{-1}$). The concentration of the free peripheral amino groups is four per repeating unit for *de*-PG2. 0.1 equivalents of S-HyNic per amino group were added from a 20 mM stock solution in dry DMF and the reaction mixture was kept at room temperature for 4 h. Free linker was then removed by repetitive ultrafiltration with buffer-2 on a Amicon Ultra-0.5, 100 kDa NMWL ultrafiltration device. Complete removal of remaining linker was monitored by UV/vis spectrophotometric analysis of the filtrate on a NanoDrop.

The concentration of available HyNic linker moieties in the obtained *de*-PG2-HyNic solution was determined as described by Solulink [113]. A stock solution of 50 mM 4-nitrobenzaldehyde was prepared in DMF and used for the preparation of a working solution of 500 µM 4-nitrobenzaldehyde in buffer-3. Immediately after mixing 5 µL of *de*-PG2-HyNic solution and 95 µL of the 500 µM 4-nitrobenzaldehyde solution the UV/vis spectrum was measured, followed by an incubation of the reaction mixture at 37 °C for 1 h. After cooling the solution to room temperature, the UV/vis spectrum was remeasured, and the difference in absorbance at 380 nm was used to calculate the concentration of the bis-aryl-hydrazone formed from HyNic and 4-nitrobenzaldehyde ($\varepsilon_{380nm}$ = 24000 $M^{-1}cm^{-1}$).

The denpol repeating unit concentration of the *de*-PG2-HyNic solution was determined with the trypan blue assay [115]. The denpol concentration was estimated from the UV/vis spectrum considering the molar absorption coefficient of the non-modified polymer ($\varepsilon_{285nm}$ = 5000 $M^{-1}cm^{-1}$) and the sample accordingly diluted to approximately 100 µM r.u. 10 µL of this solution were diluted with buffer-2 to 120 µL, mixed with 5 µL of a 0.4 mg/mL trypan blue solution, and kept at 37 °C for 1 h in a water bath. After cooling to room temperature, the sample was centrifuged at 16100 g for 20 minutes the UV/vis spectrum of the supernatant was recorded. The absorbance at 580 nm was used for analysis and correlated to a calibration curve obtained using 120 µL aliquots of *de*-PG2 of known concentration in the range of 0-15 µM r.u. for quantification of the *de*-PG2-HyNic repeating unit concentration (**Figure 5.3.1**).

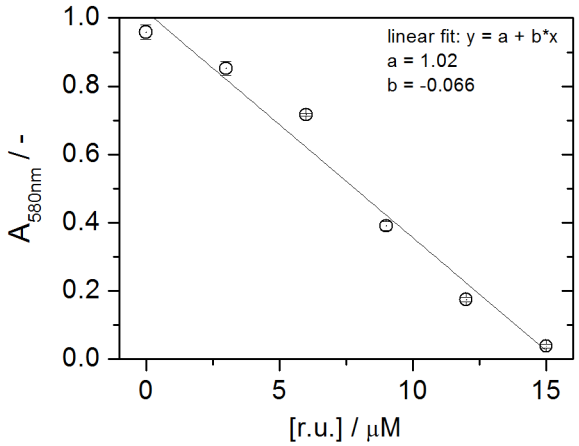


**Figure 5.3.1** Calibration curve for the determination of the *de*-PG2 concentration with the trypan blue assay.

### 5.3.2 Preparation of HRP-4FB

The modification of HRP was performed as described earlier [56]. HRP was dissolved at a concentration of approximately 4 mg/mL in buffer-4 and the exact HRP concentration was measured by UV/vis spectrophotometry using a NanoDrop ($\varepsilon_{403nm}$ = 102000 $M^{-1}cm^{-1}$ [76]). 6 eq. of S-4FB were added from a 20 mM stock solution in dry DMF and the reaction mixture was incubated for 4 h at room temperature. Remaining free linker was removed by repetitive ultrafiltration with buffer-2 using an Amicon Ultra-4, 10 kDa NMWL ultrafiltration device and complete removal of the free linker was verified by UV/vis spectrophotometric analysis of the filtrate using a NanoDrop. The linker concentration was determined by derivatization with 2-hydrazinopyridine, as described earlier [56, 113].

### 5.3.3 Preparation of GOD-4FB

For the modification of GOD with the 4FB linker moiety, 20 mg/mL GOD were dissolved in buffer-4 and the stabilizers present in the commercial product were removed by repetitive ultrafiltration with buffer-4 using an Amicon Ultra-0.5, 50 kDa NMWL ultrafiltration device. The concentration of the purified GOD was determined by UV/vis spectrophotometry ($\varepsilon_{450nm}$ = 28200 $M^{-1}cm^{-1}$ [91]). To a 50 µM GOD solution in buffer-4 1.2 eq. of S-4FB were added from a 5 mM stock solution in dry DMF and the reaction mixture was kept at room temperature for 4 h. The remaining free linker was removed by repetitive ultrafiltration with buffer-2 using an Amicon Ultra-0.5, 50 kDa NMWL ultrafiltration device and complete removal of the linker was verified by UV/vis spectroscopic analysis of the filtrate using a NanoDrop.

The modification of GOD with 4FB linker was quantified by derivatization of the 4FB moiety with 2-hydrazinopyridine as described by Solulink [113], with slight modifications. To 995 µL of 500 µM 2-hydrazinopyridine in buffer-2 5 µL of the purified GOD-4FB were added and changes in the UV/vis spectrum were recorded for 6 h. The absorbance at 450 nm was used to quantify the GOD concentration ($\varepsilon_{450nm}$ = 28200 $M^{-1}cm^{-1}$), and the change in absorbance at 350 nm was used to quantify the bis-aryl hydrazone formed by reaction of 4FB with 2-hydrazinopyridine ($\varepsilon_{350nm}$ = 24500 $M^{-1}cm^{-1}$ [113]).

### 5.3.4 Preparation of *de*-PG2-BAH-HRP

The conjugation reaction of *de*-PG2-HyNic with HRP-4FB was performed as described earlier, with slight modifications. In a 1 mm path length quartz cuvette, buffer-2, HRP-4FB (final concentration 50 µM 4FB-linker), aniline (final concentration 10 mM), and *de*-PG2-HyNic (final concentration 75 µM HyNic-linker) were mixed and a UV/vis spectrum recorded immediately. The sample was kept at 25 °C inside the spectrophotometer and the reaction monitored by recording a UV/vis spectrum every 5 minutes for 3.5 h. After removal of the crude reaction mixture from the cuvette, remaining free HRP-4FB, HRP and the aniline were removed from the conjugate by repetitive ultrafiltration with buffer-5 using an Amicon Ultra-4, 100 kDa NMWL ultrafiltration device. The complete removal of HRP was verified by UV/vis spectrophotometric analysis of the filtrate using a NanoDrop. The purified *de*-PG2-BAH-HRP conjugate was stored in buffer-5 at 4 °C.

### 5.3.5 Preparation of *de*-PG2-BAH-GOD

GOD-4FB (final concentration 50 µM 4FB-linker) and *de*-PG2-HyNic (final concentration 75 µM HyNic-linker) were mixed in buffer-6 in a 1 mm path length quartz cuvette. The temperature was kept at 25 °C and UV/vis spectra were recorded every 5 minutes for 16 h until no further significant changes were observed. To remove the free GOD-4FB and GOD from the *de*-PG2-BAH-GOD conjugate, the conjugate was precipitated from 60 % saturated ammonium sulfate solution by addition of 1.5 times the sample volume of saturated ammonium sulfate solution, incubation for 15 min, and centrifugation at 16100 g for 20 min. After removal of the supernatant containing the free GOD-4FB and GOD, the pellet was re-dissolved in buffer-5 and the precipitation was repeated 3 more times. To remove the remaining ammonium sulfate from the purified *de*-PG2-BAH-GOD, the redissolved conjugate was further purified by repetitive ultrafiltration with buffer-5

using a Centrisart I, 300 kDa MWCO ultrafiltration device. The purified *de*-PG2-BAH-GOD was stored in buffer-5 at 4 °C.

### 5.3.6 Preparation of *de*-PG2-BAH-(GOD,HRP)

*De*-PG2-BAH-(GOD,HRP) was obtained in a stepwise reaction of *de*-PG2-HyNic with GOD-4FB and then HRP-4FB. In a 1 mm path length quartz cuvette GOD-4FB (50 µM 4FB-linker) and *de*-PG2-HyNic (100 µM HyNic linker) were mixed in buffer-6 and kept at 25 °C for about 16 h, recording UV/vis spectra every 5 min. After this time, HRP-4FB (final concentration of 50 µM 4FB) was added. The HyNic concentration in the reaction mixture was about 75 µM after addition of the HRP-4FB solution and the resulting dilution. The reaction of HRP-4FB with *de*-PG2-BAH-GOD was again monitored by UV/vis spectrophotometry, recording spectra every 5 min for 16 h. The obtained *de*-PG2-BAH-(GOD,HRP) conjugate was purified by precipitation from 50 % saturated ammonium sulfate solution by addition of a corresponding volume of saturated ammonium sulfate solution, 15 min incubation at room temperature and centrifugation at 16100 g for 20 min. After removal of the supernatant containing the free GOD-4FB and HRP-4FB, the pellet was re-dissolved in buffer-5 and the precipitation repeated 3 more times. To remove the remaining ammonium sulfate, the *de*-PG2-BAH-(GOD,HRP) was further purified by repetitive ultrafiltration with buffer-5 using a Centrisart I, 300 kDa MWCO ultrafiltration device. The obtained *de*-PG2-BAH-(GOD,HRP) was stored in buffer-5 at 4 °C.

### 5.3.7 Preparation of proK-4FB

ProK was dissolved at a concentration of 10 mg/mL in buffer-9 and the protein concentration was determined by UV/vis spectrophotometry ($\varepsilon_{280nm}$ = 41000 $M^{-1}cm^{-1}$, [99]) using a NanoDrop. The modification reaction was carried out at a protein concentration of 50 µM. For a typical reaction, starting from a stock solution of 213 µM proK and a S-4FB stock solution at a concentration of 100 mM in dry DMF, 2892 µL buffer-9, 962 µL of proK (1 eq.) and 246 µL S-4FB (120 eq.) were mixed and kept at room temperature for 4 h. To remove the excess of hydrolyzed linker reagent, the proK-4FB was purified by repetitive ultrafiltration with buffer-10 using an Amicon Ultra-4, 10 kDa MWCO ultrafiltration device. The obtained proK-4FB solution was stored in buffer-10 at 4 °C until further use.

The 4FB linker was quantified by derivatization with 2-hydrazinopyridine. 10 µL of the proK-4FB stock were added to 990 µL of a 500 µM solution of 2-hydrazinopyridine in

buffer-10 and a UV/vis spectrum recorded immediately after mixing. After incubation at 25 °C for 3 h, a second UV/vis spectrum was recorded and the difference in absorption at 350 nm quantified for the determination of the amount of BAH formed ($\varepsilon_{350nm}$ = 24500 $M^{-1}cm^{-1}$, [113]).

The proK concentration in the proK-4FB stock solution was quantified with the Bradford protein assay (Sigma-Aldrich, Switzerland) using a calibration with known amounts of native proK. The contribution of the 4FB linker to the UV/vis absorption at 280 nm was determined to be about 10 % of the total absorption of proK-4FB containing about 1 linker per enzyme. This allowed direct UV/vis spectrophotometric determination of the proK concentration at λ = 280 nm for subsequent samples, correcting the measured absorption value for the 10 % contribution of the 4FB linker and calculating the enzyme concentration with the known extinction coefficient $\varepsilon_{280nm}$ = 41000 $M^{-1}cm^{-1}$ [99].

For the mass spectrometric characterization of proK-4FB, the samples were desalted by repetitive ultrafiltration with Milli-Q water using an Amicon Ultra-0.5, 10 kDa NMWL ultrafiltration device. Electrospray ionization mass spectrometric (ESI-MS) analysis of the samples was performed by the MS-Service at the laboratory of organic chemistry, ETH Zürich.

### 5.3.8 Preparation of *de*-PG2-BAH-proK

For the preparation of *de*-PG2-BAH-proK, a 2000 r.u. long *de*-PG2 was used. Modification of *de*-$PG2_{2000}$ with S-HyNic was performed as for *de*-$PG2_{1400}$ described above. Conjugation of *de*-$PG2_{2000}$-$HyNic_{500}$ and proK-4FB was performed at a concentration of 100 µM HyNic and 50 µM 4FB in buffer-10. *De*-PG2-HyNic and proK-4FB were mixed in a 1 mm path length quartz cuvette and kept in a spectrophotometer at 25 °C, recording spectra at intervals of 5 minutes. After 6 hours, the reaction mixture was recovered from the cuvette and free proK was removed by repetitive ultrafiltration, using a Centrisart I, 300 kDa MWCO ultrafiltration device. The purified *de*-PG2-BAH-proK was stored at 4 °C until further use.

## 5.4 TInAS measurements of denpol and denpol-BAH-enzyme conjugate adsorption on $SiO_2$ surfaces

Sputtered $SiO_2$ TInAS sensors were cleaned by sonication in toluene and 2-propanol, 3 x 10 min each, dried in a nitrogen stream and cleaned in an oxygen plasma for 2 min.

After assembly of the TInAS flow cells, the sensors were equilibrated with buffer-5 for several hours and mounted on the TInAS instrument. All measurements were performed using a constant flow rate of 20 µL/min controlled with a peristaltic pump. For the solution exchanges during the experiments, the flow was stopped, the new solution feed installed and the flow cell flushed with the new solution at a flow rate of 400 µL/min for 45 – 60 s.

A baseline was recorded at a constant flow of buffer-5 before each experiment. For the adsorption of *de*-PG2 a 20 µM (repeating unit concentration) solution in buffer-5 was used. For the adsorption of the denpol-enzyme conjugates containing GOD and HRP, solutions at a repeating unit concentration of about 2 µM in buffer-5 were used.

For the denpol-enzyme conjugate containing proK, a *de*-PG2-BAH-proK solution at a proK concentration of 1 µM in buffer-11 was used.

## 5.5 QCM-D monitoring of enzyme co-immobilization on $SiO_2$ surfaces

$SiO_2$ coated QCM-D sensors (QSX 303 from Q-Sense AB, Gothenburg) were cleaned as reported earlier [129]. The sensors were cleaned by 20 min UV/ozone cleaning, 30 min sonication in a 2 % sodium dodecyl sulfate solution followed by 4 times washing with Milli-Q water, drying with nitrogen and 10 min further UV/ozone treatment. All QCM-D measurements were carried out on a Q-Sense E4 instrument equipped with flow cells and using a flow rate of 25 µL/min. All data presented are records of the $5^{th}$ overtone.

The QCM-D sensors used for the study of the adsorption of silica nanoparticles on the APTMS modified surface were treated as described by Thörn *et al.* [129]. In short, the cleaned sensors were immersed in a 1 %(v/v) APTMS solution in toluene for 40 min, followed by sonication for 2 x 5 min in toluene and 2 x 5 min in ethanol. After curing in Milli-Q water at 60 °C for 30 min, the sensors were rinsed with Milli-Q water and dried with nitrogen. For the *in situ* adsorption of the HMM or non-porous particles, a suspension of 0.4 %(w/v) of the particles in 10 mM HCl was injected, followed by a washing step and buffer exchange to the buffer used for enzyme loading (buffer-5 for pH 5.0 and buffer-8 for pH 6.0). Subsequent enzyme loading was performed with solutions of GOD (2 µM) or HRP (10 µM) in buffer-5 and buffer-8.

The co-immobilization procedure of GOD and HRP was analyzed on non-modified $SiO_2$ coated sensors by injection of solutions of *de*-PG2 (20 µM r.u. in buffer-5), HMM (suspension of 0.4 %(w/v) in buffer-5), GOD or HRP (2 µM or 10 µM, respectively, in

buffer-5) and *de*-PG2-BAH-HRP or *de*-PG2-BAH-GOD (7.5 µM in buffer-7or 14 µM in buffer-5, respectively). After each adsorption step, a rinsing step was carried out using the same buffer as the preceding adsorption step, in order to remove residual non-adsorbed material from the system.

## 5.6 Immobilization of denpol-BAH-enzyme conjugates on microscopy glass coverslips

Round borosilicate glass coverslips (8 mm diameter, thickness #1.5, obtained from Science Services, Germany) were cleaned by sonication in ethanol (3 times 10 min) and dried with nitrogen. The cleaned glass coverslips were transferred into 2 mL polypropylene (PP) reaction tubes and the surface wetted with buffer-5. For the adsorption of the denpol-BAH-enzyme conjugates, the buffer was removed and the denpol-BAH-enzyme conjugate added at a concentration of about 2 µM repeating units in buffer-5. After 1 h the solution was removed from the reaction tube and the glass slide washed 3 times with buffer-5 and 3 times with buffer-7. The enzyme coated glass coverslips were stored immersed in buffer at 4°C.

## 5.7 Enzyme co-immobilization on microscopy glass coverslips with HMM and denpol-enzyme conjugates

Round microscopy glass coverslips with a diameter of 8 mm and a total surface of 1 $cm^2$ were cleaned 3 times by sonication in ethanol for 10 min, dried with $N_2$ and cleaned in an oxygen plasma for 2 min. Cleaned coverslips were immersed in buffer-5 for storage. The immobilization procedure was performed according to the conditions elaborated during characterization of the adsorption processes with the QCM-D and all adsorption steps were followed by extensive washing of the coverslips with buffer in order to remove excess of material form the reaction tubes containing the coverslips. *de*-PG2 was adsorbed from a solution of 20 µM r.u. in buffer-5, followed by 1 h incubation in buffer-5 and subsequent adsorption of HMM particles from a 0.4 % (w/v) suspension in buffer-5. The loading of the adsorbed HMM particles was performed using a 2 µM GOD solution in buffer-5 for GOD loading or a 10 µM HRP solution in buffer-5 for HRP loading. Subsequent adsorption of the covering denpol-enzyme conjugate layer was performed using a solution of about 7.5 µM r.u. *de*-PG2-BAH-HRP in buffer-7 or about 14 µM r.u. *de*-PG2-BAH-GOD in buffer-5. The coverslips supporting the immobilized enzymes were stored in buffer-7 at 4 °C until further use.

## 5.8 Enzyme immobilization inside glass micropipettes

Glass micropipettes with an inner diameter of 1.6 mm (BlauBrand intraMARK, 200 µL nominal volume) were cleaned by sonication in ethanol for 3 x 10 min and dried with nitrogen. The glass micropipettes were fitted to a 1 mL syringe with PTFE tubing and the inner surface wetted by aspiration of a volume of buffer. Enzyme immobilization inside the micropipette was performed by aspiration of a solution containing the corresponding denpol-enzyme conjugate (*de*-PG2-BAH-HRP: about 2 µM r.u. concentration, in buffer-5; *de*-PG2-BAH-GOD: about 2 µM r.u. concentration, in buffer-5; *de*-PG2-BAH-(GOD,HRP): about 2 µM r.u. concentration; *de*-PG2-BAH-proK: about 1 µM BAH concentration, in buffer-11). After incubation for 1 hour, the solution was removed and the micropipette washed (GOD and HRP conjugates: 3 times with buffer-5 and 3 times with buffer-7; proK conjugate: 3 times with buffer-11), filled with buffer (GOD and HRP conjugates: buffer-7; proK conjugate: buffer-11), the open end closed with kinked silicone tubing and the device stored at 4 °C until use.

## 5.9 AFM analysis of denpol-enzyme conjugates on mica and on microscopy glass coverslips

The AFM analysis was performed by Jozef Adamcik, Laboratory of Food and Soft Materials, D-HEST, ETH Zürich. AFM specimens for the analysis of single chains of the denpol-enzyme conjugates were prepared on freshly cleaved mica. 20 µL of a solution of *de*-PG2 (20 µM r.u. concentration) or denpol-enzyme conjugates (about 2 µM r.u. concentration) was placed on the mica surface, incubated for 2 min, rinsed with Milli-Q water and dried with air. For the analysis of the denpol-enzyme conjugates adsorbed on glass coverslips, the glass coverslips were coated as for the activity measurements (see above), rinsed with Milli-Q water and dried with $N_2$.

## 5.10 Determination of enzymatic activities and storage stabilities

### 5.10.1 HRP activity in solution

The HRP activity in solution was measured at 25 °C in buffer-7, using 1 mM $ABTS^{2-}$ and 0.2 mM $H_2O_2$ as substrates. Buffer, $ABTS^{2-}$ and HRP samples were combined in a polystyrene cuvette and the reaction started by addition of $H_2O_2$. The formation of the product $ABTS^{\bullet -}$ was quantified UV/vis spectrophotometrically. Spectra were recorded for 1 minute in intervals of 5 seconds, and the slope of the increasing absorbance at 414 nm against time was evaluated.

A calibration curve correlating the enzymatic activity to the native HRP concentration in solution was prepared in the range of 0.25 – 8 nM HRP (**Figure 5.9.1a**).

An additional calibration curve was made for the quantification of low HRP concentrations (**Figure 5.9.1b**). The procedure was the same as described for the $ABTS^{2-}$ based assay, the substrate solution was replaced with a solution of 3.14 mM OPD and 80 µM $H_2O_2$ in buffer-7, which allowed reaction times of typically 20 min. Product formation was analyzed UV/vis spectrophotometrically at 418 nm.

### 5.10.2 HRP activity on microscopy glass coverslips

The activity of HRP immobilized on microscopy glass coverslips was measured by removal of the storage buffer from the glass coverslips and immediate addition of 1 mL of assay solution containing 1 mM $ABTS^{2-}$ and 0.2 mM $H_2O_2$ to the 2 mL PP reaction tube containing the coverslip. After a defined time, typically 1 min, the assay solution was removed from the reaction tube and the product formation was measured by UV/vis

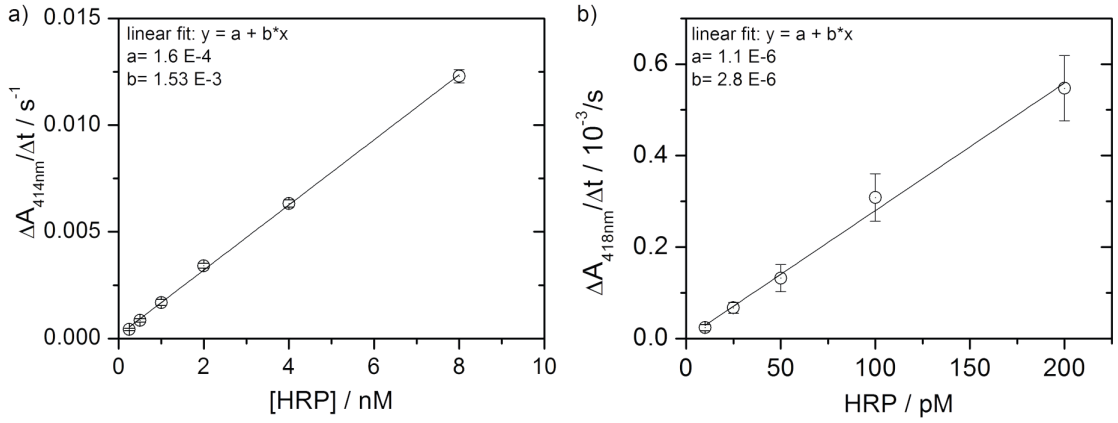


**Figure 5.9.1** Correlation of measured HRP activity with known amounts of HRP in solution. **a)** The $ABTS^{2-}$ assay was performed at pH 7.0 with 1 mM $ABTS^{2-}$ and 0.2 mM $H_2O_2$ as substrates. **b)** The OPD assay was performed at pH 7.0 with 3.14 mM OPD and 80 µM $H_2O_2$ as substrates.

spectrophotometry, using the $ABTS^{\bullet -}$ absorption band at 414 nm for quantification. The apparent surface concentration of HRP was calculated by comparison of the measured activity with the calibration curve determined under the same conditions with known amounts of HRP in solution (**Figure 5.9.1**).

### 5.10.3 GOD activity in solution

GOD activity in solution was measured at 25 °C at pH 7.0. The activity was measured using a coupled assay including 3.45 mM D-glucose and dissolved $O_2$ as substrates for GOD and 3.14 mM OPD and 2 nM HRP for the subsequent quantification of the $H_2O_2$ formed in the GOD-catalyzed oxidation of glucose. The assay was mixed in a polystyrene cuvette and the reaction started by addition of D-glucose. UV/vis spectra were recorded in intervals of 10 seconds for 20 minutes and the formation of the product of the cascade reaction, DAP, was followed at 418 nm. A calibration curve was measured using known amounts of native GOD in solution (**Figure 5.9.2**).

### 5.10.4 GOD activity on microscopy glass coverslips

The GOD activity on microscopy glass coverslips was measured by removal of the storage buffer from the PP tube containing the coverslip and addition of 1 mL of assay solution containing 3.45 mM D-glucose, dissolved $O_2$, 2 nM HRP and 3.14 mM OPD. The reaction tubes were kept in the dark for a defined time, typically 20 minutes. After removal of the assay solution from the reaction tubes, product formation was analyzed by

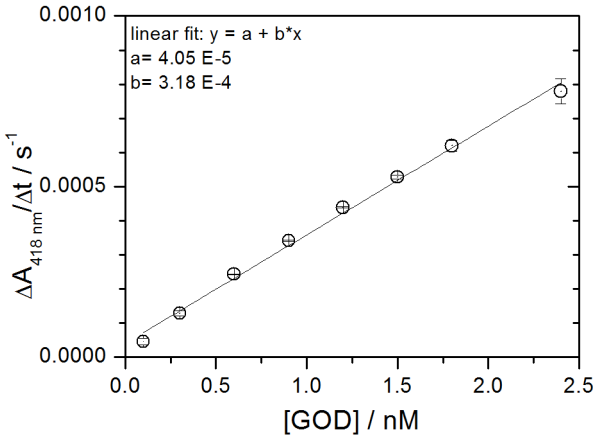


**Figure 5.9.2** Correlation of measured GOD activity with known amounts of GOD in solution. The activity assay was performed at pH 7.0 with 3.45 mM D-glucose and dissolved $O_2$ as substrates for GOD. The $H_2O_2$ formed was quantified *in situ* by HRP catalyzed oxidation of OPD and subsequent spectrophotometric determination of DAP at $\lambda$ = 418 nm.

UV/vis spectrophotometry, using the absorption band of DAP at λ = 418 nm. The apparent surface concentration of GOD was determined by comparison of activity measured with a calibration relating measured activity with known concentrations of native GOD in solution (**Figure 5.9.2**)

### 5.10.5 Measurement of enzymatic cascade reaction involving GOD and HRP

The activity assay for the enzymatic cascade reaction of GOD and HRP immobilized on microscopy glass coverslips was performed with the same assay solution as use for the GOD activity assay, except that no HRP was added to the solution. Therefore, the assay solution (pH 7.0) contained 3.45 mM D-glucose, dissolved $O_2$ and 3.14 mM OPD. To measure the catalytic cascade activity, the storage buffer solution was removed from the PP reaction tube containing the coverslip and the assay solution added to the coverslip for a defined time. During incubation, the reaction tube was stored in the dark. After incubation, the assay solution was removed from the reaction tube and product formation quantified by UV/vis spectrophotometry using the DAP absorption at λ = 418 nm.

### 5.10.6 proK activity in solution

The catalytic activity of proK in solution was measured at pH 7.0 using the protected tetrapeptide *para*-nitroanilide Suc-AAPF-pNA as substrate. 990 µL of a proK solution in buffer-11 were placed in a polystyrene cuvette and 10 µL 50 mM Suc-AAPF-pNA in DMF were added to start the reaction. UV/vis spectra were recorded in 15 second intervals for 5 minutes immediately after mixing. The rate of hydrolysis was determined by quantification of the reaction product *p*-nitroaniline using the absorption band at λ= 410 nm. A calibration correlating the measured hydrolytic activity with known amounts of native proK in solution was made using proK concentrations between 0.1 nM and 2 nM (**Figure 5.9.3**).

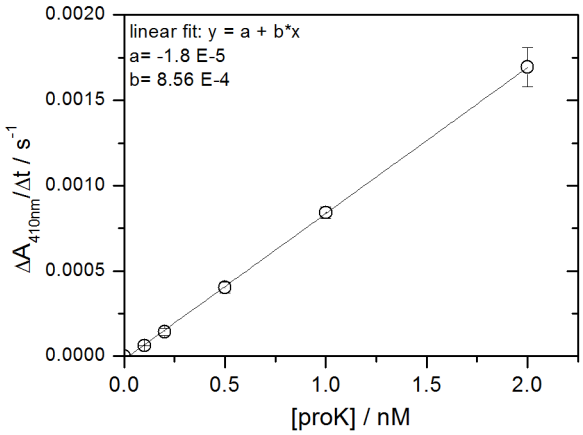


**Figure 5.9.3** Correlation of measured proK activity with known amounts of proK in solution. The activity assay was performed at pH 7.0 with 500 µM Suc-AAPF-pNA as substrate. The *p*-nitroaniline formed was quantified spectrophotometrically at λ = 410 nm.

Determination of $k_{cat}$ and $K_m$ according to the Michaelis-Menten kinetics was performed at an enzyme concentration of 5 nM for proK and proK-4FB and 16.5 nM for *de*-PG2-BAH-proK. The substrate concentration was varied from 30-250 µM. Additional DMF was added to the reaction mixture for a constant concentration of 1 vol% DMF in the final assay. UV/vis spectra were recorded in intervals of 5 seconds for 1 minute immediately after mixing. For the determination of the initial velocity, the absorption of *p*-nitroaniline was quantified at 410 nm ($\varepsilon_{4110nm}$ = 8800 $M^{-1}cm^{-1}$, [110]) and a linear fit for product concentration versus time was used for the determination of the reaction rate. The kinetic constants were obtained with a non-linear fit of the initial velocities versus substrate concentration according to the Michaelis-Menten equation.

### 5.10.7 Enzymatic activity measurements of immobilized proK on glass coverslips

The enzymatic activity of proK on microscopy glass coverslips was determined by removal of the storage solution from the PP tubes containing the coverslips and addition of an assay solution containing 500 µM Suc-AAPF-pNA in buffer-11. After a defined time, typically 5 min, the assay solutions were removed from the tubes and the UV/vis spectra measured. The rate of product formation was determined by evaluation of the absorption band of the product *p*-nitroaniline at λ = 410 nm and the apparent surface concentration of proK determined using a calibration curve made with known amounts of native proK (**Figure 5.9.3**).

## 5.11 Operational stability of adsorbed denpol-enzyme conjugates immobilized in glass micropipettes

### 5.11.1 Stability of sequential GOD-HRP cascade

A 7 cm long glass micropipette with adsorbed *de*-PG2-BAH-GOD and a 7 cm long glass micropipette with adsorbed *de*-PG2-BAH-HRP were connected with a short piece of silicone tubing. The inlet of the GOD containing micropipette was connected with PTFE tubing to a substrate feed, and the outlet of the HRP micropipette was connected to a UV/vis Z-flow cell and a peristaltic pump installed after the UV/vis cell. The substrate feed included 3.45 mM D-glucose, dissolved $O_2$ and 0.25 mM $ABTS^{2-}$ in buffer-7. The operational stability was studied at a constant flow of substrate solution controlled with the peristaltic pump at a flow rate of 230 µL/min by online UV/vis monitoring of the formation of the $ABTS^{\bullet -}$ at $\lambda$ = 414 nm.

### 5.11.2 Stability of co-immobilized GOD-HRP

The inlet of a 7 cm long glass micropipette with adsorbed *de*-PG2-BAH-(GOD,HRP) was connect with PTFE tubing to a substrate feed containing 3.45 mM D-glucose, dissolved $O_2$ and 0.25 mM $ABTS^{2-}$ in buffer-7. The outlet of the micropipette was connected to a UV/vis Z-flow cell and a peristaltic pump installed at the outlet of the flow cell. The operational stability of the device was studied by monitoring the formation of the product of the enzyme catalyzed cascade reaction, $ABTS^{\bullet -}$ with online UV/vis spectrophotometry under continuous flow conditions at a flow rate of 140 µL/min.

### 5.11.3 Stability of immobilized proK

The inlet of a 14 cm long glass micropipette with adsorbed *de*-PG2-BAH-proK was connected with PTFE tubing to a substrate feed containing 100 µM Suc-AAPF-pNA in buffer-11. The outlet of the micropipette was connected to a UV/vis Z-flow cell and a peristaltic pump. The operational stability of the device was studied at a continuous flow of 35 µL/min, monitoring the steady state level of the hydrolysis product *p*-nitroaniline by online UV/vis spectrophotometry.

## 5.12 Immobilization of proK in a microfluidic chip

Microfluidic experiments were performed in collaboration with Bernhard Sebastian and Prof. Petra Dittrich, Bioanalytics Group, D-BSSE, ETH Zürich. The design of the chip consisted of a single microchannel of 30 cm length, 100 µm width, and 40 µm height. The microfluidic channel consisted of 15 parallel channels (14 turns) of 1.84 cm length each feeding into an outlet channel of about 2 cm length. The side inlet connected to the main channel immediately after the 6$^{th}$ turn.

Microchannels were produced by cast-molding from a patterned silicon wafer using polydimethylsiloxane (PDMS, Sylgard 184 Dow, Midland, Michigan, USA). Prepolymer and curing agent were mixed 10:1 (w/w), degassed, and poured on a pattern silicon wafer, degassed again, and finally baked at 80 °C for one hour. The silicon wafer was produced in a clean room by standard soft lithography processing.

The PDMS chip was detached from the silicon wafer, cut, and connection holes were punched with a 1.5 mm diameter biopsy puncher. The chip was cleaned with soapy water and ethanol, rinsed with ultrapure water and dried with an air gun. A coverslip was cleaned with soapy water, acetone, isopropanol, and ethanol, rinsed with ultrapure water and dried with an air gun.

PDMS chip and cover slip were loaded in a plasma cleaner (Harrick Plasma, PDC-32G) for surface-activation in an air plasma for 45 seconds. The activated surfaces were brought into contact for assembly, and the chip was put on a 50 °C hot plate for 12 minutes for bonding.

The chip was primed with buffer-11 by centrifugation (Sigma 3-18K) at 800 rcf for 5 minutes. A 250 µL syringe (Agilent, Santa Clara, California, USA) was filled with *de*-PG2-BAH-proK (2 µM proK, in buffer-11). Another syringe (500 µL, Agilent, Santa Clara, California, USA) was filled with 400 µL BODIPY-FL-casein (20 µg/mL, in buffer-11) and a plug of 100 µL buffer-11 at the tip of the syringe. The syringes were connected to the microfluidic chip with PTFE tubing and controlled with syringe pumps (Nemesys, Cetoni, Korbußen, USA).

The microfluidic chip was mounted on a widefield inverted microscope (Olympus IX-70) equipped with a 4x objective (Olympus Plan, NA 0.1) and set up for bright light and fluorescence imaging. For fluorescence imaging a silver halide lamp in combination with a

470 nm/ 40 nm excitation filter, 495 nm dichroic mirror, and 525 nm/ 50 nm emission filter was used. Image acquisition was done using an Andor iXon EMCCD camera.

The conjugate was pumped through the microfluidic channel downstream of the side inlet at 2 µL/min for 60 min and then incubated at stopped flow for 30 min. To remove excess *de*-PG2-BAH-proK from the channel, the buffer plug was injected from the substrate syringe at a flow rate of 5 µL/min. After injection of the substrate, proK activity was monitored under steady state conditions at a flow rate of 14 nL/min by fluorescence imaging.

# 6 REFERENCES

[1] A. Payen, J. Persoz, Mémoire sur la diastase, les principaux produits de ses réactions et leurs applications aux arts industriels, Annales de chimie et de physique, 53 (1833) 73-92.

[2] J.J. Berzelius, Årsberättelsen om framsteg i fysik och kemi, Royal Swedish Academy of Sciences, 1835, pp. 245.

[3] J.J. Berzelius, Quelques Idées sur une nouvelle Force agissant dans les Combinaisons des Corps Organiques, Annales de chimie et de physique, 61 (1836) 146-151.

[4] D.E. Koshland, Stereochemistry and the Mechanism of Enzymatic Reactions, Biological Reviews, 28 (1953) 416-436.

[5] A.S. Bommarius, M.F. Paye, Stabilizing biocatalysts, Chemical Society Reviews, 42 (2013) 6534-6565.

[6] C. Garcia-Galan, Á. Berenguer-Murcia, R. Fernandez-Lafuente, R.C. Rodrigues, Potential of Different Enzyme Immobilization Strategies to Improve Enzyme Performance, Advanced Synthesis & Catalysis, 353 (2011) 2885-2904.

[7] I.H. Silman, E. Katchalski, Water-Insoluble Derivatives of Enzymes, Antigens, and Antibodies, Annual Review of Biochemistry, 35 (1966) 873-908.

[8] E. Katchalski-Katzir, Preparation, properties and uses of polymer-enzyme conjugates, Die Angewandte Makromolekulare Chemie, 166 (1989) 227-247.

[9] J.-Y. Wu, H.-S. Weng, Transient method for proposing the mechanisms of reactions over immobilized enzymes, Biotechnology and Bioengineering, 33 (1989) 415-421.

[10] W. Tischer, F. Wedekind, Immobilized Enzymes: Methods and Applications, in: W.-D. Fessner, A. Archelas, D. Demirjian, R. Furstoss, H. Griengl, K. Jaeger, E. Morís-Varas, R. Öhrlein, M. Reetz, J.L. Reymond, M. Schmidt, S. Servi, P. Shah, W. Tischer, F. Wedekind (Eds.) Biocatalysis - From Discovery to Application, Springer Berlin / Heidelberg, 1999, pp. 95-126.

[11] R.A. Sheldon, S. van Pelt, Enzyme immobilisation in biocatalysis: why, what and how, Chemical Society Reviews, 42 (2013) 6223-6235.

[12] A. Liese, L. Hilterhaus, Evaluation of immobilized enzymes for industrial applications, Chemical Society Reviews, 42 (2013) 6236-6249.

[13] E. Katchalski-Katzir, Immobilized enzymes — learning from past successes and failures, Trends in Biotechnology, 11 (1993) 471-478.

[14] R.A. Sheldon, Enzyme Immobilization: The Quest for Optimum Performance, Advanced Synthesis & Catalysis, 349 (2007) 1289-1307.

[15] U. Hanefeld, L. Gardossi, E. Magner, Understanding enzyme immobilisation, Chemical Society Reviews, 38 (2009) 453-468.

[16] B. Brena, P. González-Pombo, F. Batista-Viera, Immobilization of Enzymes: A Literature Survey, in: J.M. Guisan (Ed.) Immobilization of Enzymes and Cells, Humana Press, 2013, pp. 15-31.

[17] T. Jesionowski, J. Zdarta, B. Krajewska, Enzyme immobilization by adsorption: a review, Adsorption, 20 (2014) 801-821.

[18] M.H. Osman, A.A. Shah, F.C. Walsh, Recent progress and continuing challenges in bio-fuel cells. Part I: Enzymatic cells, Biosensors and Bioelectronics, 26 (2011) 3087-3102.

[19] S. Lu, Z. An, J. Li, J. He, pH-Triggered Adsorption–Desorption of Enzyme in Mesoporous Host to Act on Macrosubstrate, The Journal of Physical Chemistry B, 115 (2011) 13695-13700.

[20] C. Mateo, J.M. Palomo, G. Fernandez-Lorente, J.M. Guisan, R. Fernandez-Lafuente, Improvement of enzyme activity, stability and selectivity via immobilization techniques, Enzyme and Microbial Technology, 40 (2007) 1451-1463.

[21] C. Mateo, J.M. Palomo, M. Fuentes, L. Betancor, V. Grazu, F. López-Gallego, B.C.C. Pessela, A. Hidalgo, G. Fernández-Lorente, R. Fernández-Lafuente, J.M. Guisán, Glyoxyl agarose: A fully inert and hydrophilic support for immobilization and high stabilization of proteins, Enzyme and Microbial Technology, 39 (2006) 274-280.

[22] C. Mateo, G. Fernandez-Lorente, J. Rocha-Martin, J. Bolivar, J. Guisan, Oriented Covalent Immobilization of Enzymes on Heterofunctional-Glyoxyl Supports, in: J.M. Guisan (Ed.) Immobilization of Enzymes and Cells, Humana Press, 2013, pp. 73-88.

[23] F. López-Gallego, J. Guisán, L. Betancor, Glutaraldehyde-Mediated Protein Immobilization, in: J.M. Guisan (Ed.) Immobilization of Enzymes and Cells, Humana Press, 2013, pp. 33-41.

[24] A. Ménard, Y. Huang, P. Karam, G. Cosa, K. Auclair, Site-Specific Fluorescent Labeling and Oriented Immobilization of a Triple Mutant of CYP3A4 via C64, Bioconjugate Chemistry, 23 (2012) 826-836.

[25] E. Steen Redeker, D.T. Ta, D. Cortens, B. Billen, W. Guedens, P. Adriaensens, Protein Engineering For Directed Immobilization, Bioconjugate Chemistry, 24 (2013) 1761-1777.

[26] N.M. Green, Avidin, in: J.T.E. C.B. Anfinsen, M.R. Frederic (Eds.) Advances in Protein Chemistry, Academic Press, 1975, pp. 85-133.

[27] S. Feifel, A. Kapp, F. Lisdat, Protein Multilayer Architectures on Electrodes for Analyte Detection, in: M.B. Gu, H.-S. Kim (Eds.) Biosensors Based on Aptamers and Enzymes, Springer Berlin Heidelberg, 2014, pp. 253-298.

[28] H. Mao, T. Yang, P.S. Cremer, Design and Characterization of Immobilized Enzymes in Microfluidic Systems, Analytical Chemistry, 74 (2002) 379-385.

[29] G. Zhen, V. Eggli, J. Vörös, P. Zammaretti, M. Textor, R. Glockshuber, E. Kuennemann, Immobilization of the Enzyme β-Lactamase on Biotin-Derivatized Poly(l-lysine)-g-poly(ethylene glycol)-Coated Sensor Chips: A Study on Oriented Attachment and Surface Activity by Enzyme Kinetics and in Situ Optical Sensing, Langmuir, 20 (2004) 10464-10473.

[30] S. Fornera, T.E. Balmer, B. Zhang, A.D. Schlüter, P. Walde, Immobilization of Peroxidase on $SiO_2$ Surfaces with the Help of a Dendronized Polymer and the Avidin-Biotin System, Macromolecular Bioscience, 11 (2011) 1052-1067.

[31] C.J. Galvin, J. Genzer, Applications of surface-grafted macromolecules derived from post-polymerization modification reactions, Progress in Polymer Science, 37 (2012) 871-906.

[32] S. Tugulu, A. Arnold, I. Sielaff, K. Johnsson, H.-A. Klok, Protein-Functionalized Polymer Brushes, Biomacromolecules, 6 (2005) 1602-1607.

[33] S.P. Cullen, I.C. Mandel, P. Gopalan, Surface-Anchored Poly(2-vinyl-4,4-dimethyl azlactone) Brushes as Templates for Enzyme Immobilization, Langmuir, 24 (2008) 13701-13709.

[34] G. Decher, J.-D. Hong, Buildup of ultrathin multilayer films by a self-assembly process, 1 consecutive adsorption of anionic and cationic bipolar amphiphiles on charged surfaces, Makromolekulare Chemie. Macromolecular Symposia, 46 (1991) 321-327.

[35] G. Decher, J.D. Hong, J. Schmitt, Buildup of ultrathin multilayer films by a self-assembly process: III. Consecutively alternating adsorption of anionic and cationic

polyelectrolytes on charged surfaces, Thin Solid Films, 210-211, Part 2 (1992) 831-835.

[36] G. Decher, M. Eckle, J. Schmitt, B. Struth, Layer-by-layer assembled multicomposite films, Current Opinion in Colloid & Interface Science, 3 (1998) 32-39.

[37] J.-i. Anzai, H. Takeshita, Y. Kobayashi, T. Osa, T. Hoshi, Layer-by-Layer Construction of Enzyme Multilayers on an Electrode for the Preparation of Glucose and Lactate Sensors: Elimination of Ascorbate Interference by Means of an Ascorbate Oxidase Multilayer, Analytical Chemistry, 70 (1998) 811-817.

[38] G. Palazzo, G. Colafemmina, C. Guzzoni Iudice, A. Mallardi, Three immobilized enzymes acting in series in layer by layer assemblies: Exploiting the trehalase-glucose oxidase-horseradish peroxidase cascade reactions for the optical determination of trehalose, Sensors and Actuators B: Chemical, 202 (2014) 217-223.

[39] M. Burchardt, G. Wittstock, Kinetic studies of glucose oxidase in polyelectrolyte multilayer films by means of scanning electrochemical microscopy (SECM), Bioelectrochemistry, 72 (2008) 66-76.

[40] N.L. St. Clair, M.A. Navia, Cross-linked enzyme crystals as robust biocatalysts, Journal of the American Chemical Society, 114 (1992) 7314-7316.

[41] A.L. Margolin, M.A. Navia, Protein Crystals as Novel Catalytic Materials, Angewandte Chemie International Edition, 40 (2001) 2204-2222.

[42] L. Cao, F. van Rantwijk, R.A. Sheldon, Cross-Linked Enzyme Aggregates: A Simple and Effective Method for the Immobilization of Penicillin Acylase, Organic Letters, 2 (2000) 1361-1364.

[43] R.A. Sheldon, Cross-linked enyzme aggregates (CLEA's): stable and recyclable biocatalysts, Biochemical Society Transactions, 35 (2007) 1583-1587.

[44] S. Hudson, J. Cooney, E. Magner, Proteins in Mesoporous Silicates, Angewandte Chemie International Edition, 47 (2008) 8582-8594.

[45] C.-H. Lee, T.-S. Lin, C.-Y. Mou, Mesoporous materials for encapsulating enzymes, Nano Today, 4 (2009) 165-179.

[46] E. Magner, Immobilisation of enzymes on mesoporous silicate materials, Chemical Society Reviews, 42 (2013) 6213-6222.

[47] Z. Zhou, M. Hartmann, Progress in enzyme immobilization in ordered mesoporous materials and related applications, Chemical Society Reviews, 42 (2013) 3894-3912.

[48] N. Carlsson, H. Gustafsson, C. Thörn, L. Olsson, K. Holmberg, B. Åkerman, Enzymes immobilized in mesoporous silica: A physical–chemical perspective, Advances in Colloid and Interface Science, 205 (2014) 339-360.

[49] M. Hartmann, X. Kostrov, Immobilization of enzymes on porous silicas - benefits and challenges, Chemical Society Reviews, 42 (2013) 6277-6289.

[50] C. Thörn, N. Carlsson, H. Gustafsson, K. Holmberg, B. Åkerman, L. Olsson, A method to measure pH inside mesoporous particles using protein-bound SNARF1 fluorescent probe, Microporous and Mesoporous Materials, 165 (2013) 240-246.

[51] C. Lei, Y. Shin, J.K. Magnuson, G. Fryxell, L.L. Lasure, D.C. Elliott, J. Liu, E.J. Ackerman, Characterization of functionalized nanoporous supports for protein confinement, Nanotechnology, 17 (2006) 5531.

[52] M. Burchardt, G. Wittstock, Micropatterned Multienzyme Devices with Adjustable Amounts of Immobilized Enzymes, Langmuir, 29 (2013) 15090-15099.

[53] K. Ariga, Q. Ji, T. Mori, M. Naito, Y. Yamauchi, H. Abe, J.P. Hill, Enzyme nanoarchitectonics: organization and device application, Chemical Society Reviews, 42 (2013) 6322-6345.

[54] F. Jia, B. Narasimhan, S. Mallapragada, Materials-based strategies for multi-enzyme immobilization and co-localization: A review, Biotechnology and Bioengineering, 111 (2014) 209-222.

[55] Y. Guo, J.D. van Beek, B. Zhang, M. Colussi, P. Walde, A. Zhang, M. Kröger, A. Halperin, A.D. Schlüter, Tuning Polymer Thickness: Synthesis and Scaling Theory of Homologous Series of Dendronized Polymers, Journal of the American Chemical Society, 131 (2009) 11841-11854.

[56] A. Grotzky, T. Nauser, H. Erdogan, A.D. Schlüter, P. Walde, A Fluorescently Labeled Dendronized Polymer–Enzyme Conjugate Carrying Multiple Copies of Two Different Types of Active Enzymes, Journal of the American Chemical Society, 134 (2012) 11392-11395.

[57] A.D. Schlüter, Dendrimers with Polymeric Core: Towards Nanocylinders, in: Dendrimers, Springer Berlin Heidelberg, 1998, pp. 165-191.

[58] H. Frey, From Random Coil to Extended Nanocylinder: Dendrimer Fragments Shape Polymer Chains, Angewandte Chemie International Edition, 37 (1998) 2193-2197.

[59] A.D. Schlüter, A. Halperin, M. Kröger, D. Vlassopoulos, G. Wegner, B. Zhang, Dendronized Polymers: Molecular Objects between Conventional Linear Polymers and Colloidal Particles, ACS Macro Letters, 3 (2014) 991-998.

[60] O. Bertran, B. Zhang, A.D. Schlüter, M. Kröger, C. Alemán, Modeling Nanosized Single Molecule Objects: Dendronized Polymers Adsorbed onto Mica, The Journal of Physical Chemistry C, 119 (2015) 3746-3753.

[61] H. Yu, A.D. Schlüter, B. Zhang, Synthesis of High Generation Dendronized Polymers and Quantification of Their Structure Perfection, Macromolecules, 47 (2014) 4127-4135.

[62] B. Zhang, R. Wepf, K. Fischer, M. Schmidt, S. Besse, P. Lindner, B.T. King, R. Sigel, P. Schurtenberger, Y. Talmon, Y. Ding, M. Kröger, A. Halperin, A.D. Schlüter, The Largest Synthetic Structure with Molecular Precision: Towards a Molecular Object, Angewandte Chemie International Edition, 50 (2011) 737-740.

[63] O. Bertran, B. Zhang, A.D. Schlüter, A. Halperin, M. Kröger, C. Alemán, Computer simulation of dendronized polymers: organization and characterization at the atomistic level, RSC Advances, 3 (2013) 126-140.

[64] A. Grotzky, E. Altamura, J. Adamcik, P. Carrara, P. Stano, F. Mavelli, T. Nauser, R. Mezzenga, A.D. Schlüter, P. Walde, Structure and Enzymatic Properties of Molecular Dendronized Polymer–Enzyme Conjugates and Their Entrapment inside Giant Vesicles, Langmuir, 29 (2013) 10831-10840.

[65] A. Grotzky, Dendronized Polymers and Enzymes: A Molecular Hybrid Structure, ETH Dissertation Nr. 20689, Zürich, 2012.

[66] S. Fornera, P. Kuhn, D. Lombardi, A.D. Schlüter, P.S. Dittrich, P. Walde, Sequential Immobilization of Enzymes in Microfluidic Channels for Cascade Reactions, ChemPlusChem, 77 (2012) 98-101.

[67] S. Fornera, T. Bauer, A.D. Schlüter, P. Walde, Simple enzyme immobilization inside glass tubes for enzymatic cascade reactions, Journal of Materials Chemistry, 22 (2012) 502-511.

[68] M. Howarth, K. Takao, Y. Hayashi, A.Y. Ting, Targeting quantum dots to surface proteins in living cells with biotin ligase, Proceedings of the National Academy of Sciences of the United States of America, 102 (2005) 7583-7588.

[69] M. Howarth, D.J.F. Chinnapen, K. Gerrow, P.C. Dorrestein, M.R. Grandy, N.L. Kelleher, A. El-Husseini, A.Y. Ting, A monovalent streptavidin with a single femtomolar biotin binding site, Nature Methods, 3 (2006) 267-273.

[70] A. Viens, F. Harper, E. Pichard, M. Comisso, G. Pierron, V. Ogryzko, Use of Protein Biotinylation In Vivo for Immunoelectron Microscopic Localization of a Specific Protein Isoform, Journal of Histochemistry & Cytochemistry, 56 (2008) 911-919.

[71] E. de Boer, P. Rodriguez, E. Bonte, J. Krijgsveld, E. Katsantoni, A. Heck, F. Grosveld, J. Strouboulis, Efficient biotinylation and single-step purification of tagged transcription factors in mammalian cells and transgenic mice, Proceedings of the National Academy of Sciences, 100 (2003) 7480-7485.

[72] D.A. Schwartz, Solulink Biosciences, Inc., Hydrazine-based and carbonyl-based bifunctional crosslinking reagents, 2004, U.S. Patent 6800728.

[73] A. Dirksen, P.E. Dawson, Rapid Oxime and Hydrazone Ligations with Aromatic Aldehydes for Biomolecular Labeling, Bioconjugate Chemistry, 19 (2008) 2543-2548.

[74] A. Dirksen, S. Yegneswaran, P.E. Dawson, Bisaryl Hydrazones as Exchangeable Biocompatible Linkers, Angewandte Chemie International Edition, 49 (2010) 2023-2027.

[75] L.M. Shannon, E. Kay, J.Y. Lew, Peroxidase Isozymes from Horseradish Roots, Journal of Biological Chemistry, 241 (1966) 2166-2172.

[76] S. Aibara, H. Yamashita, E. Mori, M. Kato, Y. Morita, Isolation and Characterization of Five Neutral Isoenzymes of Horseradish Peroxidase, Journal of Biochemistry, 92 (1982) 531-539.

[77] N.C. Veitch, Horseradish peroxidase: a modern view of a classic enzyme, Phytochemistry, 65 (2004) 249-259.

[78] A.M. O'Brien, C. Ó'Fágáin, P.F. Nielsen, K.G. Welinder, Location of crosslinks in chemically stabilized horseradish peroxidase: Implications for design of crosslinks, Biotechnology and Bioengineering, 76 (2001) 277-284.

[79] K.G. Welinder, Covalent structure of the glycoprotein horseradish peroxidase (EC 1.11.1.7), FEBS Letters, 72 (1976) 19-23.

[80] K.G. Welinder, Amino Acid Sequence Studies of Horseradish Peroxidase, European Journal of Biochemistry, 96 (1979) 483-502.

[81] J.S.S. Gray, B.Y. Yang, R. Montgomery, Heterogeneity of glycans at each N-glycosylation site of horseradish peroxidase, Carbohydrate Research, 311 (1998) 61-69.

[82] N.C. Veitch, A.T. Smith, Horseradish peroxidase, in: Advances in Inorganic Chemistry, Academic Press, 2000, pp. 107-162.

[83] H.M. Theorell, Andreas C., Untersuchungen an künstlichen Peroxydasen, Acta Chemica Scandinavica, 4 (1950) 422-434.

[84] B.K. Van Weemen, A.H.W.M. Schuurs, Immunoassay using antigen—enzyme conjugates, FEBS Letters, 15 (1971) 232-236.

[85] R.E. Childs, W.G. Bardsley, The Steady-State Kinetics of Peroxidase with 2,2'-Azino-di-(3-ethylbenzthiazoline-6-sulphonic acid) as Chromogen, Biochemical Journal, 145 (1975) 93-103.

[86] C. Hempen, S. van Leeuwen, H. Luftmann, U. Karst, Liquid chromatographic/mass spectrometric investigation on the reaction products in the peroxidase-catalyzed oxidation of o-phenylenediamine by hydrogen peroxide, Analytical and Bioanalytical Chemistry, 382 (2005) 234-238.

[87] S. Fornera, P. Walde, Spectrophotometric quantification of horseradish peroxidase with o-phenylenediamine, Analytical Biochemistry, 407 (2010) 293-295.

[88] V.M. Mekler, S.M. Bystryak, Application of o-phenylenediamine as a fluorogenic substrate in peroxidase-mediated enzyme-linked immunosorbent assay, Analytica Chimica Acta, 264 (1992) 359-363.

[89] J.H. Pazur, K. Kleppe, The Oxidation of Glucose and Related Compounds by Glucose Oxidase from Aspergillus niger, Biochemistry, 3 (1964) 578-583.

[90] H.J. Hecht, H.M. Kalisz, J. Hendle, R.D. Schmid, D. Schomburg, Crystal Structure of Glucose Oxidase from Aspergillus niger Refined at 2·3 Å Reslution, Journal of Molecular Biology, 229 (1993) 153-172.

[91] B.E.P. Swoboda, V. Massey, Purification and Properties of the Glucose Oxidase from Aspergillus niger, Journal of Biological Chemistry, 240 (1965) 2209-2215.

[92] B. Solomon, N. Lotan, E. Katchalski-Katzir, Enzymic activity and conformational properties of native and crosslinked glucose oxidase, Biopolymers, 16 (1977) 1837-1851.

[93] Q.H. Gibson, B.E.P. Swoboda, V. Massey, Kinetics and Mechanism of Action of Glucose Oxidase, Journal of Biological Chemistry, 239 (1964) 3927-3934.

[94] R. Wilson, A.P.F. Turner, Glucose oxidase: an ideal enzyme, Biosensors and Bioelectronics, 7 (1992) 165-185.

[95] C. Wong, K. Wong, X. Chen, Glucose oxidase: natural occurrence, function, properties and industrial applications, Applied Microbiology and Biotechnology, 78 (2008) 927-938.

[96] I. Willner, Y.M. Yan, B. Willner, R. Tel-Vered, Integrated Enzyme-Based Biofuel Cells–A Review, Fuel Cells, 9 (2009) 7-24.

[97] D.P. Kotler, A.R. Tierney, N.S. Rosensweig, An enzymatic microassay for lactose, Analytical Biochemistry, 110 (1981) 393-396.

[98] S. Fornera, K. Yazawa, P. Walde, Spectrophotometric quantification of lactose in solution with a peroxidase-based enzymatic cascade reaction system, Analytical and Bioanalytical Chemistry, 401 (2011) 2307-2310.

[99] W. Ebeling, N. Hennrich, M. Klockow, H. Metz, H.D. Orth, H. Lang, Proteinase K from Tritirachium album Limber, European Journal of Biochemistry, 47 (1974) 91-97.

[100] W. Saenger, Chapter 714 - Proteinase K, in: Handbook of Proteolytic Enzymes, Academic Press, 2013, pp. 3240-3242.

[101] C. Betzel, S. Gourinath, P. Kumar, P. Kaur, M. Perbandt, S. Eschenburg, T.P. Singh, Structure of a Serine Protease Proteinase K from Tritirachium album limber at 0.98 Å Resolution†, Biochemistry, 40 (2001) 3080-3088.

[102] K. Morihara, H. Tsuzuki, Specificity of Proteinase K from *Tritirachium album* Limber for Synthetic Peptides, Agricultural and Biological Chemistry, 39 (1975) 1489-1492.

[103] B. Borhan, B. Hammock, J. Seifert, B.W. Wilson, Methyl and phenyl esters and thioesters of carboxylic acids as surrogate substrates for microassay of proteinase K esterase activity, Fresenius' Journal of Analytical Chemistry, 354 (1996) 490-492.

[104] V. Čeřovský, K. Martinek, Peptide synthesis catalyzed by native proteinase K in water-miscible organic solvents with low water content, Collection of Czechoslovak Chemical Communications, 54 (1989) 2027-2041.

[105] U. Wiegers, H. Hilz, A new method using 'proteinase K' to prevent mRNA degradation during isolation from HeLa cells, Biochemical and Biophysical Research Communications, 44 (1971) 513-519.

[106] U. Wiegers, H. Hilz, Rapid isolation of undegraded polysomal RNA without phenol, FEBS Letters, 23 (1972) 77-82.

[107] R.K. Räuber Norbert, K.-D. Jany, G. Pfleiderer, Ribonuclease A Digestion by Proteinase K, in: Zeitschrift für Naturforschung C, 1978, pp. 660.

[108] R.A. Bessen, R.F. Marsh, Biochemical and physical properties of the prion protein from two strains of the transmissible mink encephalopathy agent, Journal of Virology, 66 (1992) 2096-2101.

[109] R. Morales, C. Duran-Aniotz, R. Diaz-Espinoza, M.V. Camacho, C. Soto, Protein misfolding cyclic amplification of infectious prions, Nature Protocols, 7 (2012) 1397-1409.

[110] B.F. Erlanger, N. Kokowsky, W. Cohen, The preparation and properties of two new chromogenic substrates of trypsin, Archives of Biochemistry and Biophysics, 95 (1961) 271-278.

[111] E. Kraus, U. Femfert, Proteinase K from the Mold Tritirachium album Limber, Specificity and Mode of Action, Hoppe-Seyler's Zeitschrift für physiologische Chemie, 357 (1976) 937-947.

[112] D. Georgieva, N. Genov, W. Voelter, C. Betzel, Catalytic Efficiencies of Alkaline Proteinases from Microorganisms, Zeitschrift für Naturforschung C, 61c (2006) 445-452.

[113] Product Catalog & Reference Manual, Solulink, Inc., 2008.

[114] A.A. Yaroslavov, O.Y. Kuchenkova, I.B. Okuneva, N.S. Melik-Nubarov, N.O. Kozlova, V.I. Lobyshev, F.M. Menger, V.A. Kabanov, Effect of polylysine on transformations and permeability of negative vesicular membranes, Biochimica et Biophysica Acta (BBA) - Biomembranes, 1611 (2003) 44-54.

[115] A. Grotzky, Y. Manaka, S. Fornera, M. Willeke, P. Walde, Quantification of α-polylysine: a comparison of four UV/Vis spectrophotometric methods, Analytical Methods, 2 (2010) 1448-1455.

[116] G.I. Berglund, G.H. Carlsson, A.T. Smith, H. Szoke, A. Henriksen, J. Hajdu, The catalytic pathway of horseradish peroxidase at high resolution, Nature, 417 (2002) 463-468.

[117] M. Heuberger, T.E. Balmer, The transmission interferometric adsorption sensor, Journal of Physics D: Applied Physics, 40 (2007) 7245.

[118] T. Sannomiya, T.E. Balmer, M. Heuberger, J. Vörös, Simultaneous refractive index and thickness measurement with the transmission interferometric adsorption sensor, Journal of Physics D: Applied Physics, 43 (2010) 405302.

[119] T.L. McMeekin, M. Wilensky, M.L. Groves, Refractive indices of proteins in relation to amino acid composition and specific volume, Biochemical and Biophysical Research Communications, 7 (1962) 151-156.

[120] H. Ye, Simultaneous determination of protein aggregation, degradation, and absolute molecular weight by size exclusion chromatography–multiangle laser light scattering, Analytical Biochemistry, 356 (2006) 76-85.

[121] Toyobo Enzymes, Japan, http://www.toyobo-global.com/seihin/xr/enzyme/

[122] J.H. Pazur, K. Kleppe, A. Cepure, A glycoprotein structure for glucose oxidase from Aspergillus niger, Archives of Biochemistry and Biophysics, 111 (1965) 351-357.

[123] F. Vianello, L. Zennaro, M.L. Di Paolo, A. Rigo, C. Malacarne, M. Scarpa, Preparation, morphological characterization, and activity of thin films of horseradish peroxidase, Biotechnology and Bioengineering, 68 (2000) 488-495.

[124] S.M. Lane, Z. Kuang, J. Yom, S. Arifuzzaman, J. Genzer, B. Farmer, R. Naik, R.A. Vaia, Poly(2-hydroxyethyl methacrylate) for Enzyme Immobilization: Impact on Activity and Stability of Horseradish Peroxidase, Biomacromolecules, 12 (2011) 1822-1830.

[125] C. Draghici, J. Kowal, A. Darjan, W. Meier, C.G. Palivan, “Active Surfaces” Formed by Immobilization of Enzymes on Solid-Supported Polymer Membranes, Langmuir, 30 (2014) 11660-11669.

[126] F.J. Millero, F. Huang, A.L. Laferiere, The solubility of oxygen in the major sea salts and their mixtures at 25°C, Geochimica et Cosmochimica Acta, 66 (2002) 2349-2359.

[127] M. Hartmann, D. Jung, Biocatalysis with enzymes immobilized on mesoporous hosts: the status quo and future trends, Journal of Materials Chemistry, 20 (2010) 844-857.

[128] Z. Zhou, M. Hartmann, Recent Progress in Biocatalysis with Enzymes Immobilized on Mesoporous Hosts, Topics in Catalysis, 55 (2012) 1081-1100.

[129] C. Thörn, H. Gustafsson, L. Olsson, QCM-D as a method for monitoring enzyme immobilization in mesoporous silica particles, Microporous and Mesoporous Materials, 176 (2013) 71-77.

[130] A.B.D. Nandiyanto, S.-G. Kim, F. Iskandar, K. Okuyama, Synthesis of spherical mesoporous silica nanoparticles with nanometer-size controllable pores and outer diameters, Microporous and Mesoporous Materials, 120 (2009) 447-453.

[131] H. Gustafsson, E.M. Johansson, A. Barrabino, M. Odén, K. Holmberg, Immobilization of lipase from Mucor miehei and Rhizopus oryzae into mesoporous silica—The effect of varied particle size and morphology, Colloids and Surfaces B: Biointerfaces, 100 (2012) 22-30.

[132] J.M. Rosenholm, M. Lindén, Wet-Chemical Analysis of Surface Concentration of Accessible Groups on Different Amino-Functionalized Mesoporous SBA-15 Silicas, Chemistry of Materials, 19 (2007) 5023-5034.

[133] K.C. Brown, J.F. Corbett, N.P. Loveless, Spectrophotometric studies on the protonation of hydroxy and aminophenazines in aqueous solution, Spectrochimica Acta Part A: Molecular Spectroscopy, 35 (1979) 421-423.

[134] Y. Wang, F. Caruso, Mesoporous Silica Spheres as Supports for Enzyme Immobilization and Encapsulation, Chemistry of Materials, 17 (2005) 953-961.

[135] Y. Wang, F. Caruso, Enzyme encapsulation in nanoporous silica spheres, Chemical Communications, (2004) 1528-1529.

[136] H. Takahashi, B. Li, T. Sasaki, C. Miyazaki, T. Kajino, S. Inagaki, Catalytic Activity in Organic Solvents and Stability of Immobilized Enzymes Depend on the Pore Size and Surface Characteristics of Mesoporous Silica, Chemistry of Materials, 12 (2000) 3301-3305.

[137] H. Takahashi, B. Li, T. Sasaki, C. Miyazaki, T. Kajino, S. Inagaki, Immobilized enzymes in ordered mesoporous silica materials and improvement of their stability and catalytic activity in an organic solvent, Microporous and Mesoporous Materials, 44–45 (2001) 755-762.

[138] C. Spahn, S.D. Minteer, Enzyme Immobilization in Biotechnology, Recent Patents on Engineering, 2 (2008) 195-200.

[139] A. Le Nel, N. Minc, C. Smadja, M. Slovakova, Z. Bilkova, J.-M. Peyrin, J.-L. Viovy, M. Taverna, Controlled proteolysis of normal and pathological prion protein in a microfluidic chip, Lab on a Chip, 8 (2008) 294-301.

[140] C. Wang, R. Oleschuk, F. Ouchen, J. Li, P. Thibault, D.J. Harrison, Integration of immobilized trypsin bead beds for protein digestion within a microfluidic chip incorporating capillary electrophoresis separations and an electrospray mass spectrometry interface, Rapid Communications in Mass Spectrometry, 14 (2000) 1377-1383.

[141] T. Liu, S. Wang, G. Chen, Immobilization of trypsin on silica-coated fiberglass core in microchip for highly efficient proteolysis, Talanta, 77 (2009) 1767-1773.

[142] P. Liuni, T. Rob, D.J. Wilson, A microfluidic reactor for rapid, low-pressure proteolysis with on-chip electrospray ionization, Rapid Communications in Mass Spectrometry, 24 (2010) 315-320.

[143] S. Liu, H. Bao, L. Zhang, G. Chen, Efficient proteolysis strategies based on microchip bioreactors, Journal of Proteomics, 82 (2013) 1-13.

[144] M. Slovakova, N. Minc, Z. Bilkova, C. Smadja, W. Faigle, C. Futterer, M. Taverna, J.-L. Viovy, Use of self assembled magnetic beads for on-chip protein digestion, Lab on a Chip, 5 (2005) 935-942.

[145] Z. Bílková, M. Slováková, N. Minc, C. Fütterer, R. Cecal, D. Horák, M. Beneš, I. le Potier, J. Křenková, M. Przybylski, J.-L. Viovy, Functionalized magnetic micro- and nanoparticles: Optimization and application to μ-chip tryptic digestion, Electrophoresis, 27 (2006) 1811-1824.

[146] J.P. da Costa, R. Oliveira-Silva, A.L. Daniel-da-Silva, R. Vitorino, Bionanoconjugation for Proteomics applications — An overview, Biotechnology Advances, 32 (2014) 952-970.

[147] H. Wu, J. Zhai, Y. Tian, H. Lu, X. Wang, W. Jia, B. Liu, P. Yang, Y. Xu, H. Wang, Microfluidic enzymatic-reactors for peptide mapping: strategy, characterization, and performance, Lab on a Chip, 4 (2004) 588-597.

[148] J. Lee, H.K. Musyimi, S.A. Soper, K.K. Murray, Development of an Automated Digestion and Droplet Deposition Microfluidic Chip for MALDI-TOF MS, Journal of the American Society for Mass Spectrometry, 19 (2008) 964-972.

[149] M. Slováková, J.-M. Peyrin, Z. Bílková, M. Juklíčková, L. Hernychová, J.-L. Viovy, Magnetic Proteinase K Reactor as a New Tool for Reproducible Limited Protein Digestion, Bioconjugate Chemistry, 19 (2008) 966-972.

[150] L.J. Jones, R.H. Upson, R.P. Haugland, N. Panchuk-Voloshina, M. Zhou, R.P. Haugland, Quenched BODIPY Dye-Labeled Casein Substrates for the Assay of Protease Activity by Direct Fluorescence Measurement, Analytical Biochemistry, 251 (1997) 144-152.

[151] S.D. Minteer, B.Y. Liaw, M.J. Cooney, Enzyme-based biofuel cells, Current Opinion in Biotechnology, 18 (2007) 228-234.

[152] P. Dennler, A. Chiotellis, E. Fischer, D. Brégeon, C. Belmant, L. Gauthier, F. Lhospice, F. Romagne, R. Schibli, Transglutaminase-Based Chemo-Enzymatic Conjugation Approach Yields Homogeneous Antibody–Drug Conjugates, Bioconjugate Chemistry, 25 (2014) 569-578.

# 7 ACKNOWLEDGEMENTS

This work would not have been possible without the many people supporting me at work and during my free hours. I would like to say *thank you* to all of you!

First of all, Prof. Peter Walde, for giving me the opportunity to work on this project. Your open door in case of any problems or doubts and your ambition to not only support me in all my struggles with daily lab-life, but also to pass on your knowledge to deepen and broaden my understanding and to fortify my critical thinking was invaluable and is highly appreciated. I am also very grateful to Prof. A. Dieter Schlüter for the support and constructive inputs and the enthusiasm for a project at the edge of the groups focus, but never outside your concern.

Prof. Raffaele Mezzenga is acknowledged for accepting to be a co-examiner, as well as for his support for the AFM measurements, and Prof. André Studart for accepting to be a co-examiner and his valuable inputs during the 1st year project assessment.

Dr. Andrea Grotzky laid not only the groundwork for this project with her investigations of denpol-enzyme conjugates in solution. Her shared experience helped to avoid pitfalls, and the linker molecules and a batch of polymer she generously contributed were of utmost importance for a successful completion of the present work. Also Dr. Baozhon Zhang's contribution of a batch of polymer was a cornerstone of the project.

I also thank Dr. Hanna Gustafsson and Prof. Krister Holmberg for making my stay at Chalmers University in Gothenburg a very productive but also a very pleasant time. The work with mesoporous silicates, but also my becoming acquainted with all the different forms of Swedish sweets would not have been possible without them.

A big thank you also for Dr. Jozef Adamcik, who invested so many hours to obtain all the AFM images, and Dr. Tolga Goren and Christian Mathis for their help with the TInAS. Bernhard Sebastian and Prof. Petra Dittrich for their help for the microfluidic experiments, contributing their time, knowledge and equipment.

It was as well a pleasure to work with Dr. Philipp Spycher, Olivier Kreis and Prof. Roger Schibli in a collaboration bringing the insights gained a step closer towards application. Daniel Messmer kindly provided the denpol used for this collaboration.

During my time as a PhD student I had the pleasure to work with several undergraduate students, contributing to the project with their lab course work, research projects or master theses: David Hess, Julian Bleich, Rafael Hodel, Nicolas Ghéczy, Cristina Mercandetti, Alina Hauser, Livia Schneider, Ines Weber and Christos Glaros.

My lab mates over the years, Benjamin Hohl, Katja Junker, Sun Xiaoyu, Sandra Luginbühl, Lucia Sessa, and Elizabeth Chirackal Varkey helped keeping up a the good spirit in lab G520 and were available whenever I needed an additional hand or somebody for a short break and a chat.

Thomas Schweizer knew help whenever a tool or a repair was needed. Together with Martin Willeke he was also around for many informative, interesting, and entertaining discussion during lunch time.

The many friends I found during my time in the Schlüter-Group were not only a great support during working time, but were also part of many happy hours during recreation. Special thanks also to the people keeping up with the drüü coffee, Thomas Bauer, Samuel Jakob, Simon Cerqua, Chiara Gstrein, Payam Payamyar, Bernd Deffner, Marco Servalli, and all the others joining at times.

Most of all, I want to thank my parents Christine and Josef, and my brother Michael, for their invaluable support over all the years and for always being around whenever I needed them!

# 8 CURRICULUM VITAE

This chapter has been removed in the electronic version of this thesis.

# 9 PUBLICATIONS

Parts of the results of this thesis are published in the following publications:

**Enzyme immobilization on silicate glass through simple adsorption of dendronized polymer-enzyme conjugates for localized enzymatic cascade reactions**

A. Küchler, J. Adamcik, R. Mezzenga, A. D. Schlüter, P. Walde

RSC Advances, 5 (2015) 44530-44544.

**Co-immobilization of enzymes with the help of a dendronized polymer and mesoporous silica nanoparticles**

H. Gustafsson, A. Küchler, K. Holmberg, P. Walde

Journal of Materials Chemistry B, 3 (2015) 6174-6184

**Enzymatic reactions in confined environments**

A. Küchler, M. Yoshimoto, S. Luginbühl, F. Mavelli, P. Walde

Submitted

**Stable and simple immobilization of proteinase K inside glass tubes and microfluidic channels**

A. Küchler, J. N. Bleich, B. Sebastian, P. S. Dittrich, P. Walde

Submitted

**Proteinase K activity determination with β-galactosidase as sensitive macromolecular substrate**

N. Ghéczy, A. Küchler, P. Walde

In preparation

# 10 ABBREVIATIONS

| | |
|---|---|
| 4FB | 4-formylbenzamide |
| $ABTS^{\bullet-}$ | 2,2'-azino-bis(3-ethylbenzothiazoline-6-sulfonate) radical anion |
| $ABTS^{2-}$ | 2,2'-azino-bis(3-ethylbenzothiazoline-6-sulfonate) |
| AFM | atomic force microscopy |
| BAH | bis-aryl hydrazone |
| Boc | *tert*-butyloxycarbonyl- |
| DAP | 2,3-diaminophenazine |
| denpol | dendronized polymer |
| *de*-PG2 | deprotected 2nd generation dendronized polymer |
| DMF | *N*,*N*-dimethylformamide |
| dn/dc | refractive index increment |
| GOD | *Aspergillus sp*. glucose oxidase |
| HMM | hiroshima mesoporous material |
| HRP | horseradish peroxidase |
| HyNic | 6-hydrazinonicotinamide |
| $k_{cat}$ | catalytic rate constant |
| $K_m$ | Michaelis constant |
| MES | 3(*N*-morpholino)ethanesulfonic acid |
| MOPS | 3(*N*-morpholino)propanesulfonic acid |
| MWCO | molecular weight cut-off |
| NMWL | nominal molecular weight limit |
| OPD | *o*-phenylenediamine |
| PDI | polydispersity index |
| PG2 | 2nd generation dendronized polymer |
| pI | isoelectric point |
| $P_n$ | number average degree of polymerization |
| PP | polypropylene |
| proK | *Engyodontium album* proteinase K |
| PTFE | poly tetrafluoroethylene |
| QCM-D | quartz crystal microbalance with dissipation monitoring |
| r.u. | repeating unit |
| S-4FB | succinimidyl 4-formylbenzoate |

| | |
|---|---|
| SEM | scanning electron microscopy |
| Suc-AAPF-pNA | succinyl-L-alanyl-L-alanyl-Lprolyl-Lphenylalanyl-*para*-nitroanilide |
| TEM | transmission electron microscopy |
| TInAS | transmission interferometric adsorption sensor |
| UV/vis | ultraviolet and visible |
| $\Gamma_{app}$ | apparent surface concentration |
| ΔD | dissipation shift |
| Δf | frequenci shift |
| ε | molar absorption coefficient |
| λ | wavelength |